European Union
European Social Fund

OPERATIONAL PROGRAMME
EDUCATION AND LIFELONG LEARNING
investing in knowledge society
MINISTRY OF EDUCATION & RELIGIOUS AFFAIRS
MANAGING AUTHORITY

NSRF 2007-2013
programme for development
EUROPEAN SOCIAL FUND

Co-financed by Greece and the European Union

Biochemical and biophysical study of two putative polysaccharide deacetylases: Their role in osmotic stress and cell shape maintenance in the bacterium *Bacillus anthracis*

University of Crete

2015

Αφιερωμένο στους πιο ένθερμους υποστηρικτές μου,

τους αγαπημένους μου γονείς

Dedicated to my most staunch supporters,

my beloved parents

ΕΥΧΑΡΙΣΤΙΕΣ

"Aut inveniam viam aut faciam"

Αννίβας, 247-153 π.Χ., Καρχηδόνιος στρατηλάτης

Αρχικά οφείλω ένα μεγάλο ευχαριστώ στους δύο επιβλέποντες καθηγητές της παρούσας διδακτορικής διατριβής, στην Ηλέκτρα Γκιζελή και στον Βασίλη Μπουριώτη που με καθοδήγησαν καθ'όλη την διάρκεια της και με βοήθησαν να την ολοκληρώσω.

Οφείλω ακόμη ένα τεράστιο ευχαριστώ στον καθηγητή Vollmer Waldemar, ο οποίος με φιλοξένησε στο εργαστήριο του για 3 μήνες και παρά το σύντομο διάστημα της συνεργασίας μας συνέβαλλε καθοριστικά και ποικιλοτρόπως τόσο στην ολοκλήρωση της συγκεκριμένης διατριβής όσο και στην δημοσίευση της.

Waldemar, I would like to thank you and the members of your lab so much for your hospitality during my stay in Newcastle and despite the short period of our collaboration I cannot but acknowledge your priceless contribution to the completion of this thesis. You were always very generous with your ideas and your time, both during the experiments and during the writing of the paper.

Ένα ευχαριστώ επίσης στον κ. Ηλία Ηλιόπουλο και στον Πέτρο Γκιάστα που ασχολήθηκαν με την επίλυση των δομών των πρωτεινών που μελέτησα κατά τη διάρκεια του διδακτορικού μου και βοήθησαν και αυτοί με τη σειρά τους στην διαλεύκανση του βιολογικού τους ρόλου.

Θα ήθελα επίσης να ευχαριστήσω τα υπόλοιπα μέλη της επταμελούς επιτροπής μου, Νίκο Πανόπουλο, Μιχάλη Κοκκινίδη και Κρίτωνα Καλαντίδη που δέχτηκαν να συμμετάσχουν στην αξιολόγηση της διδακτορικής μου διατριβής και για τον χρόνο που μου αφιέρωσαν.

I would also like to thank Prof. Colin Harwood for providing the UM23C1-2 *Bacillus anthracis* strain and for his useful advice during my visit in Newcastle.

Δεν θα μπορούσα να παραλείψω όλα τα άτομα που στάθηκαν δίπλα μου αυτά τα χρόνια και με συντρόφευσαν σε όλη αυτή την πορεία. Ένα μεγάλο ευχαριστώ στην Μαίρη Τζανοδασκαλάκη τόσο για την βοήθεια της εντός του εργαστηρίου, μα κυρίως για την αγάπη και το ενδιαφέρον της προς το πρόσωπο μου. Επίσης ένα πολύ μεγάλο ευχαριστώ στην Εύη, στον Δημήτρη, στη Νατάσα, στην Ελένη, στον Σωτηράκη, στην Αλεξάνδρα και σε όλα τα παιδιά με τα οποία συνυπήρξαμε στο εργαστήριο που ομόρφυναν την καθημερινότητα μου αλλά και για τις πολύτιμες συμβουλές και

παρατηρήσεις τους. Νιώθω ιδιαίτερη χαρά που τους περισσότερους εκτός απο καλούς συνεργάτες μπορώ να τους αποκαλώ και καλούς φίλους.

Επίσης ενα μεγάλο ευχαριστώ σε όλους τους ανθρώπους που είχα την τύχη να γνωρίσω και να έχω τώρα το προνόμιο να είναι αγαπημένοι μου φίλοι, στον Τάσο, στον Μάνο, την Θάνια, τον Γιώργο, την Όλγα και την Έλλη. Παράλληλα ένα πολύ μεγάλο ευχαριστώ στους πολύ αγαπημένους μου φίλους που βρίσκονται στην Αθήνα αλλά και σε όλα τα μήκη και πλάτη της γης, την Αθηνά, την Ελένη, την Ευαγγελία, τη Νατάσσα και τον Δημήτρη. Μπορεί να μου λείπει η φυσική τους παρουσία, αλλά καθ'όλη την πορεία του διδακτορικού ήταν παρόντες για να χαρούν με την χαρά μου και να στεναχωρηθούν με την λύπη μου.

Τέλος το μεγαλύτερο ευχαριστώ το χρωστάω στην οικογένεια μου, στην αγαπημένη μου γιαγιά και στους λατρεμένους μου γονείς. Ένα ευχαριστώ γιατί ποτέ δεν με εμπόδισαν να ακολουθήσω αυτό που ήθελα, αλλά αντιθέτως είναι πάντα δίπλα μου σε κάθε βήμα, σιωπηλοί συνοδοιπόροι μου και οι πιο ένθερμοι υποστηρικτές μου τόσο στις επιτυχίες όσο και στις αποτυχίες μου να με στηρίζουν ψυχικά, ηθικά και υλικά. Ένα ευχαριστώ εκ βάθους καρδίας που δυστυχώς είναι λίγο και η ελπίδα ότι η ολοκλήρωση αυτής της διατριβής θα μπορέσει να τους ανταποδώσει ηθικά έστω και λίγο ότι έχουν κάνει για μένα μέχρι σήμερα.

This work was supported by the project "IRAKLITOS II - University of Crete" of the Operational Programme for Education and Lifelong Learning 2007 - 2013 (E.P.E.D.V.M.) of the NSRF (2007 - 2013), which is co-funded by the European Union (European Social Fund) and National Resources.

Table of Contents

List of Figures..... 8

List of Tables.....10

ΠΕΡΙΛΗΨΗ.....11

ABSTRACT.....13

1. INTRODUCTION 15

1.1 History Of Anthrax 15

1.2 Biology And Life Cycle Of Anthrax 16

1.3 Toxins And Pathogenesis Of Anthrax 19

1.4 Diagnosis Of Anthrax.....23

1.5 Potency Of Anthrax As Biowarfare Agent.....24

1.6 Cell envelope components of Bacillus anthracis 25

1.6.1 Cytoplasmic membrane.....25

1.6.2 Peptidoglycan 29

1.6.3 S-Layer 33

1.6.4 Capsule 34

1.7 Polysaccharide Deacetylases.....34

1.7.1 Biological Roles of Polysaccharide Deacetylases.....35

1.7.2 Structural Studies of Polysaccharide Deacetylases 37

1.8 Bacterial Cell Shape.....40

1.8.1 Cell Elongation 42

1.8.2 Cell Division 43

1.9 Fibronectin Type III (Fn3) Domain 44

1.10. Inactive enzyme homologues 45

1.11 Adaptation of bacteria to osmotic stress 48

1.11.1 Salt in cytoplasm 48

1.11.2 Organic osmolyte 49

2. MATERIALS AND METHODS 50

2.1 MATERIALS 50

2.2 METHODS 56

2.2.1 Cloning and expression of ba0330 and ba0331 genes of B. anthracis into pRSET A expression vector 56

2.2.2 Purification of recombinant BA0330 and BA0331 56

2.2.3 Preparation of radiolabelled substrate 57

2.2.4 Enzyme assays 57

2.2.5 Construction of B. anthracis *Δba0330*, *Δba0331* and *Δba0330/0331* mutants, complemented strains and gfp fusions 58

2.2.6 Peptidoglycan and neutral polysaccharide purification 59

2.2.7 Autolysis assay 59

2.2.8 Fluorescence microscopy of vegetative cells 60

2.2.9 Western blotting analysis 60

2.2.10 Transmission Electron Microscopy 60

2.2 11 Scanning Electron Microscopy 61

2.2.12 In vitro determination of lysozyme resistance 61

2.2.13 Salt stress adaptation 61

2.2.14 Peptidoglycan binding assay..... 62

2.2.15 Site-directed mutagenesis of BA0330 and BA0331..... 62

3. RESULTS 63

3.1 Computational analysis 63

3.2 BA0330 and BA0331 lack deacetylase activity against common deacetylase substrates 65

3.3 The structure of BA0330 reveals unique features of the active site.....66

3.4 Phenotypic analysis reveals roles of BA0330 and BA0331 in cell wall integrity... 70

3.5 Cells lacking BA0330 and BA0331 are more sensitive upon salt upshift 72

3.6 Lysozyme sensitivity, autolysis rate and muropeptide analysis of parental and mutant strains. 74

3.7 BA0330 and BA0331 interact with peptidoglycan 77

3.8 Gfp-fusions of BA0330 and BA0331 localize to lateral wall and distinct foci respectively 78

3.9 Deacetylase activity is not required to complement mutant phenotypes 79

3.10 Do BA0330 and BA0331 complement each other?.....80

4. DISCUSSION.....83

5. PERSPECTIVES.....89

5.1 Complementation studies.....89

5.2 Elucidation of the role of the Fn3 domain and the NodB domain.....89

5.3 Are BA0330 and/or BA0331 involved in B. anthracis virulence? 90

5.4 Dead or alive? 90

6. REFERENCES 92

List of Figures

Figure 1: *The sporulation and germination cycle in Bacillus.* 18
Figure 2: *The B. anthracis life cycle.* 19
Figure 3: *Cellular model of anthrax toxins.*.....21
Figure 4: *The three clinical forms of anthrax.* 22
Figure 5: *The biosynthetic pathway of bacterial lipoproteins.* 28
Figure 6: *Structure of peptidoglycan in gram-positive bacteria.*.....29
Figure 7: *The peptidoglycan biosynthetic pathway* 31
Figure 8: *The structure of the HF-PS repeating oligosaccharide unit from B. anthracis*.....32
Figure 9: *Cartoon representation of the 3D structures of CE4 family deacetylases.* 38
Figure 10: *Proposed catalytic mechanism for Carbohydrate Esterase Family 4 enzymes.*.....39
Figure 11: *Chemistry of peptidoglycan synthesis and processing* 41
Figure 12: *Proposed models for cell elongation and cell division machineries* 43
Figure 13: (A) *Schematic representation of BA0330 and BA0331 domains.* (B) *Gene organization of putative polysaccharide deacetylases genes ba0330, ba0331 and bc0361.* 65
Figure 14: *SDS-PAGE of the purified BA0330 and BA0331*.....65
Figure 15: (A) *The overall structure of BA0330* (B) *A surface representation of the BA0330 molecule.* 67
Figure 16: *Sequence alignment of the NodB domains of the BA0330, BA0331 proteins and representative members of the CE4 family.*....69
Figure 17: *The putative binding site of BA0330.* 70
Figure 18: *Growth curves of B. anthracis UM23C1-2 and mutant strains.* 71
Figure 19: *Phenotype analysis of parental and mutant strains.* 71
Figure 20: *Complementation of Δba0330 and Δba0331 mutant strains with BA0330 and BA0331 respectively*.....72
Figure 21: (A) *Effect of different NaCl concentrations on growth kinetics.* (B) *Growth of Δba0330 and Δba0331 mutant strains complemented*

with BA0330 and BA0331 respectively under high NaCl concentration (4,5%). 73
Figure 22: *Effect of lysozyme on UM23C1-2, Δba0330 and Δba0331 mutant strains.* 74
Figure 23: *Autolysis rate of UM23C1-2 and mutant strains.*.....75
Figure 24: (A) *HPLC analysis of muropeptide composition of peptidoglycan of UM23C1-2, Δba0330, Δba0331 and Δba0330/0331.* (B) *Proposed structures of major muropeptides.*.....76
Figure 25: *HPLC analysis of muropeptide composition of neutral polysaccharide of UM23C1-2, Δba0330 and Δba0331.* 77
Figure 26: *Peptidoglycan binding assay* 77
Figure 27: (A) *Localization of Gfp-BA0330 and Gfp-BA0331* (B) *Growth of Δba0330 and Δba0331 mutant strains complemented with Gfp-BA0330 and Gfp-BA0331 respectively under high NaCl concentration (4,5%).* 79
Figure 28: (A) *Transmission electron micrographs of Δba0330 and Δba0331 mutant strains complemented with BA0330 (D205A) and BA0331 (D212A) respectively.* (B) *Growth of Δba0330 and Δba0331 mutant strains complemented with BA0330 (Asp205Ala) and BA0331 (Asp212Ala) respectively under high NaCl concentration (4,5%).* 80
Figure 29: (A) *Transmission electron micrographs of UM23C1-2 and Δba0330, Δba0331 mutant strains complemented with BA0331 and BA0330 respectively* (B) *Growth of Δba0330 and Δba0331 mutant strains complemented with BA0330 and BA0331 under mild NaCl concentration (2,5%).*.....81
Figure 30: *Scanning electron micrographs of Δba0330/0331 mutant cells complemented with BA0330 and BA0331* 82

List of Tables

Table 1: List of oligonucleotides used in the present study.....51
Table 2: Strains and Plasmids used in this study. 54
Table 3: The putative polysaccharide deacetylases coding sequences from *B. cereus* and *B. anthracis*. 63

ΠΕΡΙΛΗΨΗ

Οι απακετυλάσες *N*-ακετυλογλυκοζαμίνης των πολυσακχαριτών ανήκουν στην οικογένεια των εστερασών CE4, η οποία περιλαμβάνει ένζυμα που χαρακτηρίζονται απο σημαντική ομολογία και λειτουργικές ομοιότητες. Αποτελεί εξαιρετικό ενδιαφέρον το γεγονός οτι τα γονιδιώματα του *Bacillus cereus* και του συγγενικού παθογόνου *Bacillus anthracis* περιέχουν 10 και 11 γονίδια αντίστοιχα με υψηλή ομολογία μεταξύ τους που κωδικοποιούν για πιθανές απακετυλάσες πολυσακχαριτών. Πρόσφατα μελετήθηκε ο βιολογικός ρόλος για 5 απο αυτές. Οι αιτίες ύπαρξης τόσο μεγάλου αριθμού γονιδίων που κωδικοποιούν για πιθανές απακετυλάσες πολυσακχαριτών στο γονιδίωμα του *B. anthracis*, σε αντίθεση με άλλα παθογόνα βακτήρια που διαθέτουν μικρότερο αριθμό αντίστοιχων γονιδίων αποτελεί βασική αναζήτηση της παρούσας μελέτης.

Τα γονίδια *ba0330* και *ba0331* αποτελούν τα δυο μοναδικά ανοιχτά πλαίσια ανάγνωσης απο τα 11 που περιέχει ο *B. anthracis* που εκτός απο πιθανές απακετυλάσες πολυσακχαριτών κωδικοποιούν και για πιθανές λιποπρωτείνες και μοιράζονται 55% ομολογία μεταξύ τους. Οι λιπορωτείνες των βακτηρίων αποτελούν μια οικογένεια μεμβρανικών πρωτεινών με ποικίλους ρόλους στα κατά Gram θετικά βακτήρια. Για την διαλεύκανση του βιολογικού ρόλου των παραπάνω ενζύμων ακολουθήθηκε συνδυασμός βιοχημικών και μοριακών τεχνικών καθώς και ο κυτταρικός εντοπισμός τους στο βακτήριο *B. anthracis*.

Συνοψίζοντας τα αποτελέσματα της παρούσας διατριβής καταλήγουμε στο συμπέρασμα ότι παρόλο που στις δύο πρωτείνες δεν ανιχνεύθηκε ενεργότητα *N*-απακετυλάσης σε ενζυμικές δοκιμές με συνήθη υποστρώματα απακετυλασών, η κατασκευή των μεταλλαγμάτων *Δba0330, Δba0331* και *Δba0330Δba0331* έδειξε ότι παίζουν σημαντικό ρόλο στην διατήρηση της ακεραιότητας του κυτταρικού τοιχώματος του βακτηρίου. Συγκεκριμένα η διαγραφή του γονιδίου *ba0330* απο το γονιδίωμα του *B. anthracis* έδειξε ότι οδηγεί στην εμφάνιση μερικής αποκόλλησης μεταξύ μεμβράνης και πεπτιδογλυκάνης, πιθανά λόγω αποδυνάμωσης της αλληλεπίδρασης μεταξύ των δύο στρωμάτων. Επίσης τα κύτταρα του στελέχους *Δba0330* είχαν πολύ χαμηλό ρυθμό ανάπτυξης συγκρινόμενα με κύτταρα αγρίου τύπου σε θρεπτικό μέσο με αυξημένη συγκέντρωση NaCl, συσχετίζοντας έτσι την BA0330 με την προσαρμογή του βακτηρίου σε συνθήκες υψηλής αλατότητας. Κατά την διαγραφή του γονιδίου *ba0331* παρατηρήθηκε αδυναμία του στελέχους να διατηρήσει το χαρακτηριστικό σχήμα του βακίλου, με αποτέλεσμα την εμφάνιση άτυπων κυτταρικών σχημάτων. Προκειμένου να διαπιστωθεί κατα πόσο οι φαινότυποι των μεταλλαγμάτων μπορούν να αποδωθούν σε πιθανή ενεργότητα *N*-απακετυλάσης, σημιακές μεταλλαγές εισήχθησαν στα δυο

γονίδια σε καθοριστικά κατάλοιπα για την διατήρηση της πιθανής ενεργότητας. Τα μεταλλλαγματα *Δba0330* και *Δba0331* στα οποία εκφράστηκαν οι αντίστοιχες πρωτείνες που έφεραν την σημιακή μετάλλαξη ανέκτησαν πλήρως τα χαρακτηριστικά του στελέχους αγρίου τύπου.

Επίσης οι δύο πρωτείνες εντοπίζονται σε διαφορετικά σημεία του κυτταρικού φακέλου: η BA0330 εντοπίζεται στην περιφέρεια του κυττάρου, ενώ η BA0331 εντοπίζεται σε διακριτά σημεία. Παράλληλα και οι δύο πρωτείνες αλληλεπιδρούν με την πεπτιδογλυκάνη του βακτηρίου.

Παρόλο που η BA0330 και η BA0331 διαθέτουν τα περισσότερα απο τα κατάλοιπα των μελών της CE4 οικογένειας που έιναι απαραίτητα και συντηρημένα για την κατάλυση, η πρόσφατη επίλυση της δομής της BA0330 έδειξε κάποιες διαφοροποιήσεις στον καταλυτικό μηχανισμό, στις οποίες θα μπορούσε να αποδωθεί η πιθανή έλλειψη ενεργότητας.

Τα αποτελέσματα της παρούσας διατριβής παρέχουν καινοτόμες και θεμελιώδεις πληροφορίες σχετικά με τον ρόλο των λιποπρωτεινών στα κατά Gram θετικά βακτήρια, καθώς για πρώτη φορά καταδεικνύεται ο ρόλος που παίζουν στην διατήρηση της ακεραιότητας των κυτταρικών τοιχωμάτων.

ABSTRACT

Bacillus anthracis is a Gram-positive, spore forming bacterium and the etiological agent of anthrax, a lethal disease sporadically affecting humans and animals. The cell wall of *B. anthracis* is composed of peptidoglycan, polysaccharides, proteins and a poly-γ-D-glutamic acid capsule.

Bacterial lipoproteins are a functionally diverse class of peripheral membrane proteins in Gram-positive bacteria, with important roles in substrate binding for ABC transporters, adhesion, antibiotic, lantibiotic and bacteriocin resistance and phage superinfection, cell envelope homeostasis, protein secretion, folding and localization, redox and sensory processes, including signaling in sporulation and germination.

Polysaccharide deacetylases belong to Carbohydrate Esterase Family 4 (CE4). Interestingly, the genomes of *Bacillus* sp., and especially of *B. cereus* sensu lato, including *B. anthracis* contain multiple putative polysaccharide deacetylase genes with high sequence homologies. The physiological role of five polysaccharide deacetylases in *B. anthracis* has been recently elucidated.

The structures of CE4 enzymes from various bacterial species have been determined and they all contain a conserved NodB homology domain and adopt a $(\alpha/\beta)_8$ barel fold. Most of the structures contain a divalent cation in the active site bound in a His-His-Asp triad. The catalytic machinery is completed by an aspartic acid and a histidine which act as the catalytic base and catalytic acid respectively.

BA0330 and BA0331 from *B. anthracis* are predicted as putative lipoproteins and polysaccharide deacetylases and share 55% sequence identity. Furthermore, BA0330 shares 91% identity with its corresponding homologue BC0361 from *B. cereus*, while a homologue of BA0331, which is present in all *B. anthracis* strains, is missing in many *B. cereus* strains including *B. cereus* ATCC 14579. BA0331 is mainly expressed during exponential phase, but is secreted at lower amounts during the stationary phase, in both the avirulent *B. anthracis* UM23C1-2 (pXO1-, pXO2-) and the wild-type virulent Vollum strain.

In this study we employed biochemical and genetic (knockout) analysis and protein localization to elucidate the biological roles of BA0330 and BA0331 from the avirulent *B. anthracis* UM23C1-2 strain. Although both proteins lack deacetylase activity towards commonly used deacetylase substrates, the construction of both single *Δba0330* and *Δba0331* and double *Δba0330Δba0331* mutants revealed a significant role for the two proteins in maintaining cell wall integrity.

Electron Microscopy revealed that the mutant cells exhibited aberrant phenotypes. In *Δba0330* cells a partial detachment of the membrane from the cell wall was observed, probably due to a weakened interaction between the two layers. Furthermore *Δba0330* cells exhibited impaired growth rate compared to wild type cells, when challenged with increased NaCl concentrations, indicating that BA0330 contributes to the adaptation of the bacterium to high salt stress. On the contrary,

Δba0331 cells had normal peptidoglycan-membrane connection but were unable to maintain the typical bacilli shape, exhibiting a distorted cell shape, a finding which was confirmed by both Transmission and Scanning Electron Microscopy. To examine the importance of the putative deacetylase activity of the proteins in vivo, a point mutation was introduced in *ba0330* and *ba0331* to replace key catalytic residues. The distorted phenotypes of *Δba0330* and *Δba0331* were restored when the mutant cells were complemented with the point mutated BA0330 and BA0331 proteins respectively.

Both proteins were located in the cell envelope but exhibited different localization patterns: BA0330 is localized in the cell periphery and enhanced at the septa and BA0331 in distinct foci with lower representation at the septa. Both BA0330 and BA0331 interact with peptidoglycan, thus reinforcing their implication in stabilizing the cell wall of *B. anthracis*. Furthermore, both proteins may affect the function of autolysins, since *Δba0330* and to a lesser extent *Δba0331* mutant strains showed decreased autolysis.

Although BA0330 and BA0331 contain most of the catalytic and zinc binding residues conserved in five catalytic motifs of enzymatically and structurally characterized CE4 esterases, the recently solved structure of BA0330 revealed that the catalytic site differs from that typically found in polysaccharide deacetylases and could explain the apparent lack of activity of this protein.

To our knowledge this is the first report of lipoproteins implicated in maintenance of cell wall integrity in Gram-positive bacteria.

INTRODUCTION

1.1 History Of Anthrax

Anthrax, caused by *B. anthracis* is a highly contagious and fatal disease. Anthrax was reported in the early literature of the Greeks, Romans and Hindus. The name anthrax originates from the Greek word “anthrakis” which means coal, because black skin lesions is the main symptom in the cutaneous form of anthrax. It is speculated that the fifth plague of Egypt, an epidemic of ancient Egypt described in the book of Genesis (1491 BC), which exterminated the Egyptian livestock without affecting the Israelites livestock, was caused by anthrax.

During the19th century, intense research on anthrax led to various medical developments. In 1850, Pierre Rayer was the first to observe filamentous formations in the blood of sheep that had died due to anthrax. Tiegel and Klebs in 1864 demonstrated that blood infected with anthrax, when filtered through a clay candle (bacterial filter), lost its ability to infect, while the material that remained on the filter was still infective [1]. Robert Koch postulated three principles for germ theory of disease considering anthrax as a model organism. In 1876, he conclusively demonstrated that *B. anthracis* was the etiological agent of anthrax, establishing the first disease whose causative form was due to a microbial agent [2]. Furthermore, by studying bacterial growing cultures, he monitored the multiplication of bacilli and found that under adverse environmental conditions, especially under conditions of oxygen deprivation, they produced round spores. The spores returned to typical bacilli cells when growth conditions were restored to optimum, demonstrating that spore formation is a self-protective mechanism of *B. anthracis*. Pasteur *et al* showed that buried corpse of animals previously infected with anthrax play a significant role in further spreading of the infection [3]. He also confirmed Koch’s finding that anthrax disease is caused by a microbe. He observed that chickens were immune to anthrax, and assumed that this was due to their high body temperature (43 ^{o}C-44 ^{o}C). When the body temperature decreased to 37 ^{o}C, chickens became susceptible to anthrax. For vaccination, Pasteur used heated anthrax cells and inoculated 25 sheep. He found that

all sheep survived, except a pregnant one, while all non-inoculated sheep died following exposure to virulent *B. anthracis*. Pasteur therefore demonstrated that while the weakened *B. anthracis* lost its ability for full virulence it could still confer immunity and this technique was termed "vaccination". Thus, the first live bacterial vaccine for anthrax was developed by Pasteur *et al* [3].

During the civil war in Zimbabwe in 1979-1980, the world's largest outbreak of anthrax was recorded. Over 9400 cutaneous anthrax cases were reported, including 182 fatalities. Before the beginning of the war, anthrax was only endemic in Zimbabwe. Since anthrax is a zoonotic disease, it first infected cattles and then spread in human population. Due to shortage in food supplies, people had to consume animals infected by anthrax, and as a consequence the occurrence of human anthrax cases increased dramatically.

During the first and second World War this extremely pathogenic bacterium served as a means of mass destruction. The most recent case of anthrax being used as a bioweapon occurred in 2001, where envelopes containing *B. anthracis* spores were sent by mail to different dignitaries in United States and 22 infections were reported [4]. This was considered as an act of bioterrorism and led to drastic increase in funding towards the detection and prevention of bioterrorism [5].

1.2 Biology And Life Cycle Of Anthrax

B. anthracis belongs to *Bacillus cereus sensu lato* group, shared by six other species namely *Bacillus cereus*, *Bacillus mycoides*, *Bacillus pseudomycoides*, *Bacillus thuringiensis*, *Bacillus weihenstephanensis*, and *Bacillus cytotoxicus* [6]. It is a Gram positive, rod-shaped, aerobic, facultative anaerobic, sporulating and capsulated bacterium, 1-1.2 μm in width and 3-5 μm in length. The identification of members of the *B. cereus* group based exclusively on chromosomal markers is difficult [7]. Notably, pathogenic strains of *B. anthracis* harbor two virulence plasmids, namely pXO1 and pXO2, which constitute a differentiation marker [8]. pXO1 size is 184.5 kb and encodes the tripartite toxin of *B. anthracis*, which participates in the pathogenicity of the bacterium. The encoding genes which comprise the toxin are *pag* (coding for protective antigen PA), *lef* (coding for lethal factor LF) and *cya* (coding for edema

factor EF) [9]. Plasmid pXO1 also encodes the *atxA* virulence factor which regulates the expression of genes encoded on pXO1 and pXO2 plasmids [10]. The second plasmid pXO2 is 95.3 kb in size and carries the genes for capsule production, degradation and regulation. The capsule of *B. anthracis* is composed of γ-linked poly-D-glutamic acid which gives mucoid appearance to the colony. Formation of capsule is important for the virulence of this bacterium. The capsule itself is non-toxic and doesn't provoke the immune system of the host. However, it contributes significantly in establishing the infection by helping the organism to escape phagocyte action, while the later phase of the disease is controlled by anthrax toxin [11]. Genes *capB, capC and capA* code for capsule synthesis, and gene *dep* codes for capsule degradation [9]. A gerX operon is also present on plasmid pXO1 and its deletion affects the germination of spores in macrophages. The operon codes for three proteins GerXA, GerXB and GerXC. These proteins interact with each other and form a receptor, which specifically detects germinants within the host [12].

Although *B. anthracis* is an aerobic organism, it is also able to survive under anaerobic conditions due to its ability to form spores. *B. anthracis* spores are extremely resistant to harsh environmental conditions such as high temperature, pressure, pH, UV radiation, chemicals and deprivation of nutrients and they can survive for years in soil, air and water [13-15]. When *B. anthracis* cells come across adverse environmental conditions, sporulation is triggered and the endospore is released from the mother vegetative cell.

Sporulation and germination processes require a series of metabolic as well as morphological alterations. In order for *B. anthracis* to form a spore the vegetative cell is divided in two asymmetric sections by a septum, the forespore and the mother cell. Each section obtains a single copy of the bacterial DNA. Following asymmetric division, the mother cell engulfs the forespore employing a double-membrane system. DNA of the mother cell is degraded and forespore DNA is surrounded by an inner membrane. Between the inner and the outer membrane of the forespore two peptidoglycan layers are synthesized, the primordial germ cell wall (inner thin layer) and the cortex (outer thick layer) [16,17]. The outer membrane of the forespore is modified by various proteins to form the coat. Thickness of the spore coat varies among different *Bacillus* species. In *B. anthracis* and *B. cereus*, the spore coat is compact, whereas it can be distinguished from *B. subtilis* [18,19] and confers both

great resistance to the spore and protection to the cortex and DNA. The formed endospores are dormant, well organized and highly resistant to various stress conditions; therefore they can remain viable for long time in the environment and can germinate into vegetative bacteria when suitable environmental and nutritional requirements are provided. In Figure 1 the sporulation and germination processes in *B. anthracis* are presented.

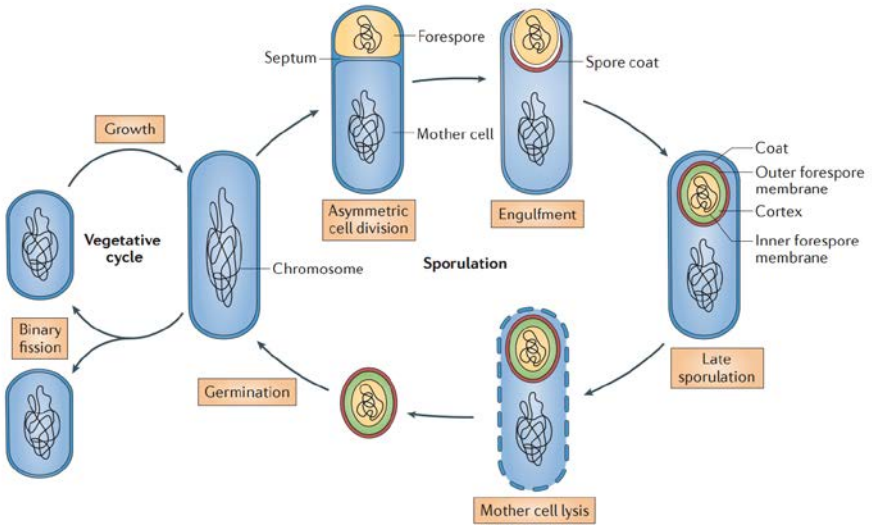

Figure 1: *The sporulation and germination cycle in Bacillus [20].*

The life cycle of *B. anthracis* is shown in Figure 2. Since *B. anthracis* is a severe zoonotic pathogen of ruminants, anthrax infection occurs when animals uptake the endospores found in the soil of agricultural areas. Inside the mamamalian host spores undergo the germination process, since they come across favorable conditions like aqueous environment and sufficient nutrients and thus are able to activate their metabolism and further multiply [21]. Germination of spores into vegetative cells plays a crucial role in pathogenesis, since the vegetative form of the bacterium produces the main virulent factors, namely the capsule and the tripartite toxin [12]. The capsule evades the host immune system and thus is a crucial factor for the

survival of the bacteria in the host. After entry into the host, vegetative cells remain in the capillaries of invaded organs and produce the lethal and edema toxins which cause the local and fatal effects of the infection. Upon death, the capsulated bacteria are released with blood into the environment through natural orifices. After being exposed to oxygen, vegetative cells are converted to spores and thus again infect the agriculture fields and subsequently grazing animals.

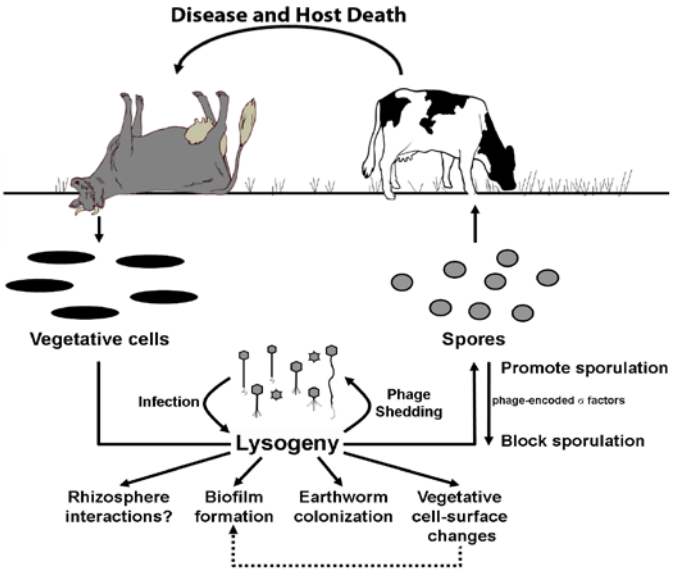

Figure 2: *The B. anthracis life cycle.*

1.3 Toxins And Pathogenesis Of Anthrax

As mentioned above, the virulence of *B. anthracis* is attributed to a tripartite anthrax toxin and a poly-γ-D-glutamic acid capsule. Capsule formation is a key defense element of *B. anthracis* against host responses, since it facilitates the invasion of the host immune system by outrunning the ability of macrophages to engulf and destroy the bacteria [22].

Three non-toxic proteins namely PA (protective antigen), LF (lethal factor) and EF (edema factor) of anthrax tripartite toxin coassemble in order to produce a series of free or cell-bound toxic complexes [23,24]. Two out of the three toxins, specifically LF and EF, are enzymes acting on substrates within the cytosolic

compartments of host cells [25], while PA binds on the receptors of host cells and forms a pore to mediate the transportation of LF and EF to the cytosol [26]. Thus, anthrax toxin is an A-B type toxin, whereas PA is the B subunit and interacts with the LF and EF, which constitute the A subunits to form the lethal toxin and edema toxin, respectively [27].

Anthrax PA is an 83 kDa precursor polypeptide which binds to anthrax toxin receptors. Once cellular proteases cleave PA, a nicked 20 kDa fragment (PA20) at N-terminus and a 63 kDa fragment (PA63) at C-terminus are generated [28]. The 63 kDa fragment self-assembles in order to form a heptameric ring, which can associate with up to three copies of EF and/or LF molecules [29]. A decreased amount of PA forms octamers (20%-30% of oligomers), which can bind up to four molecules of EF and/or LF. This structure is considered more solid than the heptameric one [30]. These complexes after endocytosis operate as a translocation machinery for LF and EF and places them in the cytosol where they disrupt the cell due to their enzymatic functions [31]

LF is a zinc dependent metalloprotease located in the cytoplasm [32],where it inactivates the members of mitogen-activated protein kinase family (MAPKK) [33-35]. Inactivation of three major MEKs *i.e.*, extracellular signal regulated kinases, c-Jun N-terminal kinases and p38 MAPKs leads to the deactivation of several cellular processes like cell division, cell differentiation, cellular response to different types of stress and ultimately results in apoptosis.

The third protein EF functions as an adenylate cyclase. It is produced as a inactive preprotein and is activated by the calcium modulated protein (calmodulin, CaM) [25]. CaM binds to the helical domain of EF by its N-terminus domain. EF interacts with the late endosomal membranes that surround the nucleus forming a perinuclear necklace [36]. In anthrax infection, these two toxins, LF and EF, are responsible for immune system failure and consequent death of host. Figure 3 demonstrates the formation of anthrax toxin on host cell surface followed by internalization and release of lethal factor.

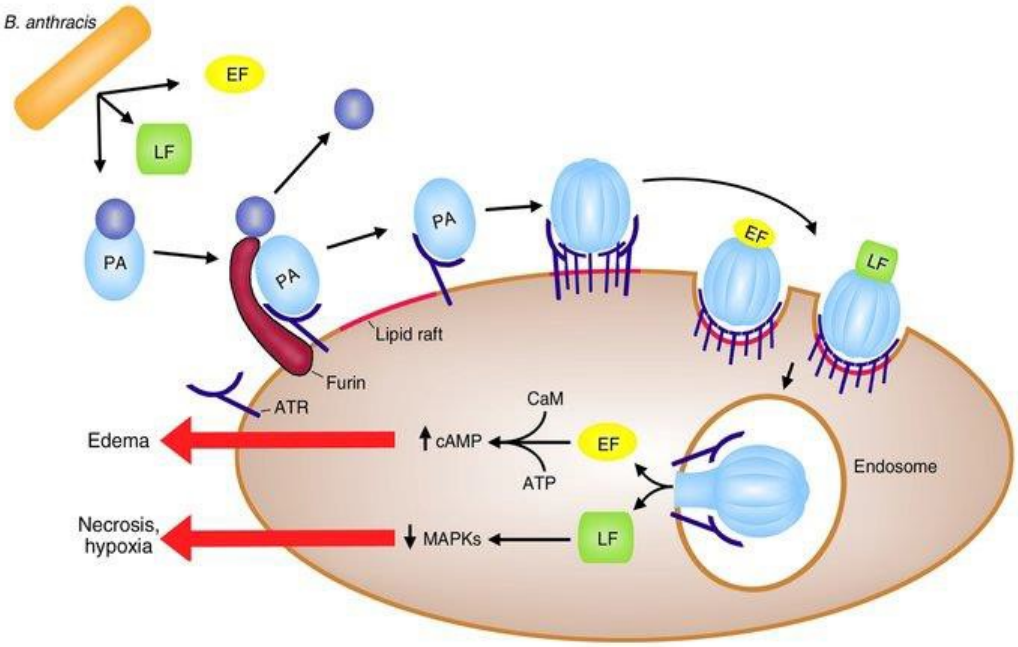

Figure 3: *Cellular model of anthrax toxins [37].*

There are three clinical forms of anthrax, namely cutaneous (skin), gastrointestinal (ingestion) and pulmonary (inhalation) anthrax [38], which are presented in Figure 4. Recently, another type of anthrax has emerged, namely injectional anthrax, related to heroin drug users who are infected by the bacterium [39,40].

The first symptom of cutaneous anthrax infection is a small itching papule resembling an insect bite at the site of infection on skin. Within a day or two, this papule grows and transforms into a painless ulcer with a depressed necrotic centre and a raised and round edge. Generally, such lesions are formed within 2-5 days at the site of spore entry on skin. Finally, after 7-10 days, a black eschar, surrounded by edema is formed, which scars the skin permanently, even after the disease has been cured. Regional lymph nodes draining the infected area may be swollen and enlarged. Cutaneous anthrax infection mostly remains painless and limited to dermis. However, in certain cases it can become systemic when bacteria enter into blood stream causing bacterimia. Hemorrhagic lesions can be developed on any part of the body and can be fatal in bacteremic anthrax [41].

Gastrointestinal (GI) anthrax occurs by consuming food, usually meat, contaminated with anthrax spores. After ingestion, spores germinate and can cause lesions anywhere in the body. Based on the lesions, gastrointestinal anthrax is

classified in two types, abdominal and oropharyngeal. In abdominal GI anthrax, lesions are formed mainly in the ileum and cecum, whereas in oropharyngeal anthrax lesions are usually formed in the oral cavity and resemble the lesions of cutaneous anthrax. Symptoms include throat pain, swallowing and swelling problem in neck due to edema and cervical lymphadenopathy [42].

Pulmonary or inhalational anthrax is the most severe form of infection and occurs by inhalation of spores into lungs. Alveolar macrophages ingest the spores and transport them to lymph nodes in mediastinum. Initially, symptoms of inhalational anthrax are similar to cold or flu with mild chest discomfort, shortness of breath, nausea and finally severe respiratory collapse. Pulmonary anthrax doesn't cause pneumonia, but causes hemorrhagic mediastinitis and pulmonary edema. Historically, mortality was 92%, but, it can be reduced significantly if treated early as only 45% mortality was observed during the 2001 anthrax attack in United States [43].

Symptoms of anthrax caused by injection remain the same as in cutaneous anthrax, but there may be infection deep under the skin or in the muscle where the drug is injected. Sometimes there is redness at the area of injection. Injectional anthrax is difficult to diagnose because several other common bacteria can cause skin and injection site infections. Therefore, it is hard to treat injectional anthrax as it spreads throughout the body very fast. *B. anthracis* secretes toxins which affect proper functioning of different organs like spleen, lymph nodes, liver, kidney, heart and brain. It becomes very difficult to cure the disease by antibiotic therapy at this stage and action of anthrax toxins ultimately leads to septic shock and death of host within 1-2 days [39].

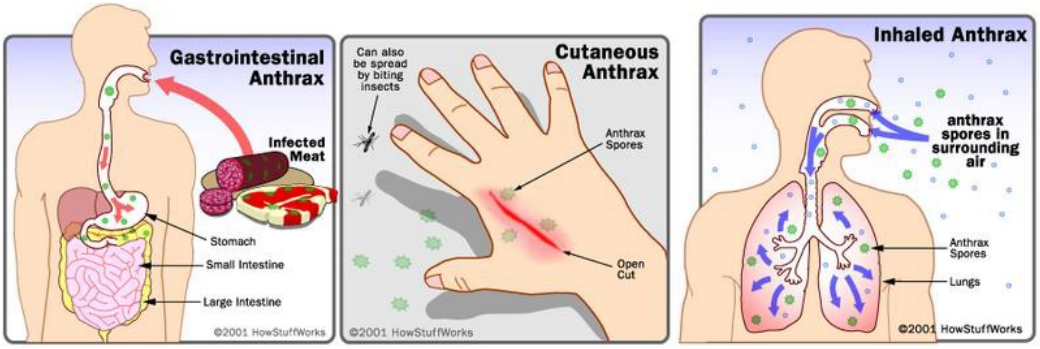

Figure 4: *The three clinical forms of anthrax.*

1.4 Diagnosis Of Anthrax

As various outbreaks of the anthrax disease occur from time to time there is an increasing need of an early and effective diagnosis in order to prevent human and animal casualties. Moreover this need has been further emphasized after the recent cases of use of anthrax in acts of bioterrorism. The early monitoring of the disease requires the detection of anthrax spores and infection both at environmental and clinical levels.

Cutaneous anthrax is diagnosed clinically mostly employing traditional microbiological methods like gram-staining or capsule staining [44,45]. A selective media containing polymyxin-B, lysozyme, EDTA and thallous acetate was used for isolation of *B. anthracis* from contaminated and suspected samples [46]. Additionally, bicarbonate agar is used to induce capsule formation for *B. anthracis* and subsequent verification of the strain. However, growth on selective media is not the proper way to identify *B. antracis*, since several closely related bacteria such as *B. cereus* and *B. subtilis* also grow well on these. Alternatively, immunoflorescent techniques have been employed for the direct identification of *B. anthracis* spores [47].

Recently, a new method utilizing genetically modified phages has been developed for detection of pathogenic *B. anthracis* from clinical sources [48]. The reporter phage displays species specificity by its inability, or significantly reduced ability, to detect members of the closely related *B. cereus* group and other common bacterial pathogens.

Nucleic acid based detection methods, which employ nucleic acid sequences unique to *B. anthracis*, have also been developed for detection of anthrax. Polymerase chain reaction (PCR) or real-time PCR amplify the specific chromosomal markers or virulence plasmids present in *B. anthracis*. This approach has gained enormous popularity for its specificity and constitutes the fastest and most accurate method of *B. anthracis* identification [49].

1.5 Potency Of Anthrax As Biowarfare Agent

The use of microorganisms as a means of conducting war or as bioterror agents is becoming a real possibility now around the world. Any biological agent from a large range of human infection causing pathogens could be considered as a potential biological weapon. However, only a small number of these agents fulfil the desirable ctiteria like ease of cultivation and dispersal or dissemination for recognition as possible biological weapons. Anthrax spores pose the biggest bioterrorism threat because it is easier to produce and preserve them. Additionally, some characteristic properties of the spores such as high resistance to temperature, pressure, pH, ionizing radiations and half life of 100 years make them a suitable bioterror agent. After production and purification, anthrax spores can be stored in a dry form which remains viable for decades. Spores may survive in the water, soil and on several surfaces for years.

Anthrax spores have already been used in the United States and it is considered the most preferable agent to be used for biothreat in the future because of high case fatality rates, rapid transmission by aerosol and its stability in the environment.

According to Center for Disease Control national occupational respiratory mortality system (CDC norms), *B. anthracis* is placed in high priority- Category A due to its ease of dissemination, high mortality rates, epidemic potential and special alertness required. In 2001, mails deliberately contaminated with *B. anthracis* spores were used to terrorize people and subsequently research for the development of anthrax vaccine speeded up. Moreover, each category A biothreat agent has its unique clinical and diagnostic features and no single system can meet the challenges of all the agents. Besides, anthrax is still a concern of human as well as veterinary public heath in several countries like India. Bioterrorism itself is an emerging problem for public health. Hence, it is not possible to look into bioterrorism and public health separately.

1.6 Cell envelope components of Bacillus anthracis

The cell envelope of *B. anthracis* has a multilayered structure. In addition to that it exhibits some unique characteristics, since apart from the membrane and the peptidoglycan layer, it also possesses the S-layer and the capsule, two structures present simultaneously only in few bacteria. The main properties of the components constituting the cell envelope of *B. anthracis* are highlighted below:

1.6.1 Cytoplasmic membrane

There has not been an extensive study regarding the cytoplasmic membrane of *B. anthracis*. It is composed of phospholipids and fatty acids. The latter are mostly composed of iso- and anteiso- branched fatty acids [50]. When *B. anthracis* cells are grown on complex media branched-chain fatty acids comprise less than a third of the total. On the contrary, when they are grown on synthetic media the ratio increases to over two-thirds of the total [51]. Cytoplasmic membrane has been demonstrated to provide resistance against cationic antimicrobial peptides due to the presence of certain phospholipids. In *B. anthracis* it has been shown that the membrane protein MprF, catalyses the addition of lysine to phospholipids, which makes the bacterium resistant towards various cationic antimicrobial peptides, but not towards cationic antibiotics [52].

Membrane associated structures

Lipoteichoic acids

Until recently it was believed that *B. anthracis* did not possess any membrane-associated polysaccharides, i.e. lipoteichoic acids, due to its low CG content. In a recent study by Missiakas *et al.* the existence of membrane anchored lipoteichoic acids in *B. anthracis* was confirmed [53]. A polymer of glycerol phosphate linked to glycolipid was identified, which is typical of lipoteichoic acids anchoring bacterial membranes [54]. Two genes coding for LtaS1 and LtaS2 housekeeping synthases, are

necessary and sufficient for lipoteichoic acid synthesis in *B. anthracis*. Disrupted synthesis of lipoteichoic acids leads to inability of *B. anthracis* for sporulation and proper cell separation during vegetative growth [53], indicating the significant role of lipoteichoic acids in the physiology of the bacterium.

Lipoproteins

Bacterial lipoproteins are a functionally diverse class of peripheral membrane proteins in Gram-positive bacteria. They are identified by the presence of a conserved N-terminus lipid modified cysteine residue which facilitates the anchoring of proteins to cell membranes [55]. The distinct feature of lipoproteins is a characteristic lipobox consensus sequence [LVI][ASTVI][GAS][C], which is the hallmark for lipid modification of proteins in bacteria. *B. anthracis* is predicted from genomic sequence analysis to have a large number of cell-associated lipoproteins, comprising ~2.5% of its proteome [56].

The biosynthetic pathway of lipoproteins in *B. anthracis* was recently studied. Two conserved genes in both gram-negative and gram-positive bacteria were identified in its genome, namely *lgt* and *lsp*. Lipoproteins are first translated as prolipoproteins and are translocated via Sec or Tat machineries. Subsequently they are further processed by the two membrane bound proteins Lgt and Lsp in the inner cytoplasmic membrane.

Modification of prolipoproteins by Lgt is the first step in lipoprotein synthesis [57].The role of Lgt , which is a lipoprotein diacylglyceryl transferase , is to transfer a diacylglyceryl moiety to the cysteine residue located within the lipobox. After lipidation the next step involves the action of Lsp, a lipoprotein signal peptidase, which cleaves the signal sequence of the lipidated prolipoprotein, leaving the cysteine of the lipobox as the new amino-terminal residue and thus forming the mature diacyl lipoprotein [57]. In *B. anthracis* and other gram-positive bacteria it has been demonstrated that *lgt* and *lsp* are dispensable, whereas in gram-negative bacteria the disruption of these two enzymes has lethal consequences [56].

Noteworthy, maturation of lipoproteins in gram-negative bacteria requires an additional step, the action of Lnt, a lipoprotein N-acyl transferase, which attaches an amide-linked fatty acid at the N-terminus cysteine residue producing the triacyl mature lipoprotein [58]. For a long time this type of lipoprotein modification

was not identified in gram-positive bacteria, until the identification of Lnt homologues in gram-positive bacteria [59] and the confirmation of the presence of triacyl mature lipoproteins also in some gram-positive bacteria [60]. In low GC content gram-positive bacteria such as members of the *Bacillaceae*, *lnt* homologues have not been identified although the existence of an unidentified enzyme that catalyses the a-amino acylation of diacylated lipoproteins has been proposed [55]. The biosynthetic pathway of lipoproteins in presented in Figure 5.

Lipoproteins have been implicated in many important cellular processes such as substrate binding for ABC transporters, antibiotic, lantibiotic and bacteriocin resistance and phage superinfection, protein secretion, folding and localization, redox and sensory processes, including signaling in sporulation and germination [61]. Additionally genome analyses revealed a number of putative lipoproteins predicted to play significant roles in cell envelope stability and homeostasis and cell wall crosslinking or remodeling such as penicillin binding proteins and peptidoglycan hydrolases [62,63]. Notably bacterial lipoproteins seem to have key role in host-pathogen interactions, by facilitating surface adhesion and initiation of inflammatory processes or by translocating virulence factors into the host cytoplasm [64]. Interestingly, lipoproteins anchored to the outer membrane of gram-negative bacteria which interact covalently or non-covalently with peptidoglycan have been reported to play a structural role [65]. Although it has been proposed that lipoproteins of gram-positive bacteria could also have equivalent structural roles, it has not been demonstrated so far [66].

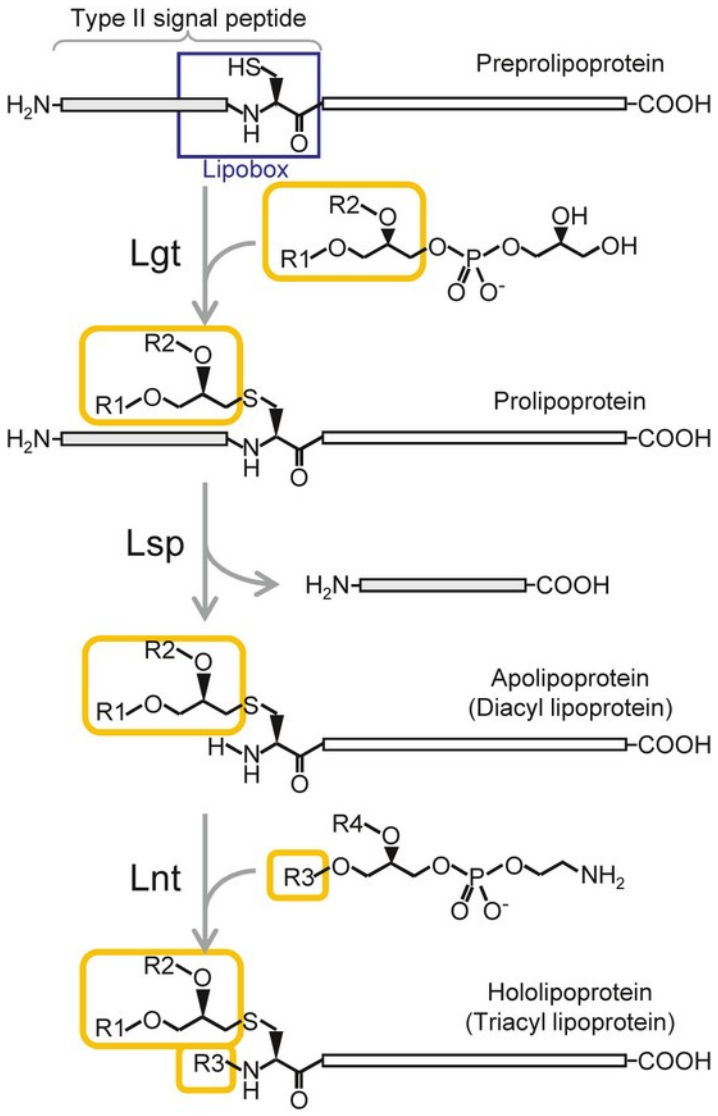

Figure 5: *The biosynthetic pathway of bacterial lipoproteins [55].*

.6.2 Peptidoglycan

Peptidoglycan structure constitutes an essential component of bacterial cell wall for shape maintenance and resistance to osmotic pressure. Constant remodelling of this highly dynamic macromolecule permits the completion of several critical cellular processes including cell growth and cell division.

The peptidoglycan layer of *B. anthracis* consists of repeating units of *N*-acetylglucosamine and *N*-acetylmuramic acid held together by β-(1-4) glycosidic bonds. *N*-acetyl-muramic acid harbours a stem peptide whose terminal amino groups are connected to the carboxyl groups of the muramyl residues via amide linkages. The stem peptide is composed of five amino acids. The first two positions are occupied by L-Ala and D-Glu respectively while the last two positions are represented by two D-Ala residues. The amino acid at the third position of the peptidoglycan stem peptide is occupied by meso-diaminopimelic acid (meso-DAP), a feature which distinguishes *B. anthracis* from the majority of gram-positive bacteria, which usually utilize L-Lys at the third position of the stem peptide. Its stem peptides are cross-linked between the amino acid at position four of the first stem peptide (D-Ala) and the third amino acid of the adjacent stem peptide (meso-Dap) at a rate of 32%. A schematic representation of peptidoglycan structure is demonstrated in Figure 6.

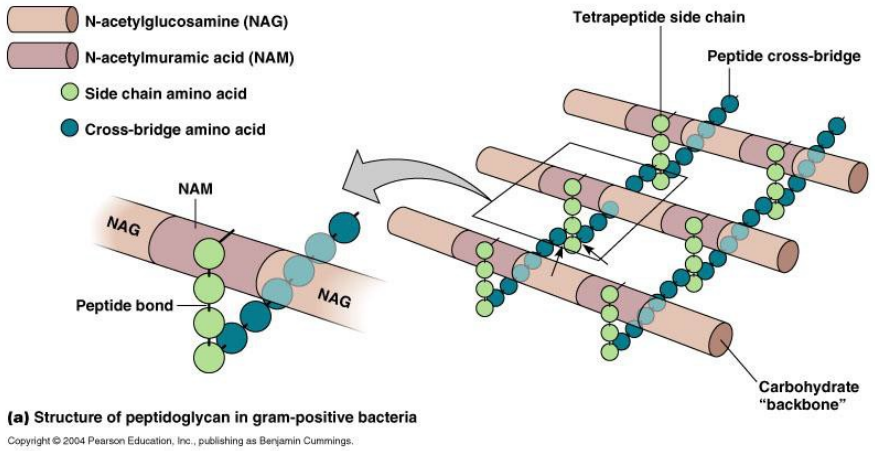

Figure 6: *Structure of peptidoglycan in gram-positive bacteria.*

A broad variety of enzymes such as transglycosylases, transpeptidases, D,D-carboxypeptidases and hydrolases employ the peptidoglycan layer as a substrate, boosting the complex structure of this macromolecule [67].

Peptidoglycan biosynthesis, which is demonstrated in Figure 7, is a three step process depending on which compartment each step takes place:

Cytoplasmic reactions (synthesis of the nucleotide precursors). In the cytoplasm, fructose-6-phosphate is converted to UDP-GlcNAc via a series of enzymatic reactions in the cytosol. Subsequently, UDP-GlcNAc is converted to UDP-MurNAc by two enzymatic reactions involving MurA and MurB. MurA tranfers the enolpyruvate moiety of phosphoenolpyruvate (PEP) to the 3-hydroxyl of UDP-GlcNAc whereas MurB reduces the UDP-GlcNAc-enolpyruvate product using one equivalent of NADPH and a solvent-derived proton. This two-electron reduction creates the lactyl ether of UDP-MurNAc. The stem peptide of UDP-MurNAc-pentapeptide is assembled by MurC,D,E,F enzymes [68].

Reactions at the inner side of the cytoplasmic membrane (synthesis of lipid-linked intermediates). Transferase MraY catalyzes the transfer of the phospho-MurNAc-pentapeptide moiety of UDP-MurNAc-pentapeptide to the membrane acceptor, undecaprenyl phosphate, forming lipid I. Transferase MurG catalyzes the addition of *N*-acetyl-glucosamine to the *N*-acetyl-muramic acid residue of lipid I yielding lipid II, the molecule responsible for transferring the complete disaccharide-peptide monomer unit: GlcNAc-β-(1-4)-MurNAc-L-Ala-γ-D-Glu-DAP (or L-Lys)-D-Ala-D-Ala [69].

Reactions at the outer side of the cytoplasmic membrane (polymerization reactions). Transfer of lipid II to the outer leaflet, initiates the extracellular steps of peptidoglycan formation. In a recent study it was demonstrated that the translocation of lipid II through the plasma membrane requires the integral membrane protein FtsW [70].Lipid II is subsequently polymerized by a transglycosylation reaction in order to form the immature peptidoglycan. Transglycosylation is followed by a transpeptidation reaction for peptidoglycan maturation and cross-bridges formation [71].

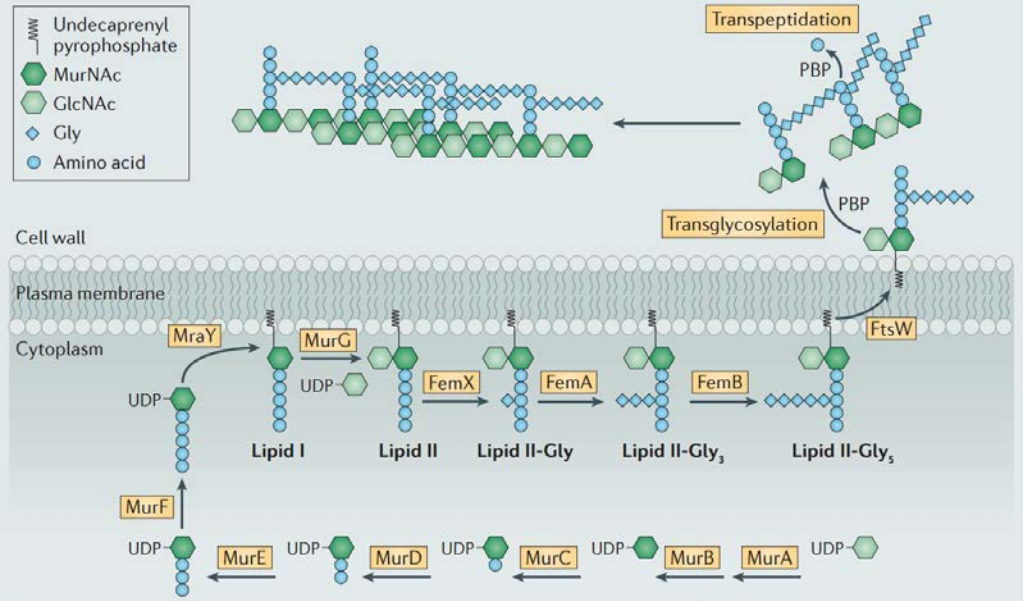

Figure 7: *The peptidoglycan biosynthetic pathway [72].*

Peptidoglycan associated polymers

Neutral polysaccharide

Gram-positive bacteria synthesize anionic polymers which are linked to peptidoglycan via covalent bonds. They are categorized in three groups: i) teichoic acids, which are polyol-phosphates, ii) teichuronic acids, which are uronic acids containing polysaccharides and iii) acidic or neutral polysaccharides. Among them teichoic acids are most probably absent from the surface of *B. anthracis*, since the phosphate concentration is very low in the cell wall and their biosynthetic pathway has not been yet identified [73].

Noteworthy, a neutral polysaccharide has been detected following treatment of the cell wall of *B. anthracis* with hydrofluoric acid. It has a molecular mass of 12 kDa and it is composed of galactose, *N*-acetylglucosamine and *N*-acetylmannosamine [74,75]. The backbone of the polysaccharide consists of an amino sugar backbone,→

6)-alpha-GlcNAc-(1→4)-beta-ManNAc-(1→4)-beta-GlcNAc-(1→, in which, with some variability, the alpha-GlcNAc residue is substituted with alpha-Gal and beta-Gal at O-3 and O-4, respectively, and the beta-GlcNAc substituted with alpha-Gal at O-3 [76]. This polymer is linked to the peptidoglycan layer via murein linkage units, i.e. a GlcNAc-MurNAc moiety that is linked to the C6 hydroxyl of MurNAc via a phosphodiester bond [77]. The neutral polysaccharide has been identified in both vegetative cell wall and spores [78] and its structure is presented in Figure 8.

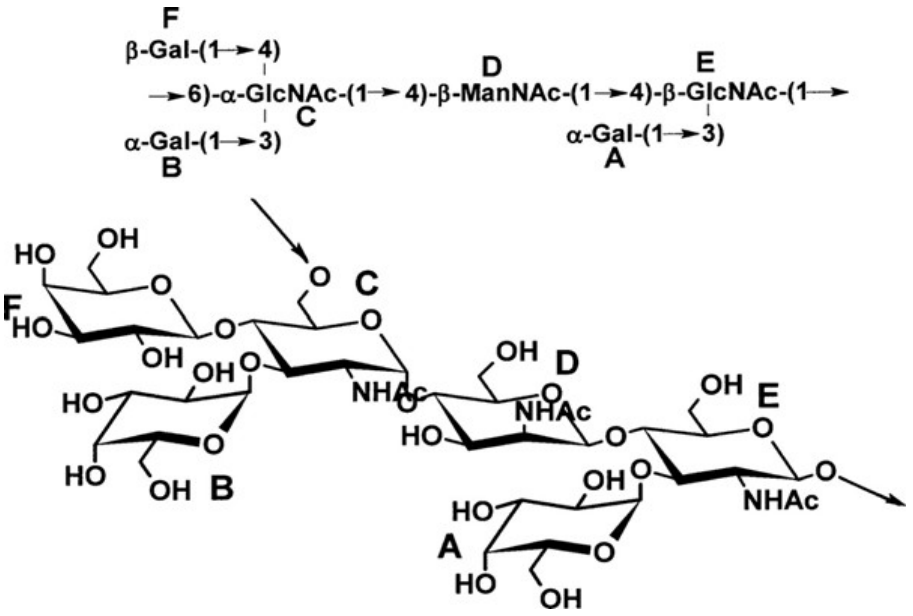

Figure 8: *The structure of the HF-PS repeating oligosaccharide unit from B. anthracis [76].*

Several roles have been attributed to the neutral polysaccharide. Isolated neutral polysaccharide has been found to be pyruvylated, an essential modification required for its interaction with SLH domain harboring proteins[79]. This is an important property, since some of the autolysins which are responsible for the proper septation of cells belong to this category of proteins. Moreover the neutral polysaccharide is immunogenic and it has been speculated that it may confer resistance to α defensins, which are cationic antimicrobial peptides active against *B. anthracis* among other bacteria [80].

1.6.3 S-Layer

In *B. anthracis* 24 proteins have been identified whose sequences contain the structurally conserved surface layer (S-layer) homology (SLH) domain. Proteins which harbor the SLH domain are bound to the neutral polysaccharide [81]. Two of these proteins, namely surface array protein (Sap) and extractable antigen 1 (EA1), self-assemble into a paracrystalline layer on the surface of bacilli and constitute the S-layer [82].These bimodular proteins are composed of an anchoring domain made of three SLH motifs and a second motif, which is suspected to play a role in their crystallization [83].

S-layer proteins cover completely the cell surface of the bacterium and it is estimated that they can represent up to 15% the total proteins. In *B. anthracis* EA1 is found only as cell-bound, while Sap is found both as cell-bound and secreted, thus indicating different regulation. The two S-layer proteins form distinct arrays according to the developmental stage of the bacterium. Sap layer is formed during the early and logarithmic growth phases of the culture, whereas EA1 wraps around the surface during the stationary growth phase, following Sap destabilization [84]. Accordingly, the *sap* gene, which encodes for Sap, is transcribed at the exponential growth phase and once the cell reaches the stationary growth phase transcription level decreases drastically, while transcription of *eag*, the gene encoding for EA1, is greatly enhanced [85]. The presence of EA1 at the cell surface provides the proper signaling for the release of Sap into the growth media, where it is accumulated.

As mentioned above SLH domain containing proteins are attached to neutral polysaccharide via electrostatic interactions with its pyruvylated moieties [79,86]. Pyruvylation of the secondary cell wall polysaccharide is catalyzed by csaB, which mediates the anchoring of the numerous SLH domain proteins of *B. anthracis*, including Sap and EA1.

Assigned roles for the S- layer include the formation of a protective coat, a component involved in cell adhesion, a molecular or ion trap or a molecular filter [87].

1.6.4 Capsule

The capsule of *B. anthracis* is the outermost layer of the cell envelope. Unlike most species, its nature is polypeptidic and not polysaccharidic. It is composed of repeating units of D-glutamic acid residues linked with γ- and not α- type linkage, as it was initially believed [88], thus glutamic acid residues are mainly linked via peptide bonds between γ-carboxyl and α-amino groups. The size of the polymer varies according to the growth conditions of the cells. In vitro fragments between 20 and 55 kDa have been isolated [88], while cells grown in vivo yield fragments up to 215 kDa [89].

Capsule synthesis is encoded by pXO2 plasmid [90], which harbors the set of genes required for its synthesis. The minimal gene set is comprised of four genes, namely capB, capC, capE and capA [91]. The poly-γ-D-glutamic acid capsule synthesis complex is membrane-anchored and uses glutamate and ATP as substrates. Capsule formation is a two step procedure, including D-glutamic acid polymerization and capsule transport through the membrane. CapB and CapC regulate capsule synthesis, while CapA and CapE facilitate its transport [92]. Finally, capD catalyzes the covalent anchoring of the poly-glutamate molecule to peptidoglycan and more precisely it catalyzes the amide bond formation between poly-γ-glutamate and the meso-diaminopimelic acid residue of the stem peptide of peptidoglycan [93].

It has been established that the capsule plays a significant role in the virulence of *B. anthracis*. Its main purpose is to inhibit phagocytosis, once the cell has infected the host, enabling it to evade the host immune responses and cause septicemia [94]. Furthermore polyglutamate capsule has been found to be weak immunogen [95], providing this polymer the main feature of not provoking an immune response.

1.7 Polysaccharide Deacetylases

Polysaccharide *N*-deacetylases are members of the carbohydrate esterase 4 (CE4) family (CAZY database, http://www.cazy.org/) and their enzymatic function is to remove acetyl groups from their polysaccharide substrates, a reaction which produces modified polysaccharides with free amines. CE4 family includes chitin deacetylases, acetylxylan esterases, xylanases, chitooligosaccharide deacetylases and

peptidoglycan deacetylases. Members of this family are metal dependent enzymes which catalyze the hydrolysis of either *N*-linked acetyl group from *N*-acetylglucosamine residues (chitin deacetylase, NodB, and peptidoglycan *N*-acetylglucosamine deacetylase) [96,97] or *O*-linked acetyl groups from *O*-acetylxylose residues (acetylxylan esterase, xylanase) [98-100]. Numerous polysaccharide deacetylases studies revealed a set of different substrates, biochemical properties and biological roles.

1.7.1 Biological Roles of Polysaccharide Deacetylases

For a long time the biological role of peptidoglycan deacetylases was tightly linked to lysozyme resistance. Lysozyme is a hydrolase and constitutes a key component of the innate immune system of mammalian host organisms. It is a 14,5 kDa cationic protein present in tears, gastric juice and milk [101]. Positively charged lysozyme binds strongly to negatively charged bacterial cell wall via electrostatic interactions and catalyses the cleavage of the β-(1,4) glycosidic bond between *N*-acetylglucosamine and *N*-acetylmuramic acid of bacterial peptidoglycan. Three properties of lysozyme contribute to its antibacterial properties, i) its muramidase action by hydrolyzing peptidoglycan, ii) the generation of peptidoglycan fragments that are recognised by different immune receptors and trigger an immune reaction to the host and iii) its function as an antimicrobial peptide.

Three modifications of the peptidoglycan backbone have been documented to confer lysozyme resistance in bacteria, *N*-glycolylation of *N*-acetylmuramic acid, *O*-acetylation of *N*-acetylmuramic acid and *N*-deacetylation of *N*-acetylglucosamine. Bacteria exploit *N*-deacetylation in order to alter the electrostatic properties of their surface and gain resistance against various antimicrobial peptides such as lysozyme, which are mainly cationic. Since the identification of the first gene encoding for a peptidoglycan deacetylase, namely *pgdA*, which was documented to confer resistance towards lysozyme [96], a plethora of functional homologues in various bacteria have been identified including *Bacillus anthracis* (*ba1977*) [102], *Bacillus cereus* (*ba1974*) [97], *Listeria monocytogenes* (*pgdA*) [103], *Lactococcus lactis* (*pgdA*) [104], *Streptococcus suis* (*pgdA*)[105] *Shigella flexneri* (*sfpgdA*) [106] and *Enterococcus faecalis* (*pgdA*) [107]. Interestingly, expression of *pgdA* gene both in the case of

Streptococcus suis and *Enterococcus faecalis* is triggered after interaction of the bacterium with neutrophils or after exposure to lysozyme respectively [105,107]. Peptidoglycan modification prevents direct killing of bacteria from host lysozymes but also their elimination by altering the host immune response.

Apart from conferring lysozyme resistance peptidoglycan deacetylases have also been implicated in the indirect regulation of autolysin activity. Autolysins are bacteriolytic enzymes that digest the peptidoglycan of the bacteria that produce them and are involved in numerous cellular processes including cell division, peptidoglycan maturation and cell wall turnover [108]. In the case of PgdA from *L. lactis* it was shown that besides conferring lysozyme resistance to the bacteriun, it also played a role in the regulation of AcmA, a major autolysin of this bacterium [107]. Likewise two recently studied peptidoglycan deacetylases from *B. anthracis*, BA1961 and BA3679 respectively, seem to impair the substrate recognition of peptidoglycan hydrolases that are crucial for autolysis and cell division [102].

In spore forming bacteria the role of polysaccharide deacetylases has been documented over a decade ago. *B. subtilis* expresses a peptidoglycan *N*-acetylmuramic acid deacetylase (PdaA) which participates in muramic δ-lactam formation during sporulation [109]. Lactamised *N*-acetyl-muramic acid residues are essential for the activity of germination lytic enzymes involved in spore cortex hydrolysis during germination. PdaA homologues are also found in other spore forming Gram-positive bacteria like *Bacillus anthracis* e.g. BA0424 that constitutes a *N*-acetyl-muramic acid deacetylase. Similarly to PdaA, a second polysaccharide deacetylase in *B. subtilis* namely PdaB, is associated with sporulation and is highly conserved among spore-forming bacteria [110].

Besides peptidoglycan, bacteria produce other carbohydrate-based polymers which decorate their cell envelope or are being secreted. Interestingly, *Pseudomonas aeruginosa* produces two distinct classes of exopolysaccharides, Psl and Pel which are both implicated in biofilm formation. Interestingly, P. *aeruginosa* produces a large 105 kDa protein, namely PelA, which exhibits structural similarity to glycoside hydrolases and additionally a C-terminal carbohydrate esterase domain was identified. PelA exhibits *N*-deacetylase activity and it considered to be essential for the formation and secretion of the Pel polymer [111]. Likewise two other polysaccharide deacetylases which employ exopolysaccharides as substrates were identified. IcaB

from *Staphylococcus epidermidis* [112] and PgaB from *E. coli* [113] have been documented the first to modify and the second to modify and export the poly-β-1,6-N-acetyl-D-glucosamine (PNAG) exopolysaccharide.

Recently two additional polysaccharide deacetylases from *B. anthracis*, namely BA5436 and BA2944 were found to participate in neutral polysaccharide attachment to peptidoglycan (BA5436) or in polysaccharide modification (BA2944) [102]. Polysaccharide deacetylases therefore have been demonstrated to play distinct and important roles in bacteria.

1.7.2 Structural Studies of Polysaccharide Deacetylases

SpPgdA form *S. pneumoniae* [114], a peptidoglycan *N*-acetylglucosamine deacetylase and BsPdaA from *B. subtilis* [115], a peptidoglycan *N*-acetylmuramic acid deacetylase, were the first two members of the CE4 family whose 3D structures were determined. Since then crystal structures of several polysaccharide deacetylases of the this family have been determined and all of them share a common NodB homology domain, which catalyses the deacetylation reaction. Notably, in same cases one or more additional domains were present at the overall structure, but their functions have not yet been identified. Most of the structures of polysaccharide deacetylases determined so far from an equivaled orientation are presented in Figure 9.

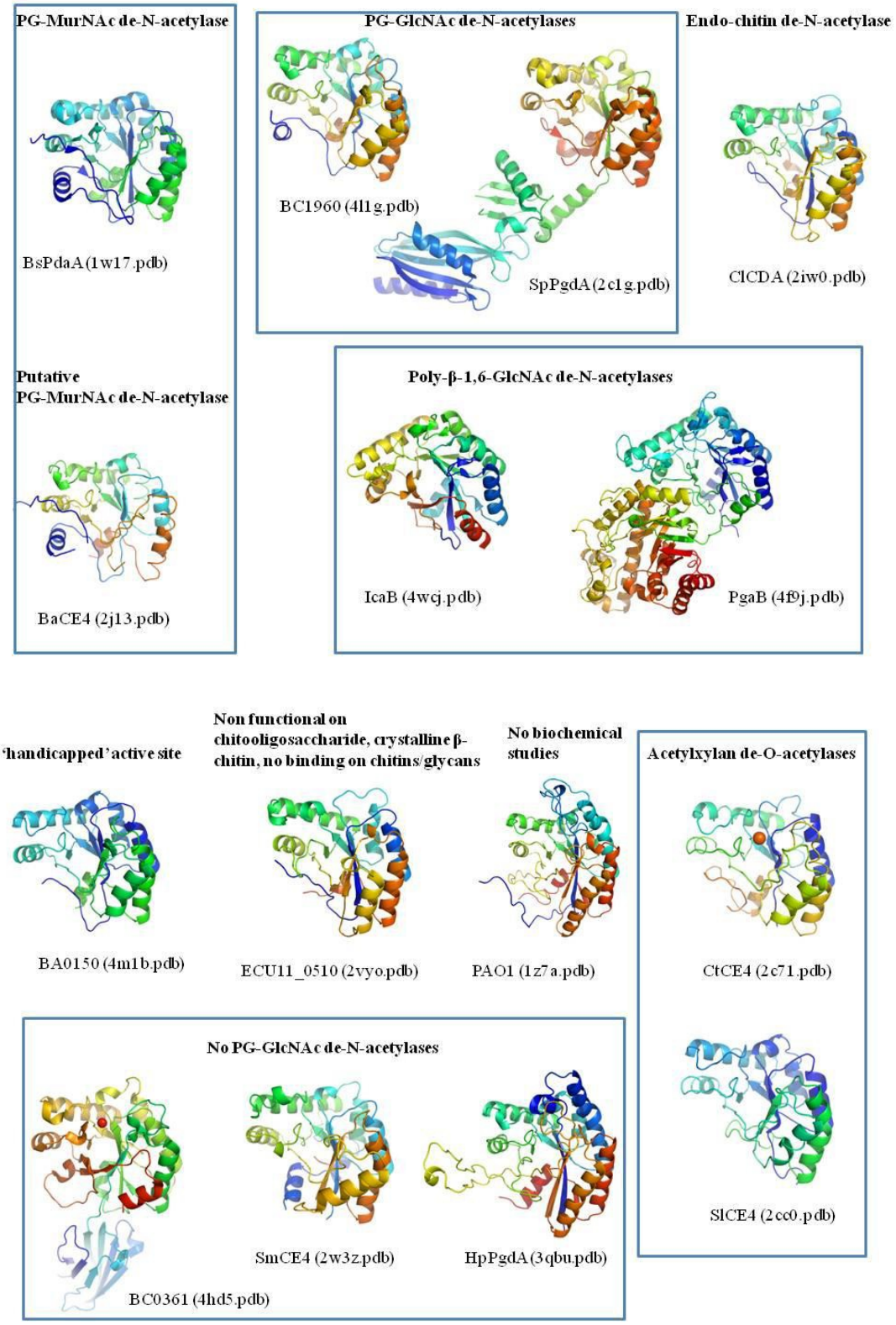

Figure 9: *Cartoon representation of the 3D structures of CE4 family deacetylases. Coloring is blue to red from N- to C-terminus. The molecules are structurally superimposed on their NodB domains and presented by the same orientation for easy comparison* [116].

CE4 enzymes adopt a distorted (α/β)8 barrel fold, with the active site lying in a groove. Since they are metalloenzymes most of the structures contain a divalent cation, usually Zn^{+2}, in the active site that is essential for enzyme activity. Blair *et al.* identified five conserved sequence motifs which are required for the activity of the NodB domain [114]. It has been proposed that catalysis follows a general acid-base mechanism. Motif 1 (TFDD) contains the catalytic base which activates the catalytic water and it occupies the first Asp residue of the motif, while the second one coordinates the metal ion. Motif 2 (H(S/T)xxH) provides the two His residues which also participate in the coordination of the metal. Motif 3 (RpPxG) contributes a conserved Arg residue which coordinates the catalytic base and a strictly conserved Pro residue. The catalytic acid is a His residue which lies in motif 5 and is coordinated by an Asp residue provided by Motif 4. It has been proposed that the interaction between the His (motif 5)/Asp (motif 4) residues raises the pKa of His which is subsequently protonated at physiological pH. The His residue can then contribute this hydrogen to the amine leaving group of substrate to mediate the breakdown of the tetrahedral intermediate. The active site is completed with the presence of a water molecule, which coordinates the metal and is located in a position suitable to perform the nucleophilic attack. Fig. 10 represents the proposed catalytic mechanism of CE4 polysaccharide deacetylases.

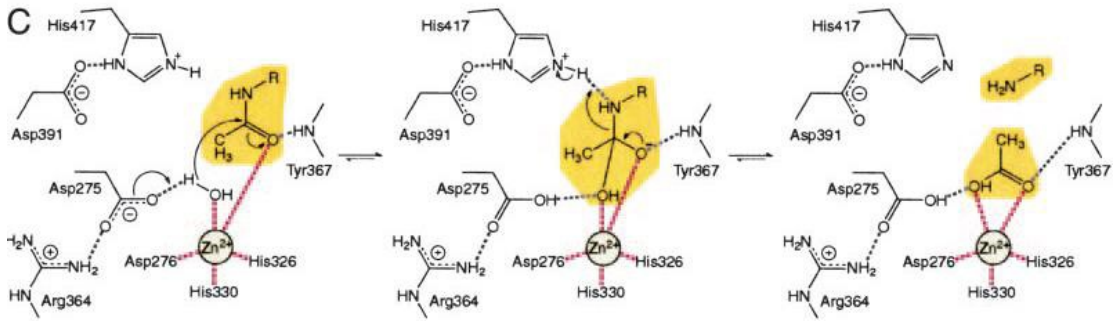

Figure 10: *Proposed catalytic mechanism for Carbohydrate Esterase Family 4 enzymes [114].*

It has been proposed that regulation of enzyme activity, substrate specificity and metal preference of CE4 family enzymes can be mediated through modifications of the five motifs. PgaB from *E. coli*, which is a β-1,6 *N*-acetylglucosamine exopolysaccharide deacetylase constitutes such a case. Although the active site contains the essential residues for catalysis, the Arg and His residues of motif 3 and motif 5 respectively, are provided by different parts of the structure. Furthermore, a water molecule is found in place of the conserved Asp residue of motif 4 which is believed to be responsible for activating the catalytic acid His [113]. According to Little *et al.* these alterations seem to provide an explanation for the reduced activity of the enzyme.

1.8 Bacterial Cell Shape

Cell shape is an important factor for the description and classification of bacterial species. Bacteria come in a variety of shapes: Cocci (e.g. *Streptococcus pneumoniae, Staphylococcus aureus*) are generally spherical or spheroid shaped; Bacilli (e.g. *Bacillus subtilis*, *Escherichia coli*) are rod shaped with hemispherical end-caps, while spirochetes (e.g. *Spiroplasma melliferum*) are named for their spiral shapes [117].

Bacteria derive and maintain a variety of shapes that carry selective benefits. For example, motile bacteria usually have rod-like shapes and are less likely to be spherical than non-motile bacteria [118]. It has been demonstrated that a rod shape increases swimming efficiency and dramatically facilitates the temporal sensing of chemical gradients, a common mechanism of chemotaxis among motile bacteria [119]. Furthermore, cell shape may also be beneficial to bacteria which colonize and form biofilms. A study observing cells colonizing in a small chamber indicated that the rod shape helps cells to self-organize into an ordered super-structure that increases nutrient access and waste evacuation efficiencies [120]. An additional, equally important selective pressure is competition for nutrients, which can be optimized by increasing the surface area relative to total cell volume. Apart from selective pressure, physical constrains are also accountable for the bacterial morphological diversity [121]. One important physical constraint is turgor pressure, which can lead to swelling

and lysis of the cells. Because of lower water activity in the cytoplasm relatively to the extracellular environment, bacteria function as essentially pressure vessels, and the cell wall must be oriented to provide sufficient strength to counteract turgor forces of several hundred kilopascals in Gram-negative bacteria and as high as three megapascals in Gram-positive bacteria [122]. For a long time the selective and physical forces mentioned above were thought to determine bacterial shape. Further studies proved that this assumption was not accurate.

Bacterial shapes are usually defined by a mechanically stiff exoskeletal cell wall, the macromolecular network of peptidoglycan, whose structure has been previously described. The growth of such a network is catalyzed by transglycosylases, which link a disaccharide precursor to an existing glycan strand by another β-1,4 glycosidic bond and transpeptidases, which form peptide cross-bridges between the pentapeptides and link the glycan strands together. Additionally, various cell-wall remodeling enzymes further digest and modify the peptidoglycan network. The main enzyme families which participate in the synthesis and processing of peptidoglycan are presented in Figure 11.

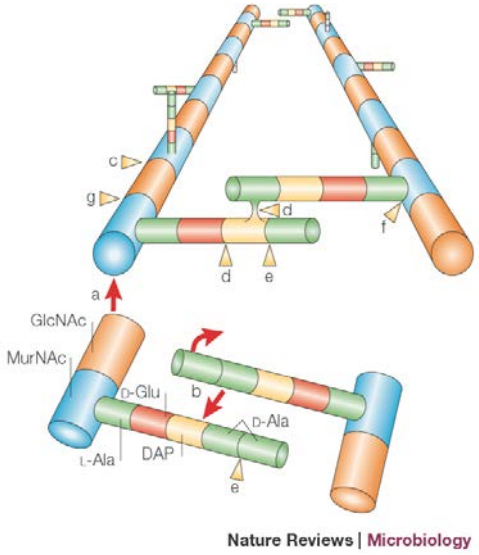

Figure 11: *Chemistry of peptidoglycan synthesis and processing [117].*

Red arrows indicate synthetic reactions and yellow arrowheads indicate hydrolytic activities. a, transglycosylase activity; b, transpeptidase activity, resulting in the loss of the terminal D-alanine on

one of the pentapeptides; c, lytic transglycosylase activity; d, endopeptidase activity; e, carboxypeptidase activity; f, amidase activity; g, N-acetylglucosaminidase activity.

The main function of the peptidoglycan layer is to maintain the cell shape and rigidity and subsequent changes will obviously affect cell morphology [117]. Yet, since peptidoglycan is highly flexible, shape determination is affected by other factors [123].

The two mechanisms known to govern bacterial morphology are cell elongation and cell division. The recently discovered bacterial cytoskeleton plays the most important role during these two cellular processes. Bacteria have homologues of all three kinds of eukaryotic cytoskeletal proteins: the actin homologue MreB, the microtubule homologue FtsZ, and the intermediate filament homologue CreS [124].

1.8.1 Cell Elongation

MreB, the actin homologue in bacteria, is required for cells to grow as rods, since naturally spherical bacteria do not encode the *mreB* gene [125]. MreB associates with many cell wall synthesis enzymes, allowing the insertion of new peptidoglycan building units into the existing peptidoglycan layer. Although previous studies had shown that MreB formed helical-like cables beneath the cytoplasmic membrane [126], recent studies proved that in *B. subtilis* neither MreB nor its two paralogs in this bacterium, MreBH and Mbl, form a long-range continuous helix [127,128]. Garner *et al.* [127] used total internal reflection fluorescence microscopy (TIRFM) to track dynamics of individual particles on the cell surface. When the same three MreB paralogs along with the peptidoglycan elongation machinery components MreC, MreD and Pbp2A were tracked, all six proteins moved with approximately equal speeds (20–30 nm per second) in linear, non-helical paths across the cell width, suggesting that they function together as a macromolecular unit. Particle tracking also confirmed that these units which are randomly distributed throughout the cell length, are independent from each other, discontinuous, and can reverse direction. The likely result of this type of movement is that new peptidoglycan is sewn together in circumferential hoops [129]. Proteins which complement the elongation machinery,

along with MreC, MreD and the peptidoglycan transpeptidase Pbp2A, are RodA and Pbp1.

1.8.2 Cell Division

The central player of cell division is the GTP-binding tubulin homolog FtsZ, which polymerizes at the site of division into a ring-like structure, the Z ring, and drives the assembly of the divisome, a multicomponent complex that mediates constriction of the division ring and subsequent cytokinesis [130]. During cell division the Z ring assembles and constricts at the division site, directing the peptidoglycan synthesis that is required for formation of the new poles [131]. Thus the role of FtsZ at the division sites implicates it as a shape determinant, as cell size is determined by cell division [117]. Precise localization of FtsZ also plays a crucial role for proper cell shape formation. Polymerization and placement of FtsZ is mediated by the MinCDE proteins, which have an inhibitory effect on Z-ring formation at the poles, and by the positions of chromosomes, which confine Z-ring formation to nucleoid free areas of the cell [132,133]. Therefore, interfering with either of these two regulatory mechanisms may alter cell shape indirectly by mislocalizing Z rings. Both cell elongation and cell division machineries are demonstrated in Figure 12.

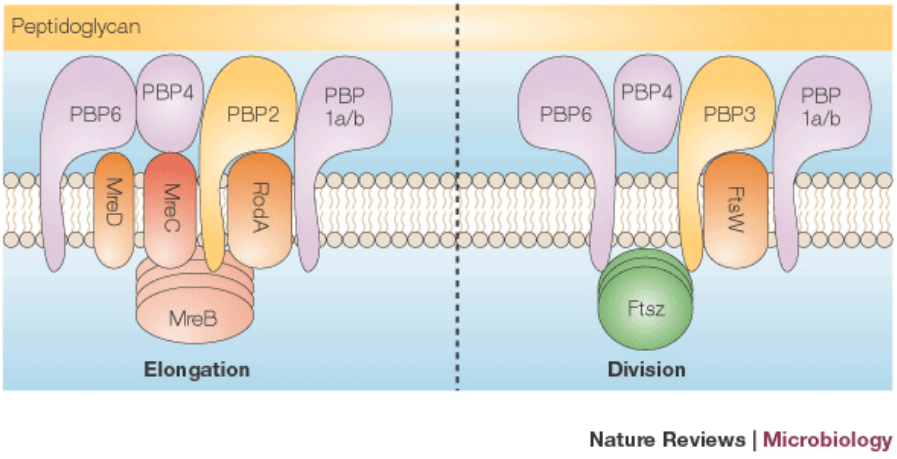

Figure 12: *Proposed models for cell elongation and cell division machineries [117].*

Noteworthy, mutant strains of several gene deletions, such as penicillin-binding proteins [134,135], exhibit phenotypes with aberrant cell shapes, so it is highly likely that other proteins can also participate either in cell shape determination or in cell shape maintenance.

1.9 Fibronectin Type III (Fn3) Domain

Fibronectin type III (Fn3) domain in higher organisms is found in extracellular matrix proteins like fibronectins, where it was initially identified, and tenascins as well as in cell surface adhesion molecules like neuroligins. In animal proteins it is a common module, occurring approximately in 2% of known sequences [136] and has a distinctive motif of a seven-stranded β sandwich similar to the immunoglobulin fold [137,138]. Despite remarkably similar tertiary structures Fn3 modules share low sequence homology with sequence identity being typically less than 20%. Furthermore, it has been shown that the Fn3 module in the fibronectin protein under specific conditions of pH and ionic strength can form dimers [139] while is also able to undertake mechanical stresses which expose cryptic self-assembly sites [140].

The first report of a bacterial protein incorporating two Fn3 domains in its structure was reported in 1990 for chitinase A1 from *Bacillus circulans* [141] and initially led to the assumption that this module must have been present in a common ancestor of prokaryotes and eukaryotes. Later studies revealed that the bacterial occurrences of Fn3 are likely the result of a single gene having been acquired from an animal source long after the divergence of prokaryotes and eukaryotes [136,142]. The bacterial distribution of the module is so far restricted to extracellular depolymerases (glycosylhydrolases) of soil bacteria as for example galacturonidases, cellulases, chitinases and amylases. This is consistent with the sporadic presence of the domain in bacterial proteins. In every case studied so far homologous proteins have been found that lack this domain. This is why for a great

number of bacterial glycosylhydrolases it is believed that the function of Fn3-like domains must be accessory and not essential [143].

The Fn3 module is a stable and convenient fold, used in different ways to provide both an adaptable functional space and a spacer. It is believed that bacterial enzymes employ the versatile binding functions of Fn3 to facilitate binding to the substrate. They might function as ligand-binding modules, simple or extendable spacers between domains or as proteins that help large enzyme complexes to remain soluble. It has been proposed that the domain is able to bind cellulosome and/or polysaccharides directly [143]. Penicillin-binding transpeptidases and chitinases are two examples of well studied bacterial family enzymes where the Fn3 domains have been sporadically found in some of their members. In penicillin-binding transpeptidases which cross link peptide chains from different glycan strands of peptidoglycan, the Fn3 domain is responsible for the proper orientation of the catalytic domain of the enzyme towards the substrate [134,144,145]. Similarly, it has been proposed that in chitinase A from *Serratia marcescens* and *Alteromonas sp.* strain O-7 the Fn3 domain interacts with the substrate and subsequently directs it towards the active site of the catalytic domain. It has been shown that a group of surface exposed tryptophans, with a subgroup of them belonging to the Fn3 domain mediates the interaction with crystalline chitin [146-148]. However, in the case of CtCel9D-Cel44A endoglucanase from *Clostridium thermocellum* this domain does not contribute to carbohydrate recognition and it has been proposed that it might function as a non-flexible spacer [149].

1.10. Inactive enzyme homologues

Over the past two decades large-scale sequencing of genomes revealed that most enzyme families contain catalytically inactive enzyme homologues. Although in the past the occurrence of inactive proteins which included evolutionary remnants of active enzymes was considered the exception, it seems that in fact they are the rule [150,151]. Unlike pseudogenes, which are non functional gene relatives that have lost their ability to express a functional protein, genes coding for inactive enzyme homologues retain the properties of being functional and able to express functional

proteins which however have lost their catalytic activity. These pseudoenzymes are well conserved, implying a selective pressure to keep them during evolution and to maintain their function [152]. Almost every enzyme family includes seemingly inactive members, and in some clans, such as the sulfotransferases that swap sulfate groups, more than half of the proteins encoded by our genome show signs of being catalytically compromised [151]. Pseudoenzymes have proven over the years to play very important biological roles, since some facilitate active enzymes to catalyze biochemical reactions by forcing them into the correct shape, while others provide platforms for protein-protein interactions. Moreover others join with receptors to help cells communicate, serve as bodyguards that escort proteins to new locations, or perform other tasks [153].

The first example of a non-catalytic relative of an enzyme was recognized in 1967, when the partial sequence of bovine α-lactalbumin was found to share about 35% sequence identity with chicken lysozyme [154]. Interestingly both proteins are involved in processing β-1,4-sugar linkages but with different outcomes and in different contexts. Hill *et al.* stated that this similarity could be due to convergent evolution, which is the independent acquisition of similar biological characteristics by unrelated phylogenetic lineages, or due to divergent evolution, whereby the acquisition of related biological characteristics emanates from diversification of a common ancestor, and argued that the latter had taken place. They also argued that similarity alone is not sufficient to prove a common ancestor and that gene duplication followed by diversification is a common route to pairs of enzymes and inactive cognates. Finally, they stated that the structural and functional legacy of enzymatic precursors is usually retained in the dead counterparts of active enzymes [154]. Since 1967, when the above study has been conducted, researchers have proposed two evolutionary explanations for the occurrence of dead enzymes, both of which involve a gene duplication event at some time in the past. The most common route for the production of a dead enzyme is the insertion of mutations which disrupt the active site of one of the two copies of the original and the duplicated gene, leading to the birth of a pseudoenzyme. Alternatively, the psudoenzyme preexisted its active counterpart, when its gene duplicated. Mutations then conferred catalytic ability on one of the versions, producing an active enzyme [153].

It is estimated that at least 10% of mammalian catalytic domains are predicted to be inactive, and the estimate for worms and flies increases to 15%.[151]. This abundance of dead cognates is also mirrored within individual enzyme classes. For example, 10% of mammalian kinases are predicted to be inactive [155] and this ratio rises to 16% for human proteases [150], and for *Drosophila melanogaster* serine proteases the percentage may be as high as 30% [156]. There is increasing annotation of these inactive homologues available; for example, individual protease families are categorized in the MEROPS and Degradome databases [157]. Important examples of inactive homologues include, among many others, proteins related to proteases, kinases, phosphatases, E2 ubiquitin-conjugating enzymes and phospholipases.

As mentioned above, most catalytically inactive enzyme homologues have lost their enzymatic properties due to mutations of critical residues that compromised their catalytic ability. However, one should always keep in mind that particularly for distantly related proteins, the substitution of critical residues may present an oversimplified picture of the basis of loss of activity and focusing on these alone may even be inappropriate. Even small conformational effects of residues distributed throughout the fold play a role in shaping the active site for complementarity and efficient catalysis [158]. Moreover a few dead enzymes owe their loss of activity, at least in part, to the disruption of the substrate binding site or the steric block of the active site cleft. For example the TIM barrel glycosyl hydrolase-like protein narbonin lacks catalytic activity, although the Glu general acid of catalytic family members is conserved. In narbonin this Glu is incorporated in a salt bridge with a spatially adjacent Arg residue, rendering the active site inaccessible to the oligosaccharides bound by its homologs [159,160].

Inactive enzymes no longer represent a small number of slightly off-beat cases, instead it seems that most enzyme families have dead relatives. Even though rather few have been studied in detail, they have been demonstrated to have important functions. In order to determine whether a putative enzyme actually performs its predicted catalytic function, one should not only rely on amino acid sequence, which can provide indication but not confirmation if a protein is not active. Further studies such as 3D structure determination and biochemical analysis are essential in order to decide if a protein is enzymatically compromised, and even then the evidence are not always decisive. The group of pseudokinases is a characteristic example of the

difficulty of identifying pseudoenzymes. According to bioinformatics prediction 10% of the kinome were thought to be pseydokinases, while later 3D structure studies revealed that in the case of WNK1, a predicted pseudokinase, although the essential key Lys residue was missing from the VAIKmotif (found in subdomain II of the kinase domain), this was structurally compensated for by a Lys residue present in the neighbouring subdomain I [161]. Similar examples of apparent pseudokinases displaying the capacity for phosphoryl transfer have been also reported for CASK [162], IRAK2 [163] and HER3 [164],leading to the conclusion that the originally estimated 10% was an overestimation.

1.11 Adaptation of bacteria to osmotic stress

Bacteria are surrounded by an ever changing external environment, where they may come across an increase or decrease of the osmotic strength and subject the cells to osmotic stress. Changes in the external osmolality trigger water fluxes along the osmotic gradient causing either swelling (and eventually cell lysis) in hypotonic environments or considerable shrinkage of the cytoplasmic volume resulting in plasmolysis under hypertonic environments. If hyperosmotic shock is not severe, plasmolysis is transient, and after some time the cytoplasmic volume will increase as a result of osmotic adjustment by the cells [165].

Bacteria have evolved two different strategies in order to cope with elevated osmolarity: a. the salt in cytoplasm type and b. the organic osmolyte type.

1.11.1 Salt in cytoplasm

This kind of adaptation is common for members of the *Halobacteriaceae* family, which includes bacteria that have a specific requirement for sodium and grow optimally at high salinity [166] and its application is strictly limited to environments of elevated osmolarity. In order to achieve salt tolerance their proteins undergo massive amino acid substitutions, such as enrichment in aspartyl, glutamyl, and weakly hydrophobic residues [167]. These alterations emerge from their need to maintain a hydration coat in an exterior environment of low water activity. According

to Zaccai *et al.* [168] the stabilization of halophilic proteins is achieved through the enzyme's tertiary or quaternary structure, which coordinates hydrated salt at a local concentration higher than that in the solvent. Therefore, the core of the protein is similar to its non-halophilic counterpart, but with loops extending outwards interacting with water and providing a large interface with the solvent [169]. This strategy has an overall impact on structure stabilization of proteins by employing tight folded conformation and strong hydrophobic interactions [170].

1.11.2 Organic osmolyte

A compatible solute or osmolyte is a small organic molecule that accumulates in cells and protects cellular components against denaturing environmental stresses [171]. Its dramatic concentration increase in the cytoplasm represents the secondary response towards elevated environmental osmolarity, following the increased levels of K^+ and its counter-ion glutamate. In general, compatible solutes are highly soluble molecules which carry no net charge at physiological pH and do not interact with proteins. In addition to their role as osmotic balancers, compatible solutes function as effective stabilizers of enzyme function, providing protection against salinity, high temperature, freeze-thaw treatment and even drying [172]. The use of only a small number of compounds as compatible solutes reflects fundamental constraints on the kind of solutes that are compatible with macromolecular and cellular function [173]. Compatible solutes are considered to have a general stabilizing effect thus avoiding the unfolding/denaturation of proteins and other labile macromolecular structures [174,175], complementary to restoring cell volume.

Bacterial cells which use compatible solutes for salt adaptation have the advantage that no great adjustments are required in the enzymatic machinery, as the cytoplasmic conditions are kept intact due to the accumulation of compatible solutes. Nevertheless the cell surface has to undergo severe changes in order to adapt to high salt concentrations, such as altered cytoplasmic membrane, adjusted cell wall properties and impaired swarming capability [176]. Furthermore, cross-linking of the peptidoglycan layer seems to adjust according to variations in the salinity stress, since NaCl challenged cells exhibited shorter peptidoglycan peptide bridges than the unstressed cells [177]

2. MATERIALS AND METHODS

2.1 MATERIALS

Primers were synthesized by the Microchemistry Facility of the Institute of Molecular Biology and Biotechnology, FORTH (Table 1). The strains and plasmids used in this study are listed in Table 2. All chromatographic materials were from Amersham Biosciences. PCR and gel extraction kits were from Qiagen and plasmid purification kit from Macherey Nagel GmbH. Substrates and common reagents were purchased from Sigma-Aldrich, Seikagaku Corporation and Merck. Fluorescamine and Brain-heart infusion (BHI) were purchased from Sigma- Aldrich. Anti-GFP rabbit serum (polyclonal antibody) was purchased from Molecular Probes.

Table 1: List of oligonucleotides used in the present study.

oligonucleotides	Sequence (5'→3')	Source or reference
Construction of *B. anthracis* mutants		
SPC-H^{+1c}	TTTTAGTTGACTTCATTTATATTTTCCTCCTTAGCCTAATTGAGAGAAGTTTCTAT	[79]
SPC-H^{+2c}	TTTTAGTTGACTCATTTATATTTTCCTCCTTAGCCTAATTGAGAGAAGTTTCTAT	[79]
SPC-H^{+3c}	TTTTAGTTGACCATTTATATTTTCCTCCTTAGCCTAATTGAGAGAAGTTTCTAT	[79]
ba0330up5	AAATGAGATAGACAAACCAA	this study
ba0330up3	TCCCCCGGGACGCCAAATTTTATATTGTA	this study
ba0331up5	TCGTTTGTTCGTTATTAACA	this study
ba0331up3	TCCCCCGGGGTAATAACTCCTTGCGTTAA	this study
ba0330/0331up5	AAATGAGATAGACAAACCAA	this study
ba0330/0331up3	TCCCCCGGGGTAATAACTCCTTGCGTTAA	this study
ba0330down5	TCCCCCGGGGCATACACCATACGACGA	this study
ba0330down3	TGTTACCTGCAAATGCTAAC	this study

ba0331down5	TCCCCCGGGTGAGTTCGCAGTAACTACT	this study
ba0331down3	TCCTTCAGCATCAACATTAT	this study
ba0330/0331down5	TCCCCCGGGGCATACACCATACGACGA	this study
ba0330/0331down3	TCCTTCAGCATCAACATTAT	this study
PR-5	AATTGGGCCCGACGTCGCATG	this study
PR-3	GAGCTCTCCCATATGGTCGAC	this study
Spec-40	GGAGAGTGTGATGATAAGTGGG	[178]
Spec-30	CGCTGTTAATGCGTAAACCACC	[178]
Construction of *gfp*-fusions		
gfpmut1frw	CATGCATGCATGAGTAAAGGAGAAGAACT	this study
gfpmut1rev	GAAGATCTCTATTTGTATAGTTCATCCAT	this study
ba0330frw	GGGGTACCATGAGAAAATACGCAGCAAT	this study
ba0330rev	CATGCATGCGGCCCGGGCCCGTTTAATCGAAGAAGCAAATTG	this study
ba0331frw	GGGGTACCATGAAAAAGTATACATATATCG	this study
ba0331rev	CATGCATGCGGCCCGGGCCCGCTTTATAAGAGATATGAATTTTT	this study
Cloning for complementation		

ba0330frw	GGGGTACCATGAGAAAATACGCAGCAAT	this study
ba0330rev	GAAGATCTTTATTTAATCGAAGAAGCAAAT	this study
ba0331frw	GGGGTACCATGAAAAAGTATACATATATCG	this study
ba0331rev	GAAGATCTTTACTTTATAAGAGATATGAATT	this study
Cloning for expression		
bα0330frw	ATGAGCAATGTAAGCCAGG	this study
bα0330rev	CCGCTCGAGTTATTTAATCGAAGAAGCAAATT	this study
bα0331frw	ATGAGTGATAAACAAATAC	this study
bα0331rev	CCGCTCGAGTTACTTTATAAGAGATATGAA	this study

Cloning for site-directed mutagenesis	(engineered codons are underlined)	
ba0330D205Afrw	TTTGTTACATTTGCTGATGGTATGAAAAATAATATG	this study
ba0330D205Arev	CATATTATTTTTCATACCATCAGCAAATGTAACAAA	this study
ba0331D212Afrw	TTCATAACAATGGCTGATGGTCGAAAAAATAATATG	this study
ba0331D212Arev	CATATTATTTTTTCGACCATCAGCCATTGTTATGAA	this study

Table 2: Strains and Plasmids used in this study.

Strains, plasmids	Description	Source or Reference
Strains		
E. coli		
DH5α	*F– Φ80lacZΔM15 Δ(lacZYA-argF) U169 recA1 endA1* *hsdR17 (rK–, mK+) phoA supE44 λ– thi-1 gyrA96 relA1*	Novagen
BL21 DE3 (pLYS)	*F^- ompT gal dcm lon $hsdS_B(r_B^- m_B^-)$ λ(DE3) pLysS(cm^R)*	Novagen
GM48	*thr-1*, *araC14*, *leuB6*(Am), *fhuA31*, *lacY1*, *tsx-78*, *glnX44*(AS), *galK2*(Oc), *galT22*, *$λ^-$*, *dcm-6*, *dam-3*, *thiE1*	Coli Genetic Stock Center (CGSC)
B. anthracis		
UM23C1-2	pXO1- pXO2- Ura- Rifr	[179]
Plasmids		
pGEM T-easy	cloning vector	Promega

pUTE583	cloning vector	[180]
pREST A	cloning vector	Novagen
pHW1520	cloning vector	Mobitec
pNF8	pAT18Ω (PdltΩgfp-mut1)	[181]
pSPCH+1 +2 +3	pUC19 carring a non-polar mutagenic SpcR cassette	[79]

2.2 METHODS

2.2.1 Cloning and expression of ba0330 and ba0331 genes of B. anthracis into pRSET A expression vector

The genes were amplified from genomic DNA of *B. anthracis* UM23C1-2 using DNA polymerase chain reaction. Primers were synthesized in order to exclude the signal peptide (1-23 amino acids) and to incorporate a blunt end at the start and an XhoI site at the end of *ba0330* and *ba0331* genes. The amplified genes were purified, digested with the corresponding enzymes and ligated into pRSET A vector. The resulting products were in-frame, non-His6 tag-fused constructs in pRSET A for *ba0330* and *ba0331* genes, placing the polysaccharide deacetylase genes under the transcriptional control of the T7 lac promoter. The two constructs were transformed into BL21(DE3) (pLys) *E. coli* strains. Twenty millilitres of saturated culture of each of the transformed deacetylase expression strains were inoculated into 1l of Luria-Bertani (LB) medium containing 100 μg ml^{-1} ampicillin and 34 μg ml^{-1} chloramphenicol as antibiotics and incubated at 37 °C on a shaker incubator to an OD_{600} of 0.6. BA0330 *E. coli* culture was transferred to 20 °C after addition of 0.5 mM isopropyl-β-D-thiogalactoside (IPTG) and BA0331 *E. coli* culture was transferred to 30 °C after addition of 0.5 mM IPTG.

2.2.2 Purification of recombinant BA0330 and BA0331

BA0330: Cells were harvested by centrifugation and resuspended in 50 mM Tris-Cl buffer, pH 7.6, 300 mM NaCl, 1 mM dithiothreitol and 0.3 mg ml^{-1} lysozyme. After 150 min incubation at 4 °C suspension was centrifuged, soluble fractions were collected and loaded onto a SP Sepharose Fast Flow adsorbent equilibrated with 50 mM HEPES-NaOH pH 6.8. Proteins were eluted using a step gradient of NaCl (500 mM). Fractions containing BA0330 were collected and loaded onto a Sephacryl S-200 HR column equilibrated with 50 mM Tris/HCl pH 7.6, 300

mM NaCl. Fractions containing BA0330 were collected, concentrated and stored at 4 °C.

BA0331: Cells were harvested by centrifugation and resuspended in 50 mM Tris-Cl buffer, pH 7.6, 300 mM NaCl, 1 mM dithiothreitol and 0.3 mg ml^{-1} lysozyme. After 150 min incubation at 4°C suspension was centrifuged, soluble fractions were collected and loaded onto a Source Q HR adsorbent equilibrated with 20 mM Tris/HCl pH 8.5. Proteins were eluted using a step gradient of NaCl (300 mM). Fractions containing BA0331 were collected and loaded onto a Sephacryl S-200 HR column equilibrated with 50 mM Tris/HCl pH 7.6, 300 mM NaCl. Fractions containing BA0331 were collected, concentrated and stored at 4 °C.

2.2.3 Preparation of radiolabelled substrate

Labeling of glycol chitin was performed using [^{3}H] acetic anhydride according to Araki *et al*., 1980 [182].

2.2.4 Enzyme assays

Enzyme assays were performed at a wide pH range and in the presence/absence of the divalent cations Co^{+2}, Zn^{+2}, Mn^{+2}, Mg^{+2}, Ni^{+2} and Cu^{+2}.

We have employed two different assays for determining polysaccharide deacetylase activity:

i. A radiometric assay: deacetylase activity was estimated using as substrate partially *O*-hydroxyethylated chitin (glycol chitin) [182].

ii. An assay based on fluorogenic labelling with fluorescamine, which labels the free amines generated by the enzymatic deacetylation of *N*-acetylchitooligosaccharides. This allowed miniaturization of the assay to 50 µl volumes suitable for a 96-well format [114]. All measurements were performed in triplicates.

2.2.5 Construction of B. anthracis *Δba0330*, *Δba0331* and *Δba0330/0331* mutants, complemented strains and gfp fusions

DNA fragments containing the sequence upstream and downstream of *ba0330*, *ba0331and ba0330/0331* were generated by PCR using the appropriate oligonucleotides (Table 1). Each fragment was cloned into pGEM vector. The constructs were then digested with SmaI/PstI in order to ligate the upstream and downstream fragments of each gene in the same plasmid. The proper cassettes that give resistance to spectinomycin (Spc) [183] from pSPCH+1, +2, +3 were incorporated in frame between the upstream and downstream fragments of each gene [79]. After digestion, the whole construction (upstream fragment – Spc cassette – downstream fragment) was ligated into the shuttle vector pUTE538 [180] and the construct was passaged through *E. coli* GM48 (*dam*$^-$) to obtain nonmethylated plasmid DNA for electroporation into *B. anthracis*. To isolate a double-crossover recombinant Spc-resistant strain, transformants were grown in BHI medium with Spc for 2 days, diluted 1:1,000 every 12 h, and then shifted to BHI medium without antibiotic to facilitate clearance of autonomous plasmids. The culture was diluted 1:1,000 in fresh medium every 12 h for several days and then plated onto BHI agar with Spc. Colonies were patch plated to score clones for Spc resistance and erythromycin (Em) sensitivity. *Δba0330*, *Δba0331* and *Δba0330/Δba0331* in *B. anthracis* were also confirmed by PCR amplification.

Complemention studies were carried out as follows: The genes were amplified from genomic DNA of *B. anthracis* UM23C1-2 using DNA polymerase chain reaction. Primers were synthesized to incorporate a KpnI site at the start and a BglII site at the end of *ba0330* and *ba0331* genes. The amplified genes were purified, digested with the corresponding enzymes and ligated into pWH1520 vector [184], placing the two genes under a xylose-inducible promoter. The constructs were passaged through *E. coli* GM48 (*dam*$^-$) to obtain nonmethylated plasmid DNA and electroporated into *B. anthracis*. BHI medium was inoculated from overnight cultures to an OD_{600} of 0.05 and incubated at 37 °C on a shaker incubator to an A_{600} of 0.6, where induction was achieved with 0,1% xylose (for expression from the xylose-inducible promoter).

To construct strains expressing Gfp translational fusions, the *gfp-mut1* gene was amplified from pNF8 [181] with specific primers, digested with SphI and BglII and ligated into the xylose-inducible plasmid pWH1520. Then, each gene (lacking the stop codon) was amplified from *B. anthracis* UM23C1-2 chromosomal DNA with the appropriate primers in order to incorporate at the C-terminal the polylinker GPGP. The amplicon was digested with KpnI and SphI and ligated in frame to the 5′ end of *gfp-mut1*. *B. anthracis* cells were then transformed with the resulting plasmids via electroporation, after initially being passaged through *E. coli* GM48 (*dam*$^-$) to obtain nonmethylated plasmid DNA. 10ml of BHI medium were inoculated from overnight cultures to an OD_{600} nm of 0.05 and incubated at 37 °C with shaking to an OD_{600} of 0.6, where induction was achieved with 0,1% xylose (final concentration).

2.2.6 Peptidoglycan and neutral polysaccharide purification

Peptidoglycan from parental *B. anthracis* UM23C1-2 and mutants was prepared from exponentially and stationary phase growing bacteria and purified as previously described [185]. Muropeptides from the native peptidoglycan were generated using the muramidase cellosyl, separated by HPLC, purified and analysed by mass spectrometry as previously described [185]. Neutral polysaccharide was extracted and purified from cell walls as described by Ekwunife *et al*. [74].

2.2.7 Autolysis assay

Ten ml of cultures in SPY [186] medium of the parental and the mutant strains at an OD_{600} of 0.5 were centrifuged and the bacterial pellet was concentrated 10 times in SPY medium devoid of sucrose to which 10 mM NaN3 was added (final concentration). The decrease in optical density of each culture was monitored for 240 min taking samples every 30 min.

2.2.8 Fluorescence microscopy of vegetative cells

Bacillus anthracis cultures of the parental and mutant strains were inoculated from fresh overnight plates to an initial OD_{600} of 0.1 and grown to stationary phase as liquid cultures in SPY medium. Cells were examined by fluorescence microscopy and the images were obtained without fixation on an inverted epifluorescence microscope Nikon E800.

2.2.9 Western blotting analysis

Bacterial cell lysates during the time points at which GFP fluorescence signal was obtained were separated by SDS-PAGE, blotted, and probed with the following antibodies: polyclonal rabbit anti-GFP primary antibody diluted 1:5000 and polyclonal goat anti-rabbit IgG horseradish peroxidase secondary antibody diluted 1:50 000.

2.2.10 Transmission Electron Microscopy

For transmission electron microscopy (TEM), vegetative and stationary cells were initially fixed with glutaraldehyde 2.5% in cacodylate buffer 0.1 M pH 7 and post-fixed in 1% osmium tetroxide in water. Samples were pelleted and embedded in low melting point 2% agar. Blocks of agar containing samples were transferred in 0.5% uranyl acetate/H_2O and then dehydrated through a series of ethanol washes. Finally, samples were embedded in epoxy resin. Blocks were then sectioned in an ultramicrotome LKB, Bromma 2088, and poststained in uranyl acetate and lead citrate. TEM analysis processed with a JEOL, JEM 2100 Transmission Electron Microscope, operated at 80KV.

2.2 11 Scanning Electron Microscopy

For scanning electron microscopy (SEM), samples were fixed in 2% glutaraldehyde, 2% paraformaldehyde (PFA) in 0.1 M sodium cacodylate buffer, pH 7.4, overnight at 4 °C, washed in the same buffer and dehydrated twice through a graded series of ethanol, 30%-50%-70%-90%-100% at 4 °C and dry ethanol (100%) at room temperature . Dehydrated samples were then dried using (Bal-Tec CPD 030) and mounted on appropriate stubs prior to sputter coating with 20 nm thickness gold/palladium Sputter Coater (Bal-Tec SCD 050). Samples were examined using a JEOL JSM-6390LV Scanning Electron Microscope, operating at 15 KV-20KV.

2.2.12 In vitro determination of lysozyme resistance

In order to test the sensitivity of the mutants in the presence of exogenous added lysozyme, overnight cultures of the parental and mutant strains were diluted to an OD_{600} of 0.1 in 1L of fresh SPY medium. The cultures were incubated at 37 ºC until an OD_{600} of 1.0. Then, each culture was divided in two equal parts of 500 ml and 10 μg ml^{-1} hen egg lysozyme was added at one of the two subcultures. The growth of both treated and untreated subcultures was monitored.

2.2.13 Salt stress adaptation

To study the effects of exposure to mild (2.5% and 3.5%) and severe (4.5%) salt stress on the growth of *B. anthracis* UM23C1-2 and mutant strains, stationary-phase cultures were diluted 1:100 (v/v) in flasks containing 50 ml fresh BHI broth and incubated at 37 °C with shaking at 200 rpm. When an optical density at OD_{600} of 0.6

was reached, BHI broth supplemented with 2.5%, 3.5%, and 4.5% (w/v) NaCl (final supplementary concentrations) was inoculated at a starting OD_{600} of 0.01. The cultures were incubated further at 37 °C with shaking at 200 rpm and growth was monitored for 9 hours. To study the effects of exposure of severe salt stress on the growth of several mutant strains of *B. anthracis*, stationary-phase cultures were diluted 1:100 (v/v) in flasks containing 50 ml fresh BHI broth and incubated at 37 °C with shaking at 200 rpm. When OD_{600} of 0.6 was reached, strains were plated on BHI solid medium containing 4.5% (w/v) NaCl (final supplementary concentration) and further incubated at 37 °C.

2.2.14 Peptidoglycan binding assay

Purified peptidoglycan (100 μg) from *B. anthracis* was incubated with purified BA0330 and BA0331 (30 μg) in 20 mM Tris-HCl (pH 8.0) in a final volume of 90 μl for 30 min at 4 ^{o}C with agitation. The suspension was centrifuged for 10 min at 15,000 g and the supernatant (soluble fraction) was kept for further analysis. The pellet was washed twice with 250 μl buffer and suspended in 90 μl of buffer (insoluble fraction). Unbound proteins in the soluble fractions and bound proteins in the insoluble fractions were analyzed by SDS-PAGE.

2.2.15 Site-directed mutagenesis of BA0330 and BA0331

Mutants were constructed using a two-step ⁄ four-primer overlap extension PCR method [187]. The amplified products were sub-cloned into the pWH1520 vector and mutant cells were transformed and examined by TEM.

3. RESULTS

3.1 Computational analysis

The genome of *B. anthracis* Ames sequence database (Genbank accession number AE016879) reveals 11 coding sequences for putative polysaccharide deacetylases of family CE4 which are listed in Table 3. Ten of them exhibit more than 90% sequence identity to their homologues from *B. cereus sensu stricto*.

Table 3: The putative polysaccharide deacetylases coding sequences from *B. cereus* and *B. anthracis*.

B. cereus **ATCC 14579**	***B. anthracis*** **str Ames**	**Possible function**	**Identity**	**Similarity**
NP_831730 (275) (BC1960)	NP_844369 (275) (BA1961)	Peptidoglycan GlcNAc deacetylase	94	97
NP_833348 (213) (BC3618)	NP_845942 (213) (BA3679)	Peptidoglycan GlcNAc deacetylase	97	100
NP_832677 (275) (BC2929)	NP_845280 (275) (BA2944)	Peptidoglycan GlcNAc deacetylase	94	97
NP_834868 (245) (BC5204)	NP_847604 (245) (BA5436)	Peptidoglycan GlcNAc deacetylase	93	96
NP_831744 (273) (BC1974)	NP_844383 (273) (BA1977)	Peptidoglycan GlcNAc deacetylase	98	99
NP_830306 (260) (BC0467)	NP_842967 (273) (BA0424)	Peptidoglycan MurNAc deacetylase	98	99
NP_830050 (254) (BC0171)	NP_842717 (254) (BA150)	Chitooligosaccharide deacetylase	95	99

NP_831543 (234) (BC1768)	NP_844255 (234) (BA1836)	Chitooligosaccharide deacetylase	92	96
NP_833526 (299) (BC3804)	NP_846187 (299) (BA3943)	Chitooligosaccharide deacetylase	95	97
NP_830200 (360) (BC0361)	NP_842877 (360) (BA0330)	Polysaccharide deacetylase	91	94
NP_830200 (360) (BC0361)	NP_842878 (367) (BA0331)	Polysaccharide deacetylase	53	69

For two of them, BA0330 and BA0331, the programs SignalP and TatP (http://www.cbs.dtu.dk/services/) predicted a signal peptide for targeting to the Sec translocation pathway. The LocateP program (http://www.cmbi.ru.nl/locatep-db/cgibin/locatepdb.py) predicted them to be *N*-terminally anchored membrane proteins with a characteristic lipobox consensus sequence [LVI][ASTVI][GAS][C], which is the hallmark for lipid modification of proteins in bacteria. In BA0330 and BA0331 Cys[19] is the lipid-modified cysteine residue as demonstrated in Figure 13A. *ba0330* and *ba0331* reside in an operon with *ba0329*, a putative aminopeptidase encoding gene and *ba0332*, a NupC-like nucleoside transporter encoding gene (Fig. 13B).

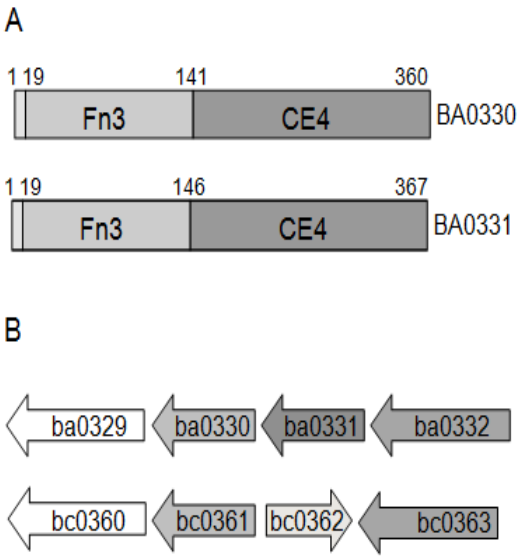

Figure 13: (A**)** *Schematic representation of BA0330 and BA0331 domains.* **(**B**)** *Gene organization of putative polysaccharide deacetylases genes ba0330, ba0331 and bc0361 in the genomes of B. anthracis UM23C1-2 and B.cereus ATCC 14579. These genes are flanked by the putative aminopeptidase genes ba0329 and ba0360, and NupC-like nucleoside transporters ba0332 and bc0363. Arrows indicate open*
reading frames. Homologous genes are indicated with the same colour.

Although this cluster of genes is highly conserved among *B. anthracis* strains, only certain *B. cereus* strains possess both putative polysaccharide deacetylases homologues.

3.2 BA0330 and BA0331 lack deacetylase activity against common deacetylase substrates

BA0330 and BA0331 were produced without containing a His6-tag and purified employing a two step procedure. For BA0330 one SP Sepharose Fast Flow and one Sephacryl S-200 HR gel filtration chromatographic columns were used, while for BA0331 one Source Q HR and one Sephacryl S-200 HR gel filtration chromatographic columns were used and the recombinant proteins were purified to near homogeneity (Figure 14). Both recombinant proteins appear to be monomers as revealed by gel filtration chromatography.

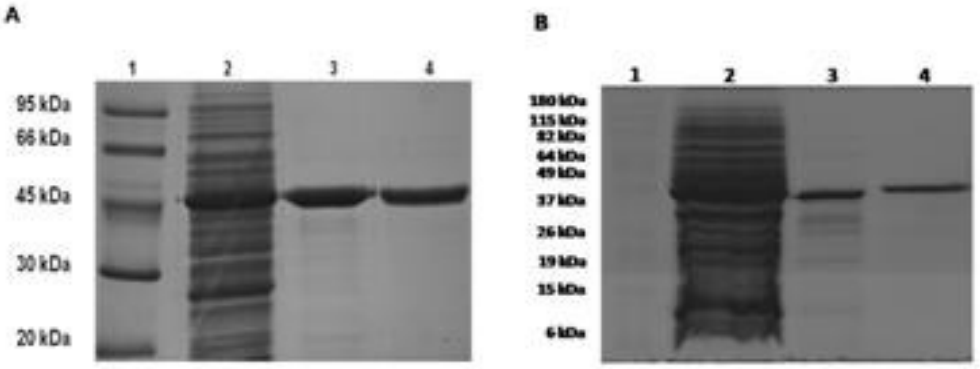

Figure 14:**.** *SDS-PAGE of the purified putative PDAs (**A**) BA0330: lane 1, molecular weight markers; lane 2, crude extract; lane 3, SP sepharose eluate; lane 4, gel filtration eluate. (**B**) BA0331: lane 1, molecular weight markers; lane 2, crude extract; lane 3, Source Q eluate; lane 4, gel filtration eluate. Samples were electrophoresed on a 12% polyacrylamide gel under denaturing and reducing conditions. Protein bands were visualized by staining with Coomassie Brilliant Blue R.*

In order to examine whether the two proteins are enzymatically active, several commonly used deacetylase substrates were tested in enzyme assays. BA0330 and BA0331 were not active against radiolabelled glycol chitin, *N*-acetyl chitooligosaccharides, the synthetic muropeptide *N*-acetyl-D-glucosaminyl-(β-1,4)-*N*-acetylmuramyl-L-alanyl-D- isoglutamine (GMDP) and p-nitrophenyl acetate (pNP-acetate) when tested at a wide pH range and in the presence or absence of the divalent cations Co^{+2}, Zn^{+2}, Mn^{+2}, Mg^{+2}, Ni^{+2} and Cu^{+2}. Both proteins were also inactive against the same substrates when they were purified from *B. anthracis* excluding that the lack of activity was due to their production in *E. coli* as recombinant proteins.

3.3 The structure of BA0330 reveals unique features of the active site

The crystal structure of BA0330 was recently determined at 1.48 Å and revealed two domains [188]. In addition to the CE4-type esterase domain there is an N-terminal Fibronectin type 3 (Fn3)-like domain (residues 45-141) consisting of a two-layered (4 + 3) β-sandwich (Figure 15A). Apart from the closely related BC0361 and BA0331 no other CE4 esterase studied so far has an Fn3-like domain. Part of the expressed protein (residues 24-44 of the N-terminus) could not be determined in the electron density maps and therefore the corresponding region was not built in the model. The CE4 domain resembles that of other deacetylases, containing a well formed groove with the Zn atom located at the bottom, as it is demonstrated in Figure 15B.

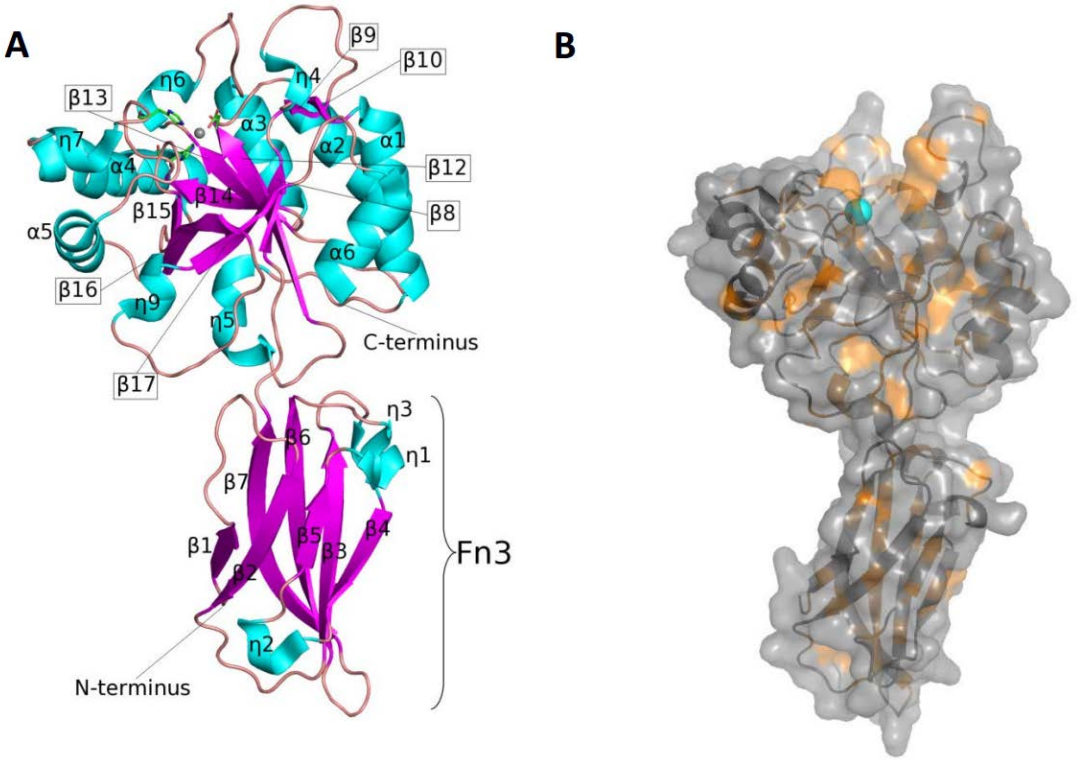

Figure 15: (**A**) *The overall structure of BA0330: helices are represented with cyan ribbons, β-strands with magenta and loops as pink strings. Zn^{2+} is shown as a gray sphere with the coordinating aminoacid residues (Asp^{206}, His^{264} and His^{268}) in stick representation.* (**B**) *A surface representation of the BA0330 molecule showing the CE4 domain (top) and the Fn3 domain (bottom). The metal containing binding cavity is located at the top of the molecule with the zinc atom (shown in cyan) exposed at the bottom of the cavity. Hydrophobic residue side chains (Leu, Ile, Val, Ala, Gly, Phe, Trp, Met) are shown in orange, the rest in gray.*

BA0330 and BA0331 retain the classical Asp-His-His arrangement as revealed by sequence alignment in Figure 16, suggesting that they could bind a metal cation within their binding site, and they contain most of the catalytic and zinc binding residues conserved in five catalytic motifs of enzymatically and structurally characterized CE4 esterases, including chitin deacetylase ClCDA, peptidoglycan deacetylases SpPgdA, BsPdaA, BC1960 and BC1974, putative polysaccharide deacetylase BC0361 and acetylxylan esterase SlCE4.

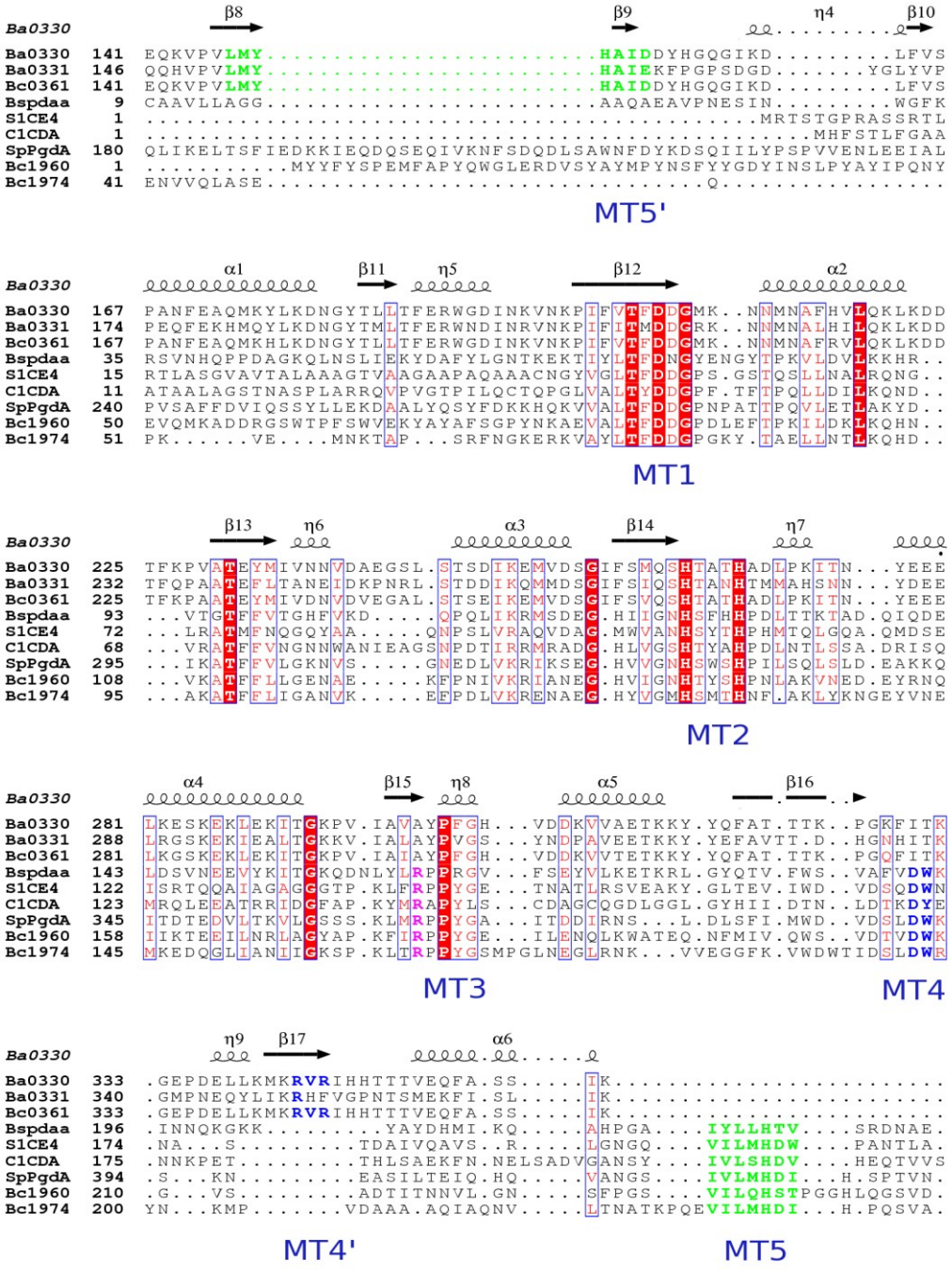

Figure 16: *Sequence alignment of the NodB domains of the BA0330, BA0331 proteins and representative members of the CE4 family including the putative PDA BC0361, the chitin deacetylase ClCDA, the acetylxylan esterase SlCE4 and the peptidoglycan deacetylases SpPdgA, BsPdaA, BC1960 and BC1974. The secondary structure elements of the BA0330 structure are shown at the top of the alignment, while the CE4 active-site motifs (MT1 to MT5) are shown at the bottom. The alignment was performed with T-coffee [189] and plotted with the ESPRIPT [190]. Strictly conserved residues are colored white in red background and similar residues are red and boxed. The residues participating at the MT4 and MT5 motifs are shown in blue and green color, respectively. Structural alignment of the proteins that contain an Fn3-like domain demonstrates a charge reversal in the MT4 region labeled as MT4'. Similarly, they present a shift of the MT5 region, which is located close to the N-terminus of the NodB domain (labeled as MT5').*

However, arrangements and alterations in both proteins occurred in motifs 4 and 5.Specifically, motif 5 is located close to the N-terminus of the NodB domain and motif 4 is shifted towards the C-terminus. Additionally, in both proteins motif 4 is electrostatically altered, as the conserved aspartic acid present in the other members of the CE4 family (Asp^{388} in SpPgdA), is replaced by an arginine (Arg^{345} in BA0330).

The catalytic site of BA0330 differs from that typically found in polysaccharide deacetylases in the following points: (i) The Arg which interacts with the catalytic Asp is usually found at the start of motif 3. Here, this Arg^{343} is provided from the last beta strand (β17, Fig. 3). (ii) The catalytic histidine (His^{150}), which is usually within motif 5, is located at a non-conserved sequence position in BA0330. (iii) BA0330 lacks the aspartic acid, which is usually provided by motif 4 and it is believed to be responsible for tuning the pKa of the catalytic histidine (His^{150}). Instead, the structure of BA0330 reveals an arginine residue (Arg^{345}) in close proximity to His^{150} and a possible interaction between them through a water molecule. In addition, Asp^{162} may interact with the catalytic His^{150} through two reactive water molecules. The catalytic site of BA0330 is presented in detail in Figure 17.

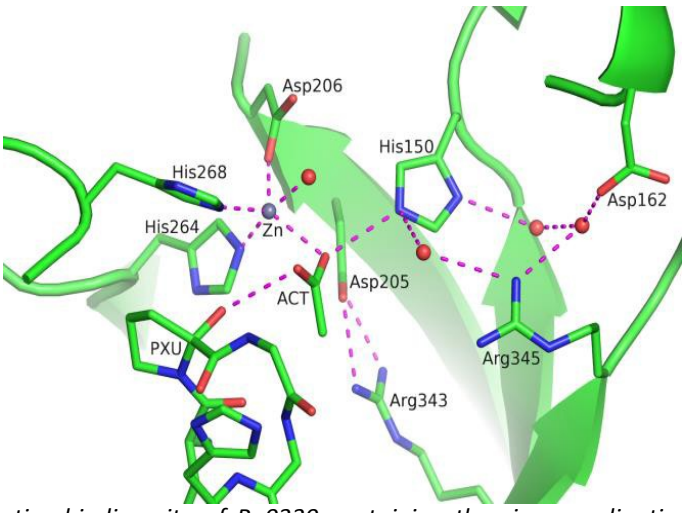

Figure 17: *The putative binding site of Ba0330 containing the zinc coordination residues (Asp^{206}, His^{264} and His^{268}), the acetate ion and a water molecule shown in red sphere. Additionally, the catalytic residues Asp^{205}, Arg^{343}, His^{150}, Asp^{162} and Arg^{345} are shown, while the whole network of interactions, either direct or through water molecules, is presented in dashed magenta lines.*

3.4 Phenotypic analysis reveals roles of BA0330 and BA0331 in cell wall integrity

To elucidate the biological roles of BA0330 and BA0331, the single mutants *Δba0330* and *Δba0331*, and the double mutant *Δba0330Δba0331* were constructed in *B. anthracis* UM23C1-2 (pXO1-, pXO2-). All mutant cells were able to grow in various liquid media (BHI broth, SPY medium), indicating that the genes were not required for *B. anthracis* viability and growth (Figure 18).

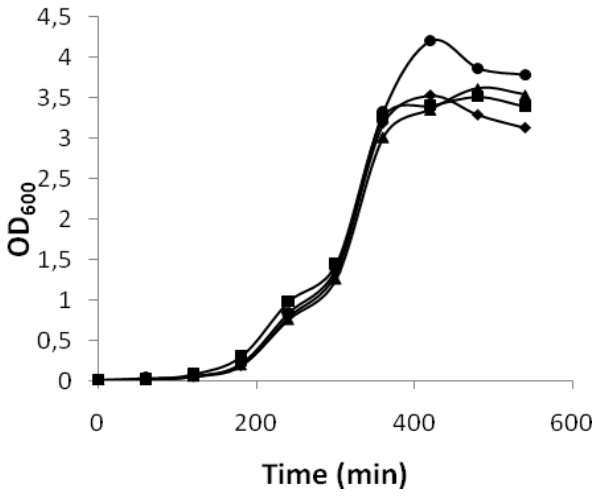

Figure 18: *Growth curves of B. anthracis UM23C1-2 and mutant strains. Cultures of B. anthracis UM23C1-2 parental strain (–●–) and Δba0330 (–◆–), Δba0331 (–▲–) and Δba0330Δba0331 (–■–) derivative strains were prepared in SPY liquid broth and grown at 37^{0}C.*

We next used electron microscopy to investigate possible cell wall alterations in the mutant strains. Exponentially and late stationary phase growth cells were fixed and imaged by TEM and SEM. While wild type cells showed the typical appearance for Gram-positive bacilli, the mutant cells exhibited different phenotypes. In *Δba0330* cells we observed a partial detachment of the membrane from the cell wall, presumably due to a weakened interaction between the two layers. In contrast, *Δba0331* cells had normal peptidoglycan-membrane connection but showed a distorted cell shape. The morphological changes were best seen by SEM showing variable cell diameter in stationary *Δba0331*cells and extensive clumping and lysis of *Δba0330Δba0331* cells. These maintained the partial cell wall detachment from the membrane during vegetative growth, and showed extensive lysis during stationary growth, indicating that both proteins together are needed to maintain cell shape and integrity (Figure 19. The same phenotypes were observed in three independent experiments, excluding thus the possibility of EM artifacts.

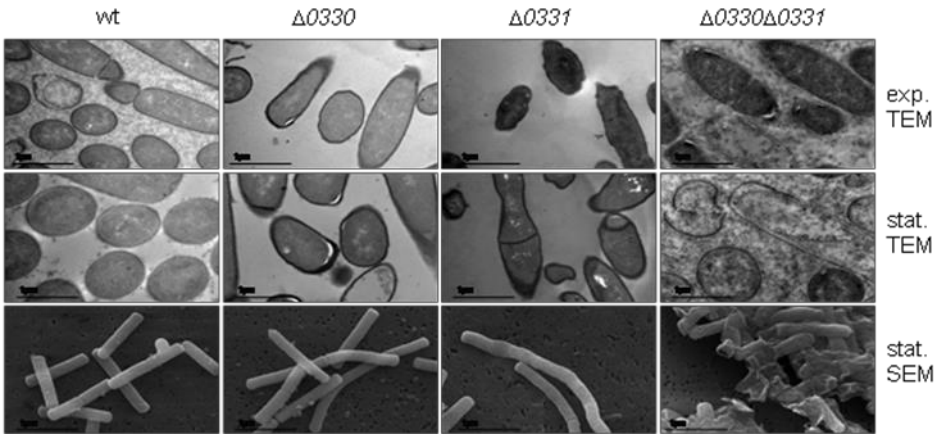

Figure 19: *Phenotype analysis of parental and mutant strains. Transmission electron micrographs of UM23C1-2 and Δba0330, Δba0331, Δba0330/0331 mutant cells during vegetative and stationary growth. Scanning electron micrographs of UM23C1-2 and Δba0330, Δba0331, Δba0330/0331 mutant cells during stationary growth. Δba0330 strain exhibited sites of detachments of peptidoglycan from the cell membrane, Δba0331 an atypical cell shape and Δba0330/0331 exhibited a virtually complete detachment of the membrane from the cell wall and formation of aggregates during stationary growth phase.*

The complemented strains fully recovered the wild-type phenotype when imaged by TEM (Fig. 20).

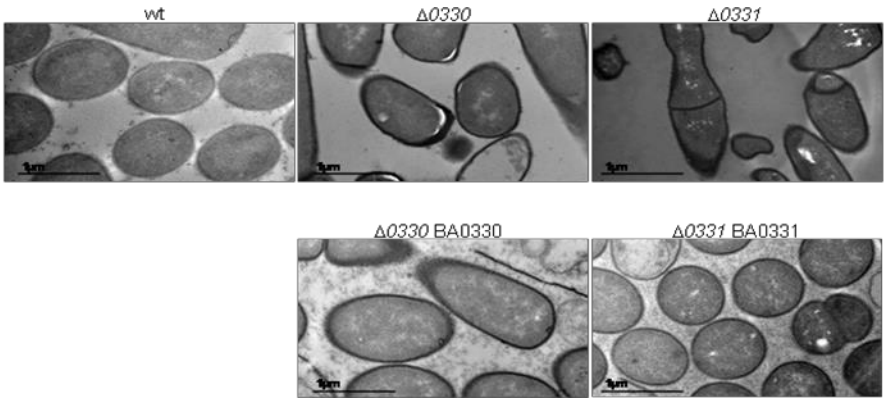

Figure 20: *Transmission electron micrographs of UM23C1-2 and Δba0330, Δba0331 mutant strains complemented with BA0330 and BA0331 respectively, during stationary growth. Both Δba0330 and Δba0331 recovered wild type phenotype after trans complementation with BA0330 and BA0331 respectively.*

3.5 Cells lacking BA0330 and BA0331 are more sensitive upon salt upshift

Previous studies in Gram-positive bacteria *Bacillus subtilis* and *Lactobacillus casei* revealed that high salt (NaCl) concentration reduced growth and resulted in detachment of cell wall from the cytoplasmic membrane [177, 191]. We therefore tested the growth of our mutants in the presence of increasing NaCl concentrations. In contrast to the wild type strain, both mutant strains grew slower at high NaCl concentrations (Figure 21A), a phenotype which was much more pronounced in *Δba0330* for concentrations higher than 3.5% NaCl. Moreover, the cell clumping and formation of filamentous cells forming visible aggregates was observed at 3.5% NaCl concentration and enhanced at higher salt conditions. These effects were enhanced in *Δba0330Δba0331* cells even under mild salt stress conditions (2.5%), preventing reliable growth monitoring for this strain. Monitoring of growth on agar plates under the presence of 4,5% NaCl of parental and mutant strains *Δba0330* and *Δba0331* confirmed the above observations. Interestingly when the mutant strains were

complemented with the corresponding protein they fully recovered the wild type phenotype, as shown in Figure 21B. Therefore, we conclude that BA0330, and to a lesser extent BA0331, are important for adaptation of *B. anthracis* to grow at high salt concentrations.

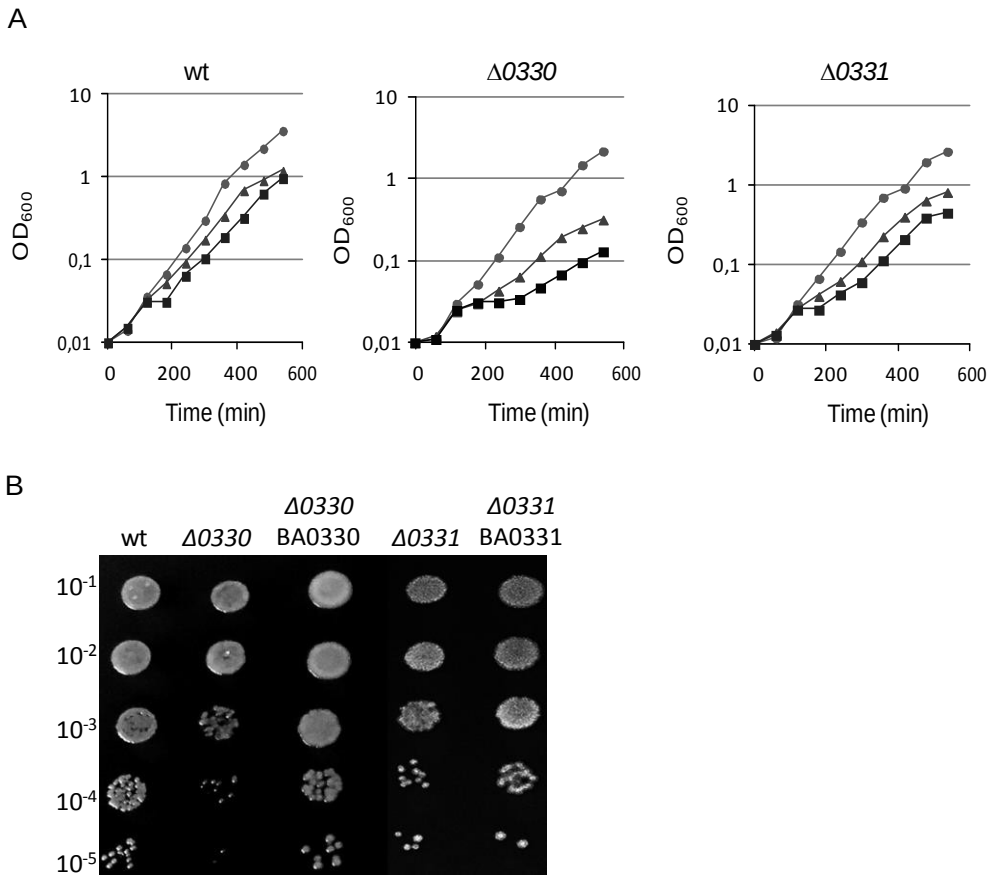

Figure 21: **(A)** *Effect of different NaCl concentrations on growth kinetics. Exponentially growing cells of parental strain and mutants were challenged with 2,5% NaCl (–●–), 3,5% NaCl (–▲–) and 4,5% NaCl ( )–■–nd the changes in growth kinetics were monitored by changes in absorbance at 600 nm. Δba0330 showed greater sensitivity at increasing concentrations of NaCl, while Δba0331 was less affected.* (**B**) *Growth of Δba0330 and Δba0331 mutant strains complemented with BA0330 and BA0331 respectively under high NaCl concentration (4,5%). B. anthracis UM23C1-2 was used as a control. While increased salt concentration inhibited growth of Δba0330 and Δba0331 mutant strains compared to the wild type strain, the complemented strains recovered the wild type phenotype. Numbers on the left axis indicate dilution factors of the cultures.*

3.6 Lysozyme sensitivity, autolysis rate and muropeptide analysis of parental and mutant strains.

Many bacterial peptidoglycan deacetylases described so far contribute to lysozyme resistance [96, 103, 105, 107]. However, *Δba0330* or *Δba0331* mutant cells grown in SPY medium did not display an altered sensitivity to lysozyme compared to the wild-type in the exponential or stationary growth phases as shown in Figure 22.

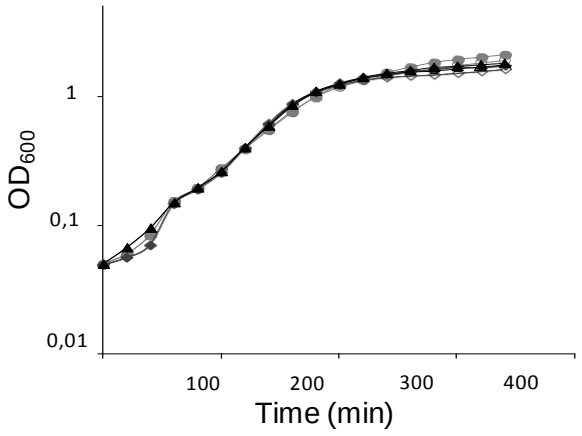

Figure 22: *Effect of lysozyme on UM23C1-2 (–○–), Δba0330 (–◇–) and Δba0331 (–△–) mutant strains. Strains were grown in SPY liquid broth at 37ºC. Closed symbols indicate the corresponding strains treated with 10 μg ml^{-1} hen egg lysozyme. None of the mutant strains was affected by the addition of lysozyme.*

We next tested the autolytic activity of parental *B. anthracis* UM23C1-2 strain and the putative polysaccharide deacetylase mutants by addition of NaN_3, a known inducer of autolysis in growing cells [192]. *Δba0330* and to a lesser extent *Δba0331* mutant strains showed decreased autolysis under these conditions compared to that of the parental strain, while *Δba0330Δba0331* did not lyse (Figure 23), indicating that both proteins affect the function of one or more autolysins.

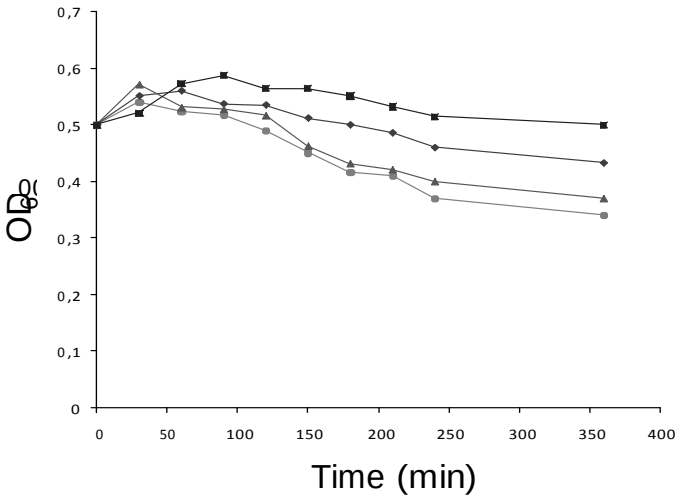

Figure 23: *Autolysis rate of UM23C1-2 and mutant strains. Autolysis was induced by the addition of 10 mM sodium azide to cultures of B. anthracis UM23C1-2 parental strain (–●–) and Δba0330 (–◆–), Δba0331 (–▲–) and Δba0330Δba0331 (–■–) derivative strains. Cell lysis was monitored by loss of absorbance at 600 nm. Δba0330Δba0331 strain was not affected by autolysis, Δba0330 strain was affected to a lesser degree compared to the wild type, while Δba0331 strain exhibited a similar pattern to the wild type strain.*

Since peptidoglycan is a major polysaccharide of *B. anthracis*, we determined the muropeptide composition of the peptidoglycan of each mutant. The peptidoglycan composition from the exponential phase cells of *Δba0330*, *Δba0331* and *Δba0330Δba0331* mutants and of the parental strain UM23C1-2 were analysed by HPLC (Fig. 24A) and main muropeptides were identified by mass spectrometry (Fig. 24B). The overall muropeptide profiles derived from all mutant strains were similar to that of the parental strain, with the exception of the abundance of tetrapeptides and tripeptides, which varied between wild type and *Δba0331* and *Δba0330Δba0331* mutant strains (Fig. 24A). Importantly, there was no significant difference in the abundance of deacetylated muropeptides.

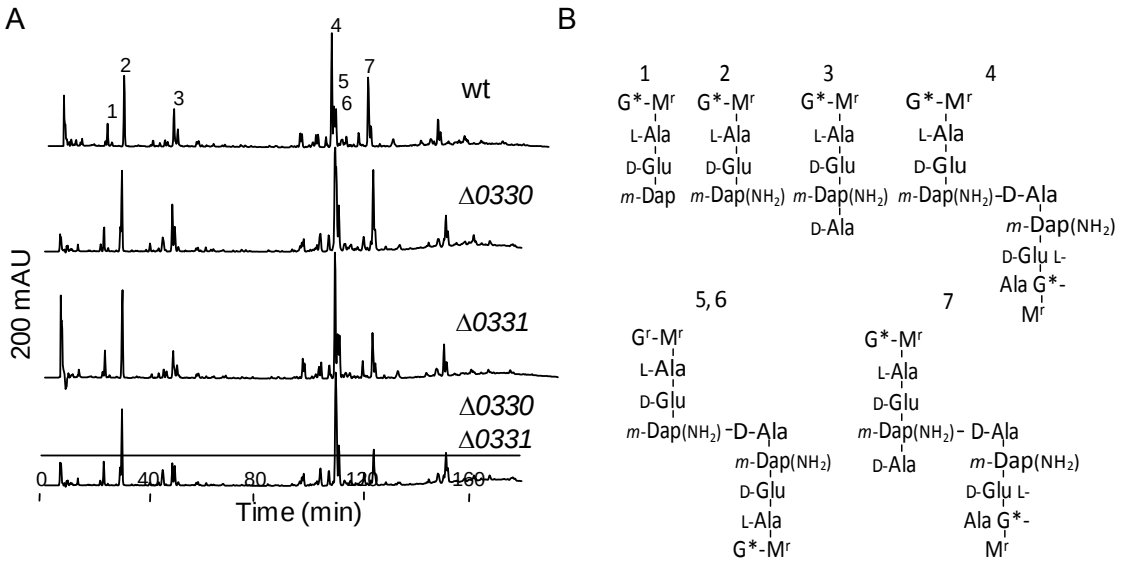

Figure 24: (**A**) *HPLC analysis of muropeptide composition of PG from vegetative cells of UM23C1-2, Δba0330, Δba0331 and Δba0330/0331. Peaks 1-7 were analysed by mass spectrometry.* (**B**) *Proposed structures of major muropeptides number 1 to 7 detected in (A) peak identification. Deacetylated monosaccharides are indicated with *; G, N-acetylglucosamine, G*, glucosamine; M^r, N-acetylmuramitol, m-Dap(NH2), amidated meso-diaminopimelic acid.*

Similarly, isolated peptidoglycan from exponential phase cells grown in the presence of 2,5% NaCl did not reveal any important differences in the muropeptide profiles from *Δba0330* and *Δba0331* in comparison to the parental strain.

Isolated neutral polysaccharide from *Δba0330* and *Δba0331* mutant strains displayed identical chromatograms (A_{206}) to that of the wild type strain (Figure 25).

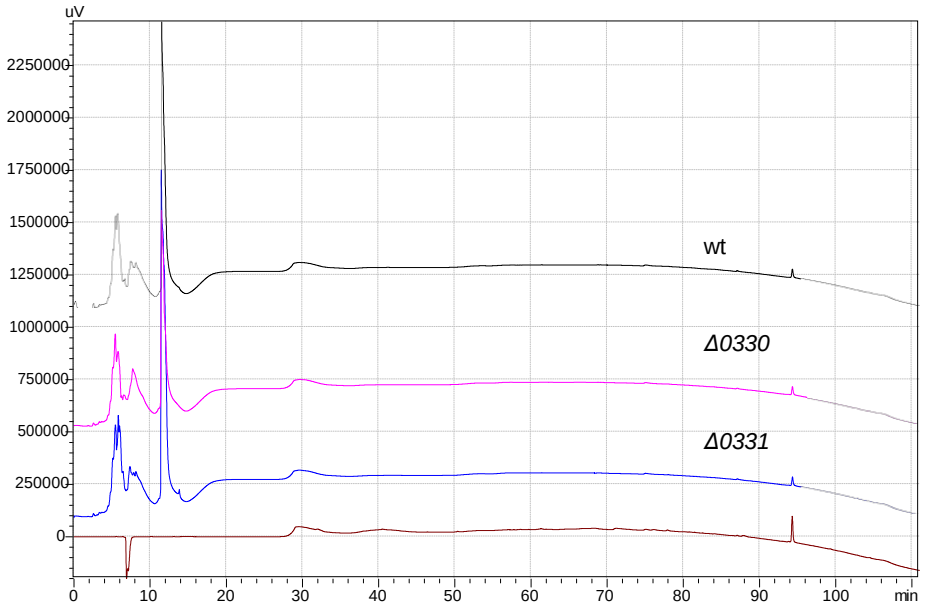

Figure 25: *HPLC analysis of muropeptide composition of neutral polysaccharide from stationary cells of UM23C1-2, Δba0330 and Δba0331.No significant differences were identified.*

These results indicate that BA0330 and BA0331 do not function to significantly change the level of *N*-acetylation of the peptidoglycan and the neutral polysaccharide.

3.7 BA0330 and BA0331 interact with peptidoglycan

A pull-down assay was used to investigate whether the two proteins bind to insoluble peptidoglycan. Both BA0330 and BA0331 were found to interact with isolated peptidoglycan from each of the corresponding mutant strain, as the proteins were detected in the pellet fraction after the pull-down experiment (Figure 26). These results suggest that the two lipoproteins, which are attached via their lipid moiety to the cell membrane, span to and interact with the peptidoglycan layer.

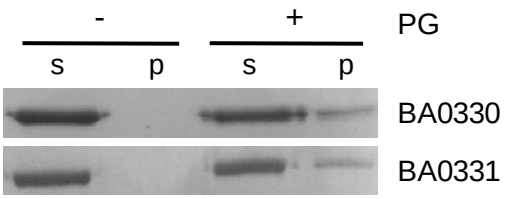

Figure 26: *BA0330 and BA0331 interact with peptidoglycan. Purified BA0330 and BA0331 proteins were incubated with or without peptidoglycan (PG) followed by sedimentation of the peptidoglycan by ultracentrifugation. Peptidoglycan was washed and sedimented again before proteins were separated by SDS-PAGE and visualized by Coomassie-staining. A fraction of each protein was pulled-down with peptidoglycan. S, supernatant after centrifugation; P, resuspended pellet.*

3.8 Gfp-fusions of BA0330 and BA0331 localize to lateral wall and distinct foci respectively

To gain more insights into the physiological roles of the two putative deacetylases, we determined the subcellular localization of C-terminal Gfp-fused proteins by fluorescence microscopy in UM23C1-2 cells. Fluorescent signal was obtained for each deacetylase during the exponential phase of growth and the expression of the Gfp-fused proteins was confirmed by Western blot analysis. BA0330-Gfp localized at the lateral wall of the cell and was enhanced at the septum. BA0331-Gfp displayed a different localization pattern, with fluorescence label distributed as distinct patches with lower fluorescence at the septa. Gfp localization of the two proteins is presented in Figure 27A. Membrane localization was consistent with the prediction of the two putative polysaccharide deacetylases as lipoproteins. The Gfp tag did not affect the function of the two proteins, since mutant strains transformed with the respective Gfp-fused proteins exhibited the same phenotype as wild type when grown under high salt concentration (Figure 27B).

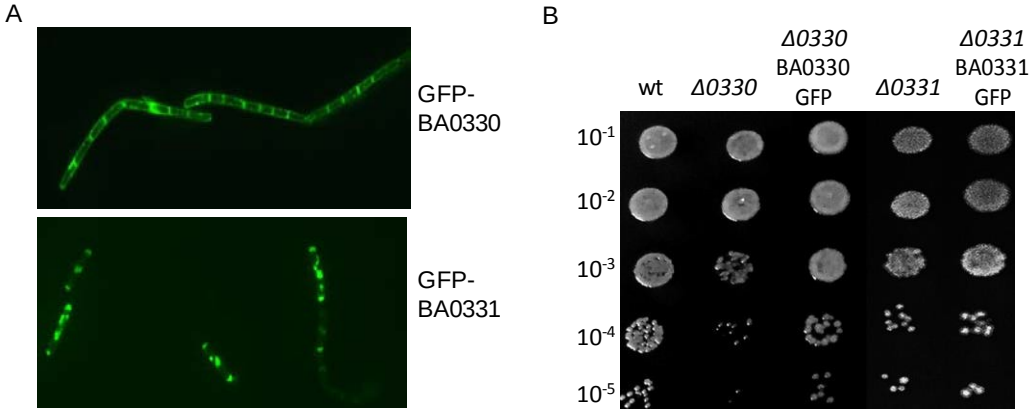

Figure 27: (A) *Localization of Gfp-BA0330 and Gfp-BA0331. Fusion proteins were constructed using the B. anthracis UM23C1-2 parental strain and were functional. Gfp-BA0330 localizes at the cell periphery and is enhanced at the septa. Gfp-BA0331 localizes at distinct spots at periphery and exhibits low fluorescence at septa. Scale bars, 5 µm.* **(B)** *Growth of Δba0330 and Δba0331 mutant strains complemented with Gfp-BA0330 and Gfp-BA0331 respectively under high NaCl concentration (4,5%). B. anthracis UM23C1-2 was used as a control. While increased salt concentration inhibited growth of Δba0330 and Δba0331 mutant strains compared to the wild type strain, the complemented strains recovered the wild type phenotype. Numbers on the left axis indicate dilution factors of the cultures.*

3.9 Deacetylase activity is not required to complement mutant phenotypes

To examine the importance of the putative deacetylase activity of the proteins *in vivo*, a point mutation was introduced in *ba0330* and *ba0331* to replace a predicted key catalytic aspartic acid residue with alanine generating BA0330 ($Asp^{205}Ala$) and BA0331 ($Asp^{212}Ala$), respectively. A shuttle vector expressing the mutated genes was introduced in the *B. anthracis* mutant strains and the resulting strains were examined by TEM. Interestingly, the mutant cells expressing the point mutated proteins lost their distorted phenotypes and fully recovered the wild type phenotype (Figure 28A), indicating that the enzymatic activity of the two proteins is not important for the observed phenotype of the mutants. Similarly, when inactive proteins were expressed in *Δba0330* and *Δba0331* mutant strains in the presence of 4.5% NaCl the wild type phenotype was restored (Figure 28B). Hence, cell wall stability and cell shape maintenance do not require enzymatically active proteins.

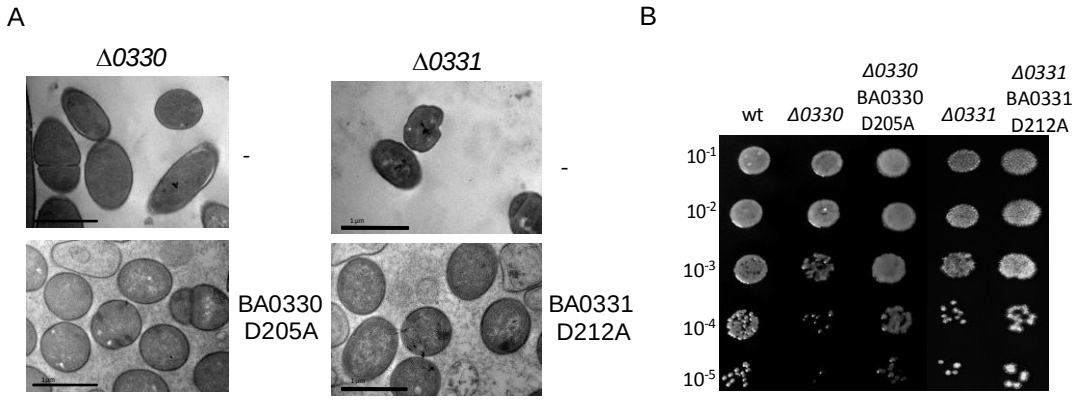

Figure 28: (**A**) *Site-directed mutagenesis of a predicted key enzymatic residue of BA0330 and BA0331. BA0330 and BA0331 with a point mutation in a key catalytic residue were expressed in Δba0330 and Δba0331 cells, respectively. Cells were grown until late stationary phase and samples for TEM observation were prepared. Δba0330 exhibited characteristic detachments, while the same strain complemented with BA0330 (Asp^{205}Ala) recovered the phenotype of the parental strain. Δba0331 cells exhibited irregular cell shape, while the same strain complemented with BA0331 (Asp^{212}Ala) recovered the typical bacilli shape.* (**B**) *Growth of Δba0330 and Δba0331 mutant strains complemented with BA0330 (Asp^{205}Ala) and BA0331 (Asp^{212}Ala) respectively under high NaCl concentration (4,5%). B. anthracis UM23C1-2 was used as a control. While increased salt concentration inhibited growth of Δba0330 and Δba0331 mutant strains compared to the wild type strain, the complemented strains recovered the wild type phenotype. Numbers on the left axis indicate dilution factors of the cultures.*

3.10 Do BA0330 and BA0331 complement each other?

Although *ΔbA0330* and *ΔbA0331* exhibit different phenotypes, the corresponding proteins BA0330 and BA0331 are highly homologous and have similar structures (personal communication Eliopoulos E.). In order to determine if the two proteins are redundant a series of preliminary experiments were conducted.

Electron microscopy was used to examine whether BA0330 and BA0331 can restore the abnormal phenotypes of *Δba0331* and *Δba0330* respectively. Noteworthy, under TEM examination the two proteins were able to complement the mutant strains and recover the wild phenotype (Figure 29A). Furthermore, when cells of parental and mutant strains were grown under mild NaCl concentration (2,5%), the complemented strains also exhibited the wild type phenotype, thus confirming the above observation (Figure 29B). Notably in the complementation of *Δba0330* mutant strain with

BA0331, except from the recovery of the wild type growth rate, the opacity of the colony is also restored.

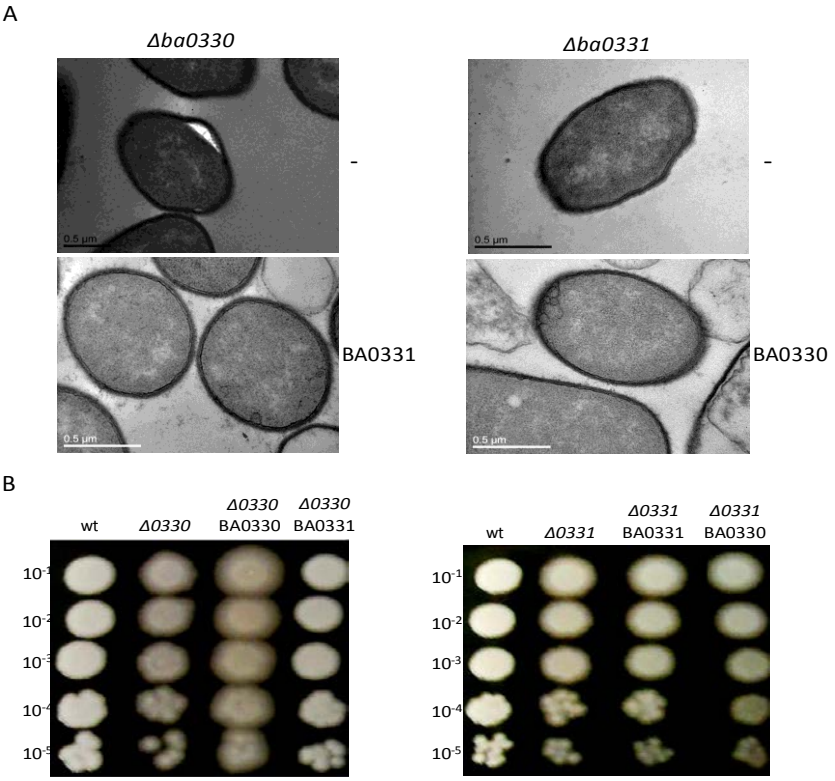

Figure 29: (**A**) *Transmission electron micrographs of UM23C1-2 and Δba0330, Δba0331 mutant strains complemented with BA0331 and BA0330 respectively, during stationary growth. Both Δba0330 and Δba0331 recovered wild type phenotype after trans complementation with BA0330 and BA0331 respectively.* (**B**) *Growth of Δba0330 and Δba0331 mutant strains complemented both with BA0330 and BA0331 under mild NaCl concentration (2,5%). B. anthracis UM23C1-2 was used as a control. The complemented strains with both proteins recovered the wild type phenotype. Numbers on the left axis indicate dilution factors of the cultures.*

In order to demonstrate which of the two proteins contributes mostly to the aberrant phenotype of the double mutant, *Δba0330ba0331* was complemented with BA0330 and BA0331 and samples from exponential and stationary growth phases were observed under SEM (Figure 30). Expression of BA0331 in the double mutant seems to restore the wild type phenotype to a higher extent in comparison to BA0330, since *Δba0330ba0331* complemented with BA0330 continues to exhibit extensive clumping and cell lysis.

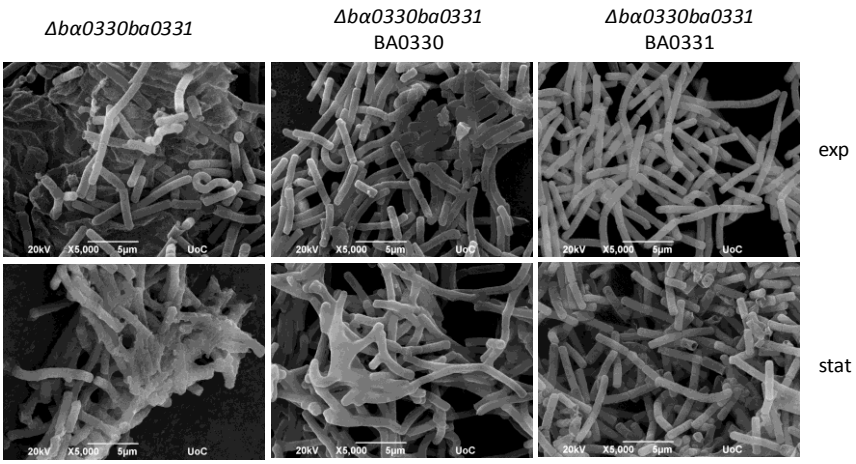

Figure 30: *Scanning electron micrographs of Δba0330/0331 mutant cells complemented with BA0330 and BA0331 during exponential and stationary growth. Expression of BA0331 seems to restore the wild type phenotype to higher extent in comparison to the expression of BA0330 in the double mutant.*

4. DISCUSSION

Bacterial lipoproteins are a functionally diverse class of peripheral membrane proteins in Gram-positive bacteria, with important roles in substrate binding for ABC transporters, adhesion, antibiotic, lantibiotic and bacteriocin resistance and phage superinfection, cell envelope homeostasis, protein secretion, folding and localization, redox and sensory processes, including signaling in sporulation and germination [61]. Some Gram-negative bacteria covalently anchor an abundant outer membrane lipoprotein (Lpp) to peptidoglycan to stabilize the cell envelope by forming tight connections between peptidoglycan and the outer membrane [193]. For Gram-positive bacteria, which lack an outer membrane, structural interactions between lipoproteins and peptidoglycan have not yet been reported [194].

Polysaccharide deacetylases belong to Carbohydrate Esterase Family 4 (CE4). The biological role of several polysaccharide deacetylases of different bacterial species has been elucidated and they have been demonstrated to play key roles in:

a) Lysozyme resistance
b) Evasion of host innate immune system
c) Cell physiology
d) Spore germination
e) Adhesion/invasion to host cells
f) Surface attachment and biofilm formation

Interestingly, the genomes of *Bacillus* sp., and especially of *B. cereus* sensu lato, including *B. anthracis* contain multiple putative polysaccharide deacetylase genes with high sequence homologies. The physiological role of five polysaccharide deacetylases in *B. anthracis* has been recently elucidated. BA1977 associated with lateral peptidoglycan synthesis, is the only deacetylase involved in resistance to host lysozyme and required for full virulence. BA1961 and BA3679 deacetylate peptidoglyan during both cell division and elongation, while BA5436 and BA2944 are important for peptidoglycan attachment of neutral polysaccharide, which anchors S-layer proteins, and for polysaccharide modification, respectively [102].

The structures of CE4 enzymes from various bacterial species have been determined, including peptidoglycan deacetylases from *Streptococcus pneumoniae* [114] and *Bacillus subtilis* [115] acetylxylan esterases from *Clostridium*

*therm*ocellum and *Streptomyces lividans* [195], poly-β-1,6-*N*-acetyl-D-glucosamine deacetylase from *E. coli* [113] and *Staphylococcus epidermitis* [196], putative polysaccharide deacetylases from *B. anthracis* [197, 198], *B. cereus* [199] and *Streptococcus mutans* [200]. CE4 enzymes contain a conserved NodB homology domain and adopt a $(\alpha/\beta)_8$ barel fold. Most of the structures contain a divalent ion in the active site bound in a His-His-Asp triad. The catalytic machinery is completed by an aspartic acid and a histidine which act as the catalytic base and catalytic acid, respectively [114].

BA0330 and BA0331 from *B. anthracis* are predicted as putative lipoproteins and polysaccharide deacetylases and share 55% sequence identity. Furthermore, BA0330 shares 91% identity with its corresponding homologue BC0361 from *B. cereus*, while a homologue of BA0331, which is present in all *B. anthracis* strains, is missing in many *B. cereus* strains including *B. cereus* ATCC 14579. BA0331 is mainly expressed during exponential phase, but is secreted at lower amounts during the stationary phase, in both the avirulent *B. anthracis* UM23C1-2 (pXO1-, pXO2-) and the wild-type virulent Vollum strain [201, 202].

In this study we employed biochemical and genetic (knockout) analysis and protein localization to elucidate the biological roles of BA0330 and BA0331 from the avirulent *B. anthracis* UM23C1-2 strain.

Surprisingly, in contrast to most other polysaccharide deacetylases, BA0330 and BA0331 were not active on a wide range of different substrates such as glycolchitin, *N*-acetylchitooligomers ($GlcNAc_{2-6}$), GMDP, pNP-acetate. Furthermore, inactivation of *ba0330*, *ba0331* and *ba0330/ba0331* did not result in a measurable change in the levels of peptidoglycan deacetylation, as shown by our analysis of the muropeptide composition (Fig. 24A, B).

The crystal structure of BA0330 has a well formed groove on the esterase domain that is lined with some hydrophobic residues and oriented towards the active-site residues (Fig. 15B). Futhermore, BA0330 and its homologue BC0361 from *B. cereus* contain a Cα-modified proline at its active site, which was modeled as an α-hydroxy-L-proline [199].How this proline becomes modified and whether this modification has any function is currently not known.

BA0330 has the characteristic Zn binding (His, His, Asp) and catalytic (Asp, His) motifs of polysaccharide deacetylase (Fig. 15A). Interestingly, Arg^{345} is found in

place of a conserved aspartic acid which is believed to be responsible for tuning the pKa of the catalytic histidine (His^{150}) (Fig. 17). Regulation of enzyme activity, altered substrate specificity or metal preference of CE4 family enzymes may be effected via modifications of the five CE4 motifs. It has been previously reported that mutation $Asp^{391}Asn$ in SpPgdA completely inactivated the enzyme [114]. A similar observation has been reported for PgaB from *E. coli* whereby a water molecule is found in place of this conserved aspartic acid [113], possibly explaining the reduced efficiency of the enzyme. By superimposing the active sites of SpPgdA and BA0330 (Fig. 17) it is apparent that the conserved His pKa modulator (Asp^{391} in SpPgdA) is replaced by a Leu in BA0330. However, the nearby Arg^{345} in BA0330 may act as a titratable catalytic group (His^{150}) modulator. We cannot predict the effect of the differentiation of the catalytic motifs of BA0330 and BA0331 on the activity of the two putative polysaccharide deacetylases.

BA0330 and BA0331 lacked deacetylase activity in our assays and their absence did not change lysozyme resistance (Fig. 22), but both did bind to purified peptidoglycan (Fig. 26). Therefore, we consider the possibility that the main functions of these proteins do not involve an enzymatic activity but they rather have a structural, cell wall stabilizing role. Putative enzymes which are inactive and have another than an enzymatic function have been previously reported. For example the *E. coli* peptidoglycan protein EnvC classified as a LytM-type endopeptidase, was initially thought to be a septum-splitting peptidoglycan hydrolase [203], until later studies revealed that EnvC and its homologue NlpD are inactive due to mutations in key catalytic residues, and that their main role is to activate the septum-splitting amidases [204]. However, we cannot strictly exclude that BA0330 and BA0331 have an enzymatic activity that is limited to a restricted cell surface area and not detectable by our techniques, or that they have an as-yet-unidentified substrate in the *B. anthracis* cell wall. Among the possible alternative substrates, not presently identified polysaccharides, distinct from the neutral polysaccharide of *B. anthacis* or specific GlcNAc residues for subsequent anchoring of cell wall polymers as previously demonstrated for BA1961 and BA3679 [205] are included.

Notably, the crystal structures of both BA0330 and BA0331 (BA0330 [188]; BA0331, personal communication Eliopoulos E., currently under structural optimization) revealed the presence of an N-terminal fibronectin type 3 (Fn3) domain,

which is unique for this family, and a carboxyterminal catalytic domain (Fig. 13A). Together with BC0361 from *B. cereus* these are the first putative polysaccharide deacetylases characterized to date with an Fn3 domain. These are often found in bacterial extracellular carbohydrases such as chitinases, amylases, cellulases etc., and it is believed that they participate in promotion of the hydrolysis of carbohydrate substrates by modifying their surfaces, while they can also play important functional roles by formation of protein-protein interfaces [206]. Fn3 domains are present in various peptidoglycan hydrolyzing enzymes, such as DD-carboxypeptidases PPB5 and PBP6 in *E. coli* [207, 208]. It has been previously proposed that differences in the Fn3 domains might affect protein localization, enzymatic activity, or interactions with other components of the peptidoglycan biosynthetic machinery [208]. It is possible that different localization of BA0330 and BA0331 is due to different functions of their Fn3 domains. The Fn3 domains of both proteins might be involved in their interaction with peptidoglycan. However, we cannot exclude the possibility that they act as spacers between the membrane linked N-terminal and the catalytic domain [209]. Experiments in order to clarify the roles of the Fn3 modules in the two lipoproteins are ongoing.

Furthermore, muropeptide composition analysis (Fig. 24A, B) revealed that the *Δba0331* and *Δba0330/Δba0331* mutants exhibited reduced amounts of tetrapeptides with a concominant increase in tripeptide content as compared to wild type and the *Δba0330* mutant. It is highly unlikely, that these changes are caused by an enzymatic activity of BA0331, which according to the sequence and structure of its homologue BA0330 does not modify tri- and tetrapeptides in peptidoglycan. Such function is rather associated with LD-carboxypeptidases, which trim the tetrapeptides to tripeptides. Several LD-carboxypeptidase genes have been identified [210-212] and recently the structure of the LdcB LD-carboxypeptidase from *B. subtilis*, which is unrelated to those of BA0330 and BA0331, has been elucidated [213]. Further experiments are required to test whether BA0331 is involved in regulating LD-carboxypeptidase activity.

The *Δba0330* mutant strain showed a reduced autolysis rate compared to wild type (Fig. 23), suggesting an effect of BA0330 on the endogenous peptidoglycan hydrolases. A reduced lysis is a property of most members of deacetylases' family, since from the polysaccharide deacetylase mutants of *B. anthracis* examined so far,

only *Δba1977* lysed with rates comparable to that of the wild type [102]. TEM revealed partial detachment of peptidoglycan from the membrane of *Δba0330* mutant cells during both the exponential and stationary phase of growth (Fig. 19) suggesting a structural role for BA0330, possibly stabilizing the interaction between the membrane and peptidoglycan. Similar structural roles have been reported for lipoproteins anchored to the outer membrane of Gram-negative bacteria which interact covalently or non-covalently with peptidoglycan [214]. Although it has been proposed that lipoproteins of Gram-positive bacteria could also have equivalent structural roles [66], to the best of our knowledge this is the first report of a lipoprotein from a Gram-positive bacterium involved in interactions with peptidoglycan, probably by reinforcing the anchoring of peptidoglycan on the membrane. In support of this role, Gfp-BA0330 was distributed along the cell membrane and was slightly enhanced at division sites (Fig. 27A). Furthermore, growth of *Δba0330* was strongly impaired at increasing concentrations of NaCl, especially above 3.5% NaCl, at which the wild type strain was only slightly affected (Fig. 21A), indicating that BA0330 is required to adapt to growth at high osmolarity. Several *Bacillus* and *Bacillus* related genera have been identified among haloalkalophilic bacteria. [215]. Exposure to NaCl has been shown to induce a protective response to *B. cereus*, a close relative of *B. anthracis* [216] and proteins playing a significant role in outgrowth of *B. cereus* have been identified [217]. To the best of our knowledge similar studies have not been presently reported for *B. anthracis.*

The *Δba0331* mutant was not sensitive to lysozyme (Fig. 22) and lysed similarly to wild type (Fig. 23). Interestingly, the cells had an abnormal cell shape with variable cell diameter. Although the mechanism is not yet known, BA0331 could either have a stabilizing role at the lateral wall, or involved with guiding cell elongation [117]. Intriguingly, Gfp-BA0331 exhibited a different localization pattern than BA0330, distributed in discrete patches around the cell periphery in exponentially growing cells (Fig. 27A). Whether BA0331 participates in the construction of a normally shaped cell wall as a component of the cell elongation machinery needs to be addressed in future studies. A structural role of BA0331 is supported by a virtually complete detachment of the membrane from the cell wall in stationary cells of the double mutant *Δba0330/Δba0331*, to a higher degree than in the

single *Δba0330* mutant, indicating that both gene products contribute to maintaining cell wall integrity (Fig. 19).

To determine if the morphological alteration of the *Δba0330* and *Δba0331* mutants are due to the putative de-*N*-acetylase enzymatic activity, we expressed protein versions lacking the catalytic aspartic acid residue, BA0330 ($Asp^{205}Ala$) and BA0331 ($Asp^{212}Ala$). Remarkably, these inactive BA0330 and BA0331 versions fully complemented the morphological aberrancies of the respective mutants, indicating that the phenotypes are not caused by the lack of enzymatic activity and supporting our conclusion that the main function of the two proteins is non enzymatic (Fig. 28A).

In this study we present experimental support for novel functions of two lipoproteins, putative polysaccharide deacetylases from *B. anthracis* in the adaptation of the bacterium under salt stress (BA0330), in cell shape maintenance (BA0331) and structural integrity of the bacterial envelope (BA0330, BA0331). Further characterization of this system should provide a better understanding of the mechanisms by which lipoproteins maintain cell wall integrity in gram positive bacteria and of how bacteria generate and maintain different shapes, a fundamental question in cell biology.

5. PERSPECTIVES

5.1 Complementation studies

Although BA0330 and BA0331 are highly homologous and they exhibit structural similarity (Eliopoulos E., unpublished data), they have different localization patterns and the mutant strains exhibit different phenotypes. From preliminary complementation studies the two proteins appear to substitute one another. Remarkably, when the *Δba0330* mutant strain is complemented with BA0331, not only the wild type phenotype is recovered, but the opacity of the colony is also restored. Further complementation studies are needed in order to elucidate whether the two proteins are redundant.

Another interesting observation is that although all *B. anthracis* strains possess both *ba0330* and *ba0331* homologues, certain *B. cereus* strains possess only *ba0330* homologues and are devoid of *ba0331* ones. It would be interesting to delete the homologue of *ba0330* gene in a *B. cereus* strain which lacks the *ba0331* homologue and examine its phenotype. The comparison of mutants from *Bacillus* strains which contain either both or solely one of the two genes can reveal significant information on whether the two proteins are redundant.

5.2 Elucidation of the role of the Fn3 domain and the NodB domain

Noteworthy, BA0330, its homologue in *B. cereus* BC0361 [188] and BA0331 are the only polysaccharide deacetylases described so far to possess an Fn3 domain in their structure. There are three main functions of Fn3 domains presently reported

a. They mediate protein-protein interactions,

b. act as a spacer to get the required biological function in the right place, or

c. they facilitate binding to the substrate in bacterial extracellular enzymes.

It is of great interest to further investigate the role of the Fn3 domains in these proteins and determine if they share the same function.

Furthermore, it would be equally challenging to determine whether the observed phenotypes of the mutant strains can be attributed solely to the function of one of the two domains or if both of them are necessary in order that the two proteins fulfill their biological role. Combined techniques need to be employed in order to study each of the two distinct domains of the two proteins.

5.3 Are BA0330 and/or BA0331 involved in B. anthracis virulence?

The involvement of BA0330 and BA0331 in the pathogenicity of *B. anthracis* has not been studied so far. The present study did not reveal potential implication of the two proteins in the virulence of the bacterium. Nonetheless, the two proteins are the only two lipoproteins among the 11 putative or known polysaccharide deacetylases of *B. anthracis* and it is well established that lipoproteins may play important roles in virulence of several pathogenic bacteria [218, 219]. In order to explore this possibility, fully virulent *B. anthracis* strains must be employed and the virulence of the mutant strains in a subcutaneous mouse model of infection in comparison to the the wild type strain should be studied. Attenuation of mutant strains after subcutaneous injection in mice will confirm their contribution to *B. anthracis* in vivo virulence.

5.4 Dead or alive?

Finally the biggest challenge of all is to conclusively determine if BA0330 and BA0331 are the inactive forms of polysaccharide deacetylases or if they deacetylate a presently not identified substrate. Our studies so far have not detected any changes in the deacetylation pattern resulting from the function of the two proteins, so more sensitive techniques such as NMR must be employed in order to exclude the possibility that the proteins perform the deacetylation reaction at a limited surface area which is not detectable with the methods used in this study. Furthermore the identification of novel polysaccharides of *B. anthracis* could lead to identification of

potential substrates for BA0330 and BA0331. It has been demonstrated by Candela *et al* [205] that *B. cereus* ATCC14579 can synthesize not only one as previously reported but two structurally unrelated polysaccharides. The first one is constantly expressed at the surface of the bacteria whereas the expression of the second is tightly regulated by culture conditions and growth states, planctonic or biofilm. We cannot therefore exclude that BA0330 and/or BA0331 act to de-*N*-acetylate other not presently identified polysaccharides from *B. anthracis*. RNA-sequencing technique can be employed in order to identify genes that could participate in the synthesis of not presently identified polysaccharides during different developmental stages of *B. anthracis*. Subsequent isolation of the putative polysaccharides from wild type and *Δba0330* and *Δba0331* mutant strains and verification via mass spectrometry and NMR of their structure is required in order to identify new potential substrates for BA0330 and BA0331.

6. REFERENCES

1 Topley W.C. & Wilson A.A. Topley and Wilson's principles of bacteriology and immunity. *Immunology* **8** (1864).

2 Koch, R. Die Aetiologie der Milzbrand-Krankheit, begrundet auf die Entwicklungs geschichte des Bacillus anthracis. *Beitrage zur Biologie der Pflanzen* **2**, 4 (1876).

3 Pasteur, L. & Roux, E. Compte rendu sommaire des experiences faites a Pouilly-le-Fort, pres Melun, sur la vaccination charbonneuse. *Comptes rendus des seances de l'academie des sciences* **92**, 6 (1881).

4 Inglesby, T. V., O'Toole, T., Henderson, D. A., Bartlett, J. G., Ascher, M. S., Eitzen, E., Friedlander, A. M., Gerberding, J., Hauer, J., Hughes, J., McDade, J., Osterholm, M. T., Parker, G., Perl, T. M., Russell, P. K., Tonat, K. & Working Group on Civilian, B. Anthrax as a biological weapon, 2002: updated recommendations for management. *Jama* **287**, 2236-2252 (2002).

5 Jernigan, J. A., Stephens, D. S., Ashford, D. A., Omenaca, C., Topiel, M. S., Galbraith, M., Tapper, M., Fisk, T. L., Zaki, S., Popovic, T., Meyer, R. F., Quinn, C. P., Harper, S. A., Fridkin, S. K., Sejvar, J. J., Shepard, C. W., McConnell, M., Guarner, J., Shieh, W. J., Malecki, J. M., Gerberding, J. L., Hughes, J. M., Perkins, B. A. & Anthrax Bioterrorism Investigation, T. Bioterrorism-related inhalational anthrax: the first 10 cases reported in the United States. *Emerging infectious diseases* **7**, 933-944 (2001).

6 Soufiane, B. & Cote, J. C. Discrimination among Bacillus thuringiensis H serotypes, serovars and strains based on 16S rRNA, gyrB and aroE gene sequence analyses. *Antonie van Leeuwenhoek* **95**, 33-45 (2009).

7 Pilo, P. & Frey, J. Bacillus anthracis: molecular taxonomy, population genetics, phylogeny and patho-evolution. *Infection, genetics and evolution : Journal of molecular epidemiology and evolutionary genetics in infectious diseases* **11**, 1218-1224 (2011).

8 Koehler, T. M., Dai, Z. & Kaufman-Yarbray, M. Regulation of the Bacillus anthracis protective antigen gene: CO2 and a trans-acting element activate transcription from one of two promoters. *Journal of bacteriology* **176**, 586-595 (1994).

9 Dixon, T. C., Meselson, M., Guillemin, J. & Hanna, P. C. Anthrax. *The New England journal of medicine* **341**, 815-826 (1999).

10 Fouet, A., Namy, O. & Lambert, G. Characterization of the operon encoding the alternative sigma(B) factor from Bacillus anthracis and its role in virulence. *Journal of bacteriology* **182**, 5036-5045 (2000).

11 Turnbull, P. C. Definitive identification of Bacillus anthracis--a review. *Journal of applied microbiology* **87**, 237-240 (1999).

12 Mock, M. & Fouet, A. Anthrax. *Annual review of microbiology* **55**, 647-671 (2001).

13 Dragon, D. C. & Rennie, R. P. The ecology of anthrax spores: tough but not invincible. *The Canadian veterinary journal. La revue veterinaire canadienne* **36**, 295-301 (1995).

14 Dutz, W. & Kohout-Dutz, E. Anthrax. *International journal of dermatology* **20**, 203-206 (1981).

15 Ibrahim, K. H., Brown, G., Wright, D. H. & Rotschafer, J. C. Bacillus anthracis: medical issues of biologic warfare. *Pharmacotherapy* **19**, 690-701 (1999).

16 Tipper, D. J. & Linnett, P. E. Distribution of peptidoglycan synthetase activities between sporangia and forespores in sporulating cells of Bacillus sphaericus. *Journal of bacteriology* **126**, 213-221 (1976).

17 Driks, A. The Bacillus anthracis spore. *Molecular aspects of medicine* **30**, 368-373 (2009).

18 Santo, L. Y. & Doi, R. H. Ultrastructural analysis during germination and outgrowth of Bacillus subtilis spores. *Journal of bacteriology* **120**, 475-481 (1974).

19 Driks, A. Maximum shields: the assembly and function of the bacterial spore coat. *Trends in microbiology* **10**, 251-254 (2002).

20 McKenney, P. T., Driks, A. & Eichenberger, P. The Bacillus subtilis endospore: assembly and functions of the multilayered coat. *Nature reviews. Microbiology* **11**, 33-44 (2013).

21 Setlow, B., Cowan, A. E. & Setlow, P. Germination of spores of Bacillus subtilis with dodecylamine. *Journal of applied microbiology* **95**, 637-648 (2003).

22 Ezzell, J. W. & Welkos, S. L. The capsule of bacillus anthracis, a review. *Journal of applied microbiology* **87**, 250 (1999).

23 Turk, B. E. Manipulation of host signalling pathways by anthrax toxins. *The Biochemical journal* **402**, 405-417 (2007).

24 Young, J. A. & Collier, R. J. Anthrax toxin: receptor binding, internalization, pore formation, and translocation. *Annual review of biochemistry* **76**, 243-265 (2007).

25 Leppla, S. H. Anthrax toxin edema factor: a bacterial adenylate cyclase that increases cyclic AMP concentrations of eukaryotic cells. *Proceedings of the National Academy of Sciences of the United States of America* **79**, 3162-3166 (1982).

26 Collier, R. J. Membrane translocation by anthrax toxin. *Molecular aspects of medicine* **30**, 413-422 (2009).

27 Singh, Y., Klimpel, K. R., Goel, S., Swain, P. K. & Leppla, S. H. Oligomerization of anthrax toxin protective antigen and binding of lethal factor during endocytic uptake into mammalian cells. *Infection and immunity* **67**, 1853-1859 (1999).

28 Klimpel, K. R., Molloy, S. S., Thomas, G. & Leppla, S. H. Anthrax toxin protective antigen is activated by a cell surface protease with the sequence specificity and catalytic properties of furin. *Proceedings of the National Academy of Sciences of the United States of America* **89**, 10277-10281 (1992).

29 Collier, R. J. & Young, J. A. Anthrax toxin. *Annual review of cell and developmental biology* **19**, 45-70 (2003).

30 Kintzer, A. F., Thoren, K. L., Sterling, H. J., Dong, K. C., Feld, G. K., Tang, II, Zhang, T. T., Williams, E. R., Berger, J. M. & Krantz, B. A. The protective antigen component of anthrax toxin forms functional octameric complexes. *Journal of molecular biology* **392**, 614-629 (2009).

31 Abrami, L., Reig, N. & van der Goot, F. G. Anthrax toxin: the long and winding road that leads to the kill. *Trends in microbiology* **13**, 72-78 (2005).

32 Guidi-Rontani, C., Weber-Levy, M., Mock, M. & Cabiaux, V. Translocation of Bacillus anthracis lethal and oedema factors across endosome membranes. *Cellular microbiology* **2**, 259-264 (2000).

33 Duesbery, N. S., Webb, C. P., Leppla, S. H., Gordon, V. M., Klimpel, K. R., Copeland, T. D., Ahn, N. G., Oskarsson, M. K., Fukasawa, K., Paull, K. D. & Vande Woude, G. F. Proteolytic inactivation of MAP-kinase-kinase by anthrax lethal factor. *Science* **280**, 734-737 (1998).

34 Park, J. M., Greten, F. R., Li, Z. W. & Karin, M. Macrophage apoptosis by anthrax lethal factor through p38 MAP kinase inhibition. *Science* **297**, 2048-2051 (2002).

35 Vitale, G., Pellizzari, R., Recchi, C., Napolitani, G., Mock, M. & Montecucco, C. Anthrax lethal factor cleaves the N-terminus of MAPKKS and induces tyrosine/threonine phosphorylation of MAPKS in cultured macrophages. *Journal of applied microbiology* **87**, 288 (1999).

36 Zornetta, I., Brandi, L., Janowiak, B., Dal Molin, F., Tonello, F., Collier, R. J. & Montecucco, C. Imaging the cell entry of the anthrax oedema and lethal toxins with fluorescent protein chimeras. *Cellular microbiology* **12**, 1435-1445 (2010).

37 Prince, A. S. The host response to anthrax lethal toxin: unexpected observations. *The Journal of clinical investigation* **112**, 656-658 (2003).

38 Goossens, P. L. Animal models of human anthrax: the Quest for the Holy Grail. *Molecular aspects of medicine* **30**, 467-480 (2009).

39 Price, E. P., Seymour, M. L., Sarovich, D. S., Latham, J., Wolken, S. R., Mason, J., Vincent, G., Drees, K. P., Beckstrom-Sternberg, S. M., Phillippy, A. M., Koren, S., Okinaka, R. T., Chung, W. K., Schupp, J. M., Wagner, D. M., Vipond, R., Foster, J. T., Bergman, N. H., Burans, J., Pearson, T., Brooks, T. & Keim, P. Molecular epidemiologic investigation of an anthrax outbreak among heroin users, Europe. *Emerging infectious diseases* **18**, 1307-1313 (2012).

40 Hicks, C. W., Sweeney, D. A., Cui, X., Li, Y. & Eichacker, P. Q. An overview of anthrax infection including the recently identified form of disease in injection drug users. *Intensive care medicine* **38**, 1092-1104 (2012).

41 Akdeniz, N., Calka, O., Ozkol, H. U. & Akdeniz, H. Cutaneous anthrax resulting in renal failure with generalized tissue damage. *Cutaneous and ocular toxicology* **32**, 327-329 (2013).

42 Maddah, G., Abdollahi, A. & Katebi, M. Gastrointestinal anthrax: clinical experience in 5 cases. *Caspian journal of internal medicine* **4**, 672-676 (2013).

43 Kaur, M., Singh, S. & Bhatnagar, R. Anthrax vaccines: present status and future prospects. *Expert review of vaccines* **12**, 955-970 (2013).

44 Ivins, B. E., Welkos, S. L., Little, S. F., Crumrine, M. H. & Nelson, G. O. Immunization against anthrax with Bacillus anthracis protective antigen combined with adjuvants. *Infection and immunity* **60**, 662-668 (1992).

45 Iacono-Connors, L. C., Welkos, S. L., Ivins, B. E. & Dalrymple, J. M. Protection against anthrax with recombinant virus-expressed protective antigen in experimental animals. *Infection and immunity* **59**, 1961-1965 (1991).

46 Marston, C. K., Beesley, C., Helsel, L. & Hoffmaster, A. R. Evaluation of two selective media for the isolation of Bacillus anthracis. *Letters in applied microbiology* **47**, 25-30 (2008).

47 Goel, A. K., Tamrakar, A. K., Kamboj, D. V. & Singh, L. Direct immunofluorescence assay for rapid environmental detection of Vibrio cholerae O1. *Folia microbiologica* **50**, 448-452 (2005).

48 Schofield, D. A., Sharp, N. J., Vandamm, J., Molineux, I. J., Spreng, K. A., Rajanna, C., Westwater, C. & Stewart, G. C. Bacillus anthracis diagnostic detection and rapid

antibiotic susceptibility determination using 'bioluminescent' reporter phage. *Journal of microbiological methods* **95**, 156-161 (2013).

49 Safari Foroshani, N., Karami, A. & Pourali, F. Simultaneous and Rapid Detection of Salmonella typhi, Bacillus anthracis, and Yersinia pestis by Using Multiplex Polymerase Chain Reaction (PCR). *Iranian Red Crescent medical journal* **15**, e9208, doi:10.5812/ircmj.9208 (2013).

50 Kaneda, T. Iso- and anteiso-fatty acids in bacteria: biosynthesis, function, and taxonomic significance. *Microbiological reviews* **55**, 288-302 (1991).

51 Lawrence, D., Heitefuss, S. & Seifert, H. S. Differentiation of Bacillus anthracis from Bacillus cereus by gas chromatographic whole-cell fatty acid analysis. *Journal of clinical microbiology* **29**, 1508-1512 (1991).

52 Samant, S., Hsu, F. F., Neyfakh, A. A. & Lee, H. The Bacillus anthracis protein MprF is required for synthesis of lysylphosphatidylglycerols and for resistance to cationic antimicrobial peptides. *Journal of bacteriology* **191**, 1311-1319 (2009).

53 Garufi, G., Hendrickx, A. P., Beeri, K., Kern, J. W., Sharma, A., Richter, S. G., Schneewind, O. & Missiakas, D. Synthesis of lipoteichoic acids in Bacillus anthracis. *Journal of bacteriology* **194**, 4312-4321 (2012).

54 Reichmann, N. T. & Grundling, A. Location, synthesis and function of glycolipids and polyglycerolphosphate lipoteichoic acid in Gram-positive bacteria of the phylum Firmicutes. *FEMS microbiology letters* **319**, 97-105 (2011).

55 Nakayama, H., Kurokawa, K. & Lee, B. L. Lipoproteins in bacteria: structures and biosynthetic pathways. *The FEBS journal* **279**, 4247-4268 (2012).

56 Okugawa, S., Moayeri, M., Pomerantsev, A. P., Sastalla, I., Crown, D., Gupta, P. K. & Leppla, S. H. Lipoprotein biosynthesis by prolipoprotein diacylglyceryl transferase is required for efficient spore germination and full virulence of Bacillus anthracis. *Molecular microbiology* **83**, 96-109 (2012).

57 Tokunaga, M., Tokunaga, H. & Wu, H. C. Post-translational modification and processing of Escherichia coli prolipoprotein in vitro. *Proceedings of the National Academy of Sciences of the United States of America* **79**, 2255-2259 (1982).

58 Kovacs-Simon, A., Titball, R. W. & Michell, S. L. Lipoproteins of bacterial pathogens. *Infection and immunity* **79**, 548-561 (2011).

59 Tschumi, A., Nai, C., Auchli, Y., Hunziker, P., Gehrig, P., Keller, P., Grau, T. & Sander, P. Identification of apolipoprotein N-acyltransferase (Lnt) in mycobacteria. *The Journal of biological chemistry* **284**, 27146-27156 (2009).

60 Kurokawa, K., Kim, M. S., Ichikawa, R., Ryu, K. H., Dohmae, N., Nakayama, H. & Lee, B. L. Environment-mediated accumulation of diacyl lipoproteins over their triacyl counterparts in Staphylococcus aureus. *Journal of bacteriology* **194**, 3299-3306 (2012).

61 Hutchings, M. I., Palmer, T., Harrington, D. J. & Sutcliffe, I. C. Lipoprotein biogenesis in Gram-positive bacteria: knowing when to hold 'em, knowing when to fold 'em. *Trends in microbiology* **17**, 13-21 (2009).

62 Sutcliffe, I. C. & Harrington, D. J. Pattern searches for the identification of putative lipoprotein genes in Gram-positive bacterial genomes. *Microbiology* **148**, 2065-2077 (2002).

63 Sutcliffe, I. C. & Harrington, D. J. Lipoproteins of Mycobacterium tuberculosis: an abundant and functionally diverse class of cell envelope components. *FEMS microbiology reviews* **28**, 645-659 (2004).

64 Das, S., Kanamoto, T., Ge, X., Xu, P., Unoki, T., Munro, C. L. & Kitten, T. Contribution of lipoproteins and lipoprotein processing to endocarditis virulence in Streptococcus sanguinis. *Journal of bacteriology* **191**, 4166-4179 (2009).

65 Dramsi, S., Magnet, S., Davison, S. & Arthur, M. Covalent attachment of proteins to peptidoglycan. *FEMS microbiology reviews* **32**, 307-320 (2008).

66 Sutcliffe, I. C. & Russell, R. R. Lipoproteins of gram-positive bacteria. *Journal of bacteriology* **177**, 1123-1128 (1995).

67 Boneca, I. G. The role of peptidoglycan in pathogenesis. *Current opinion in microbiology* **8**, 46-53 (2005).

68 Barreteau, H., Kovac, A., Boniface, A., Sova, M., Gobec, S. & Blanot, D. Cytoplasmic steps of peptidoglycan biosynthesis. *FEMS microbiology reviews* **32**, 168-207 (2008).

69 van Heijenoort, J. Lipid intermediates in the biosynthesis of bacterial peptidoglycan. *Microbiology and molecular biology reviews : MMBR* **71**, 620-635 (2007).

70 Mohammadi, T., van Dam, V., Sijbrandi, R., Vernet, T., Zapun, A., Bouhss, A., Diepeveen-de Bruin, M., Nguyen-Disteche, M., de Kruijff, B. & Breukink, E. Identification of FtsW as a transporter of lipid-linked cell wall precursors across the membrane. *The EMBO journal* **30**, 1425-1432 (2011).

71 Lovering, A. L., Gretes, M. & Strynadka, N. C. Structural details of the glycosyltransferase step of peptidoglycan assembly. *Current opinion in structural biology* **18**, 534-543 (2008).

72 Pinho, M. G., Kjos, M. & Veening, J. W. How to get (a)round: mechanisms controlling growth and division of coccoid bacteria. *Nature reviews. Microbiology* **11**, 601-614 (2013).

73 Read, T. D., Peterson, S. N., Tourasse, N., Baillie, L. W., Paulsen, I. T., Nelson, K. E., Tettelin, H., Fouts, D. E., Eisen, J. A., Gill, S. R., Holtzapple, E. K., Okstad, O. A., Helgason, E., Rilstone, J., Wu, M., Kolonay, J. F., Beanan, M. J., Dodson, R. J., Brinkac, L. M., Gwinn, M., DeBoy, R. T., Madpu, R., Daugherty, S. C., Durkin, A. S., Haft, D. H., Nelson, W. C., Peterson, J. D., Pop, M., Khouri, H. M., Radune, D., Benton, J. L., Mahamoud, Y., Jiang, L., Hance, I. R., Weidman, J. F., Berry, K. J., Plaut, R. D., Wolf, A. M., Watkins, K. L., Nierman, W. C., Hazen, A., Cline, R., Redmond, C., Thwaite, J. E., White, O., Salzberg, S. L., Thomason, B., Friedlander, A. M., Koehler, T. M., Hanna, P. C., Kolsto, A. B. & Fraser, C. M. The genome sequence of Bacillus anthracis Ames and comparison to closely related bacteria. *Nature* **423**, 81-86 (2003).

74 Ekwunife, F. S., Singh, J., Taylor, K. G. & Doyle, R. J. Isolation and purification of cell wall polysaccharide of Bacillus anthracis (delta Sterne). *FEMS microbiology letters* **66**, 257-262 (1991).

75 Fox, A., Black, G. E., Fox, K. & Rostovtseva, S. Determination of carbohydrate profiles of Bacillus anthracis and Bacillus cereus including identification of O-methyl methylpentoses by using gas chromatography-mass spectrometry. *Journal of clinical microbiology* **31**, 887-894 (1993).

76 Choudhury, B., Leoff, C., Saile, E., Wilkins, P., Quinn, C. P., Kannenberg, E. L. & Carlson, R. W. The structure of the major cell wall polysaccharide of Bacillus anthracis is species-specific. *The Journal of biological chemistry* **281**, 27932-27941 (2006).

77 Schneewind, O. & Missiakas, D. M. Protein secretion and surface display in Gram-positive bacteria. *Philosophical transactions of the Royal Society of London. Series B, Biological sciences* **367**, 1123-1139 (2012).

78 Leoff, C., Saile, E., Rauvolfova, J., Quinn, C. P., Hoffmaster, A. R., Zhong, W., Mehta, A. S., Boons, G. J., Carlson, R. W. & Kannenberg, E. L. Secondary cell wall polysaccharides of Bacillus anthracis are antigens that contain specific epitopes which cross-react with three pathogenic Bacillus cereus strains that caused severe disease, and other epitopes common to all the Bacillus cereus strains tested. *Glycobiology* **19**, 665-673 (2009).

79 Mesnage, S., Fontaine, T., Mignot, T., Delepierre, M., Mock, M. & Fouet, A. Bacterial SLH domain proteins are non-covalently anchored to the cell surface via a conserved

mechanism involving wall polysaccharide pyruvylation. *The EMBO journal* **19**, 4473-4484 (2000).

80 Mayer-Scholl, A., Hurwitz, R., Brinkmann, V., Schmid, M., Jungblut, P., Weinrauch, Y. & Zychlinsky, A. Human neutrophils kill Bacillus anthracis. *PLoS pathogens* **1**, e23, doi:10.1371/journal.ppat.0010023 (2005).

81 Fouet, A. & Mesnage, S. Bacillus anthracis cell envelope components. *Current topics in microbiology and immunology* **271**, 87-113 (2002).

82 Kern, J., Ryan, C., Faull, K. & Schneewind, O. Bacillus anthracis surface-layer proteins assemble by binding to the secondary cell wall polysaccharide in a manner that requires csaB and tagO. *Journal of molecular biology* **401**, 757-775 (2010).

83 Mesnage, S., Tosi-Couture, E., Mock, M., Gounon, P. & Fouet, A. Molecular characterization of the Bacillus anthracis main S-layer component: evidence that it is the major cell-associated antigen. *Molecular microbiology* **23**, 1147-1155 (1997).

84 Couture-Tosi, E., Delacroix, H., Mignot, T., Mesnage, S., Chami, M., Fouet, A. & Mosser, G. Structural analysis and evidence for dynamic emergence of Bacillus anthracis S-layer networks. *Journal of bacteriology* **184**, 6448-6456 (2002).

85 Mignot, T., Mesnage, S., Couture-Tosi, E., Mock, M. & Fouet, A. Developmental switch of S-layer protein synthesis in Bacillus anthracis. *Molecular microbiology* **43**, 1615-1627 (2002).

86 Kern, J., Wilton, R., Zhang, R., Binkowski, T. A., Joachimiak, A. & Schneewind, O. Structure of surface layer homology (SLH) domains from Bacillus anthracis surface array protein. *The Journal of biological chemistry* **286**, 26042-26049 (2011).

87 Fouet, A. The surface of Bacillus anthracis. *Molecular aspects of medicine* **30**, 374-385 (2009).

88 Bruckner, V., Kovacs, J. & Denes, G. Structure of poly-D-glutamic acid isolated from capsulated strains of B. anthracis. *Nature* **172**, 508 (1953).

89 Record, B. R. & Wallis, R. G. Physico-chemical examination of polyglutamic acid from Bacillus anthracis grown in vivo. *The Biochemical journal* **63**, 443-447 (1956).

90 Green, B. D., Battisti, L., Koehler, T. M., Thorne, C. B. & Ivins, B. E. Demonstration of a capsule plasmid in Bacillus anthracis. *Infection and immunity* **49**, 291-297 (1985).

91 Persson, B. & Argos, P. Prediction of transmembrane segments in proteins utilising multiple sequence alignments. *Journal of molecular biology* **237**, 182-192 (1994).

92 Candela, T. & Fouet, A. Poly-gamma-glutamate in bacteria. *Molecular microbiology* **60**, 1091-1098 (2006).

93 Candela, T. & Fouet, A. Bacillus anthracis CapD, belonging to the gamma-glutamyltranspeptidase family, is required for the covalent anchoring of capsule to peptidoglycan. *Molecular microbiology* **57**, 717-726 (2005).

94 Makino, S., Uchida, I., Terakado, N., Sasakawa, C. & Yoshikawa, M. Molecular characterization and protein analysis of the cap region, which is essential for encapsulation in Bacillus anthracis. *Journal of bacteriology* **171**, 722-730 (1989).

95 Roelants, G. E., Senyk, G. & Goodman, J. W. Immunochemical studies on the poly-gamma-D-glutamyl capsule of Bacillus anthracis. V. The in vivo fate and distribution in rabbits of the polypeptide in immunogenic and nonimmunogenic forms. *Israel journal of medical sciences* **5**, 196-208 (1969).

96 Vollmer, W. & Tomasz, A. The pgdA gene encodes for a peptidoglycan N-acetylglucosamine deacetylase in Streptococcus pneumoniae. *The Journal of biological chemistry* **275**, 20496-20501 (2000).

97 Psylinakis, E., Boneca, I. G., Mavromatis, K., Deli, A., Hayhurst, E., Foster, S. J., Varum, K. M. & Bouriotis, V. Peptidoglycan N-acetylglucosamine deacetylases from Bacillus cereus, highly conserved proteins in Bacillus anthracis. *The Journal of biological chemistry* **280**, 30856-30863 (2005).

98 Caufrier, F., Martinou, A., Dupont, C. & Bouriotis, V. Carbohydrate esterase family 4 enzymes: substrate specificity. *Carbohydrate research* **338**, 687-692 (2003).

99 Tsigos, I., Martinou, A., Kafetzopoulos, D. & Bouriotis, V. Chitin deacetylases: new, versatile tools in biotechnology. *Trends in biotechnology* **18**, 305-312 (2000).

100 Kafetzopoulos, D., Martinou, A. & Bouriotis, V. Bioconversion of chitin to chitosan: purification and characterization of chitin deacetylase from Mucor rouxii. *Proceedings of the National Academy of Sciences of the United States of America* **90**, 2564-2568 (1993).

101 Hoq, M. I. & Ibrahim, H. R. Potent antimicrobial action of triclosan-lysozyme complex against skin pathogens mediated through drug-targeted delivery mechanism. *European journal of pharmaceutical sciences* **42**, 130-137 (2011).

102 Balomenou, S., Fouet, A., Tzanodaskalaki, M., Couture-Tosi, E., Bouriotis, V. & Boneca, I. G. Distinct functions of polysaccharide deacetylases in cell shape, neutral polysaccharide synthesis and virulence of Bacillus anthracis. *Molecular microbiology* **87**, 867-883 (2013).

103 Boneca, I. G., Dussurget, O., Cabanes, D., Nahori, M. A., Sousa, S., Lecuit, M., Psylinakis, E., Bouriotis, V., Hugot, J. P., Giovannini, M., Coyle, A., Bertin, J., Namane,

A., Rousselle, J. C., Cayet, N., Prevost, M. C., Balloy, V., Chignard, M., Philpott, D. J., Cossart, P. & Girardin, S. E. A critical role for peptidoglycan N-deacetylation in Listeria evasion from the host innate immune system. *Proceedings of the National Academy of Sciences of the United States of America* **104**, 997-1002 (2007).

104 Meyrand, M., Boughammoura, A., Courtin, P., Mezange, C., Guillot, A. & Chapot-Chartier, M. P. Peptidoglycan N-acetylglucosamine deacetylation decreases autolysis in Lactococcus lactis. *Microbiology* **153**, 3275-3285 (2007).

105 Fittipaldi, N., Sekizaki, T., Takamatsu, D., de la Cruz Dominguez-Punaro, M., Harel, J., Bui, N. K., Vollmer, W. & Gottschalk, M. Significant contribution of the pgdA gene to the virulence of Streptococcus suis. *Molecular microbiology* **70**, 1120-1135 (2008).

106 Kaoukab-Raji, A., Biskri, L., Bernardini, M. L. & Allaoui, A. Characterization of SfPgdA, a Shigella flexneri peptidoglycan deacetylase required for bacterial persistence within polymorphonuclear neutrophils. *Microbes and infection* **14**, 619-627 (2012).

107 Benachour, A., Ladjouzi, R., Le Jeune, A., Hebert, L., Thorpe, S., Courtin, P., Chapot-Chartier, M. P., Prajsnar, T. K., Foster, S. J. & Mesnage, S. The lysozyme-induced peptidoglycan N-acetylglucosamine deacetylase PgdA (EF1843) is required for Enterococcus faecalis virulence. *Journal of bacteriology* **194**, 6066-6073 (2012).

108 Smith, T. J., Blackman, S. A. & Foster, S. J. Autolysins of Bacillus subtilis: multiple enzymes with multiple functions. *Microbiology* **146 (Pt 2)**, 249-262 (2000).

109 Fukushima, T., Yamamoto, H., Atrih, A., Foster, S. J. & Sekiguchi, J. A polysaccharide deacetylase gene (pdaA) is required for germination and for production of muramic delta-lactam residues in the spore cortex of Bacillus subtilis. *Journal of bacteriology* **184**, 6007-6015 (2002).

110 Fukushima, T., Tanabe, T., Yamamoto, H., Hosoya, S., Sato, T., Yoshikawa, H. & Sekiguchi, J. Characterization of a polysaccharide deacetylase gene homologue (pdaB) on sporulation of Bacillus subtilis. *Journal of biochemistry* **136**, 283-291 (2004).

111 Colvin, K. M., Alnabelseya, N., Baker, P., Whitney, J. C., Howell, P. L. & Parsek, M. R. PelA deacetylase activity is required for Pel polysaccharide synthesis in Pseudomonas aeruginosa. *Journal of bacteriology* **195**, 2329-2339 (2013).

112 Vuong, C., Kocianova, S., Voyich, J. M., Yao, Y., Fischer, E. R., DeLeo, F. R. & Otto, M. A crucial role for exopolysaccharide modification in bacterial biofilm formation, immune evasion, and virulence. *The Journal of biological chemistry* **279**, 54881-54886 (2004).

113 Little, D. J., Poloczek, J., Whitney, J. C., Robinson, H., Nitz, M. & Howell, P. L. The structure- and metal-dependent activity of Escherichia coli PgaB provides insight into

the partial de-N-acetylation of poly-beta-1,6-N-acetyl-D-glucosamine. *The Journal of biological chemistry* **287**, 31126-31137 (2012).

114 Blair, D. E., Schuttelkopf, A. W., MacRae, J. I. & van Aalten, D. M. Structure and metal-dependent mechanism of peptidoglycan deacetylase, a streptococcal virulence factor. *Proceedings of the National Academy of Sciences of the United States of America* **102**, 15429-15434 (2005).

115 Blair, D. E. & van Aalten, D. M. Structures of Bacillus subtilis PdaA, a family 4 carbohydrate esterase, and a complex with N-acetyl-glucosamine. *FEBS letters* **570**, 13-19 (2004).

116 Balomenou, S., Arnaouteli, S., Koutsioulis, D., Fadouloglou, V. & Bouriotis V. Polysaccharide Deacetylases: New antimicrobial drug targets. *Frontiers in Anti-Infective Drug Discovery* Vol. **4,** Chapter 3, Bentham Science Publishers (2015).

117 Cabeen, M. T. & Jacobs-Wagner, C. Bacterial cell shape. *Nature reviews. Microbiology* **3**, 601-610 (2005).

118 Dusenbery, D. B. Fitness landscapes for effects of shape on chemotaxis and other behaviors of bacteria. *Journal of bacteriology* **180**, 5978-5983 (1998).

119 Cooper, P. J. & Goodyer, I. Prevalence and significance of weight and shape concerns in girls aged 11-16 years. *The British journal of psychiatry : the journal of mental science* **171**, 542-544 (1997).

120 Cho, H., Jonsson, H., Campbell, K., Melke, P., Williams, J. W., Jedynak, B., Stevens, A. M., Groisman, A. & Levchenko, A. Self-organization in high-density bacterial colonies: efficient crowd control. *PLoS biology* **5**, e302, doi:10.1371/journal.pbio.0050302 (2007).

121 Young, K. D. The selective value of bacterial shape. *Microbiology and molecular biology reviews : MMBR* **70**, 660-703 (2006).

122 Koch, A. L. The bacterium's way for safe enlargement and division. *Applied and environmental microbiology* **66**, 3657-3663 (2000).

123 Young, K. D. Bacterial shape: two-dimensional questions and possibilities. *Annual review of microbiology* **64**, 223-240 (2010).

124 Gitai, Z. The new bacterial cell biology: moving parts and subcellular architecture. *Cell* **120**, 577-586 (2005).

125 Carballido-Lopez, R. The bacterial actin-like cytoskeleton. *Microbiology and molecular biology reviews : MMBR* **70**, 888-909 (2006).

126 Jones, L. J., Carballido-Lopez, R. & Errington, J. Control of cell shape in bacteria: helical, actin-like filaments in Bacillus subtilis. *Cell* **104**, 913-922 (2001).

127 Garner, E. C., Bernard, R., Wang, W., Zhuang, X., Rudner, D. Z. & Mitchison, T. Coupled, circumferential motions of the cell wall synthesis machinery and MreB filaments in B. subtilis. *Science* **333**, 222-225 (2011).

128 Dominguez-Escobar, J., Chastanet, A., Crevenna, A. H., Fromion, V., Wedlich-Soldner, R. & Carballido-Lopez, R. Processive movement of MreB-associated cell wall biosynthetic complexes in bacteria. *Science* **333**, 225-228 (2011).

129 Eraso, J. M. & Margolin, W. Bacterial cell wall: thinking globally, actin locally. *Current biology : CB* **21**, R628-630, doi:10.1016/j.cub.2011.06.056 (2011).

130 Jonas, K. To divide or not to divide: control of the bacterial cell cycle by environmental cues. *Current opinion in microbiology* **18**, 54-60 (2014).

131 Errington, J., Daniel, R. A. & Scheffers, D. J. Cytokinesis in bacteria. *Microbiology and molecular biology reviews : MMBR* **67**, 52-65 (2003).

132 Yu, X. C. & Margolin, W. FtsZ ring clusters in min and partition mutants: role of both the Min system and the nucleoid in regulating FtsZ ring localization. *Molecular microbiology* **32**, 315-326 (1999).

133 Lutkenhaus, J. Dynamic proteins in bacteria. *Current opinion in microbiology* **5**, 548-552 (2002).

134 Nelson, D. E. & Young, K. D. Contributions of PBP 5 and DD-carboxypeptidase penicillin binding proteins to maintenance of cell shape in Escherichia coli. *Journal of bacteriology* **183**, 3055-3064 (2001).

135 Nelson, D. E. & Young, K. D. Penicillin binding protein 5 affects cell diameter, contour, and morphology of Escherichia coli. *Journal of bacteriology* **182**, 1714-1721 (2000).

136 Bork, P. & Doolittle, R. F. Proposed acquisition of an animal protein domain by bacteria. *Proceedings of the National Academy of Sciences of the United States of America* **89**, 8990-8994 (1992).

137 Baron, M., Main, A. L., Driscoll, P. C., Mardon, H. J., Boyd, J. & Campbell, I. D. 1H NMR assignment and secondary structure of the cell adhesion type III module of fibronectin. *Biochemistry* **31**, 2068-2073 (1992).

138 Leahy, D. J., Hendrickson, W. A., Aukhil, I. & Erickson, H. P. Structure of a fibronectin type III domain from tenascin phased by MAD analysis of the selenomethionyl protein. *Science* **258**, 987-991 (1992).

139 Johnson, K. J., Sage, H., Briscoe, G. & Erickson, H. P. The compact conformation of fibronectin is determined by intramolecular ionic interactions. *The Journal of biological chemistry* **274**, 15473-15479 (1999).

140 Van Obberghen-Schilling, E., Tucker, R. P., Saupe, F., Gasser, I., Cseh, B. & Orend, G. Fibronectin and tenascin-C: accomplices in vascular morphogenesis during development and tumor growth. *The International journal of developmental biology* **55**, 511-525 (2011).

141 Watanabe, T., Suzuki, K., Oyanagi, W., Ohnishi, K. & Tanaka, H. Gene cloning of chitinase A1 from Bacillus circulans WL-12 revealed its evolutionary relationship to Serratia chitinase and to the type III homology units of fibronectin. *The Journal of biological chemistry* **265**, 15659-15665 (1990).

142 Doolittle, R. F. & Bork, P. Evolutionarily mobile modules in proteins. *Scientific American* **269**, 50-56 (1993).

143 Little, E., Bork, P. & Doolittle, R. F. Tracing the spread of fibronectin type III domains in bacterial glycohydrolases. *Journal of molecular evolution* **39**, 631-643 (1994).

144 Nicholas, R. A., Krings, S., Tomberg, J., Nicola, G. & Davies, C. Crystal structure of wild-type penicillin-binding protein 5 from Escherichia coli: implications for deacylation of the acyl-enzyme complex. *The Journal of biological chemistry* **278**, 52826-52833 (2003).

145 Typas, A., Banzhaf, M., Gross, C. A. & Vollmer, W. From the regulation of peptidoglycan synthesis to bacterial growth and morphology. *Nature reviews. Microbiology* **10**, 123-136 (2012).

146 Uchiyama, T., Katouno, F., Nikaidou, N., Nonaka, T., Sugiyama, J. & Watanabe, T. Roles of the exposed aromatic residues in crystalline chitin hydrolysis by chitinase A from Serratia marcescens 2170. *The Journal of biological chemistry* **276**, 41343-41349 (2001).

147 Papanikolau, Y., Prag, G., Tavlas, G., Vorgias, C. E., Oppenheim, A. B. & Petratos, K. High resolution structural analyses of mutant chitinase A complexes with substrates provide new insight into the mechanism of catalysis. *Biochemistry* **40**, 11338-11343 (2001).

148 Orikoshi, H., Nakayama, S., Hanato, C., Miyamoto, K. & Tsujibo, H. Role of the N-terminal polycystic kidney disease domain in chitin degradation by chitinase A from a marine bacterium, Alteromonas sp. strain O-7. *Journal of applied microbiology* **99** (2005).

149 Najmudin, S., Guerreiro, C. I., Carvalho, A. L., Prates, J. A., Correia, M. A., Alves, V. D., Ferreira, L. M., Romao, M. J., Gilbert, H. J., Bolam, D. N. & Fontes, C. M. Xyloglucan is recognized by carbohydrate-binding modules that interact with beta-glucan chains. *The Journal of biological chemistry* **281**, 8815-8828 (2006).

150 Puente, X. S., Sanchez, L. M., Overall, C. M. & Lopez-Otin, C. Human and mouse proteases: a comparative genomic approach. *Nature reviews. Genetics* **4**, 544-558 (2003).

151 Pils, B. & Schultz, J. Inactive enzyme-homologues find new function in regulatory processes. *Journal of molecular biology* **340**, 399-404 (2004).

152 Adrain, C. & Freeman, M. New lives for old: evolution of pseudoenzyme function illustrated by iRhoms. *Nature reviews. Molecular cell biology* **13**, 489-498 (2012).

153 Leslie, M. Molecular biology. 'Dead' enzymes show signs of life. *Science* **340**, 25-27 (2013).

154 Brew, K., Vanaman, T. C. & Hill, R. L. Comparison of the amino acid sequence of bovine alpha-lactalbumin and hens egg white lysozyme. *The Journal of biological chemistry* **242**, 3747-3749 (1967).

155 Manning, G., Whyte, D. B., Martinez, R., Hunter, T. & Sudarsanam, S. The protein kinase complement of the human genome. *Science* **298**, 1912-1934 (2002).

156 Ross, J., Jiang, H., Kanost, M. R. & Wang, Y. Serine proteases and their homologs in the Drosophila melanogaster genome: an initial analysis of sequence conservation and phylogenetic relationships. *Gene* **304**, 117-131 (2003).

157 Rawlings, N. D., Barrett, A. J. & Bateman, A. MEROPS: the database of proteolytic enzymes, their substrates and inhibitors. *Nucleic acids research* **40**, D343-350 (2012).

158 Todd, A. E., Orengo, C. A. & Thornton, J. M. Sequence and structural differences between enzyme and nonenzyme homologs. *Structure* **10**, 1435-1451 (2002).

159 Hennig, M., Schlesier, B., Dauter, Z., Pfeffer, S., Betzel, C., Hohne, W. E. & Wilson, K. S. A TIM barrel protein without enzymatic activity? Crystal-structure of narbonin at 1.8 A resolution. *FEBS letters* **306**, 80-84 (1992).

160 Hennig, M., Pfeffer-Hennig, S., Dauter, Z., Wilson, K. S., Schlesier, B. & Nong, V. H. Crystal structure of narbonin at 1.8 A resolution. *Acta crystallographica. Section D, Biological crystallography* **51**, 177-189 (1995).

161 Min, X., Lee, B. H., Cobb, M. H. & Goldsmith, E. J. Crystal structure of the kinase domain of WNK1, a kinase that causes a hereditary form of hypertension. *Structure* **12**, 1303-1311 (2004).

162 Mukherjee, K., Sharma, M., Urlaub, H., Bourenkov, G. P., Jahn, R., Sudhof, T. C. & Wahl, M. C. CASK Functions as a Mg2+-independent neurexin kinase. *Cell* **133**, 328-339 (2008).

163 Kawagoe, T., Sato, S., Matsushita, K., Kato, H., Matsui, K., Kumagai, Y., Saitoh, T., Kawai, T., Takeuchi, O. & Akira, S. Sequential control of Toll-like receptor-dependent responses by IRAK1 and IRAK2. *Nature immunology* **9**, 684-69 (2008).

164 Shi, F., Telesco, S. E., Liu, Y., Radhakrishnan, R. & Lemmon, M. A. ErbB3/HER3 intracellular domain is competent to bind ATP and catalyze autophosphorylation. *Proceedings of the National Academy of Sciences of the United States of America* **107**, 7692-7697 (2010).

165 Csonka, L. N. Physiological and genetic responses of bacteria to osmotic stress. *Microbiological reviews* **53**, 121-147 (1989).

166 Martin, D. D., Ciulla, R. A. & Roberts, M. F. Osmoadaptation in archaea. *Applied and environmental microbiology* **65**, 1815-1825 (1999).

167 Lanyi, J. K. Salt-dependent properties of proteins from extremely halophilic bacteria. *Bacteriological reviews* **38**, 272-290 (1974).

168 Zaccai, G., Cendrin, F., Haik, Y., Borochov, N. & Eisenberg, H. Stabilization of halophilic malate dehydrogenase. *Journal of molecular biology* **208**, 491-500 (1989).

169 Zaccai, G., Wachtel, E. & Eisenberg, H. Solution structure of halophilic malate dehydrogenase from small-angle neutron and X-ray scattering and ultracentrifugation. *Journal of molecular biology* **190**, 97-106 (1986).

170 Sleator, R. D. & Hill, C. Bacterial osmoadaptation: the role of osmolytes in bacterial stress and virulence. *FEMS microbiology reviews* **26**, 49-71 (2002).

171 Bolen, D. W. & Baskakov, I. V. The osmophobic effect: natural selection of a thermodynamic force in protein folding. *Journal of molecular biology* **310**, 955-963 (2001).

172 Welsh, D. T. Ecological significance of compatible solute accumulation by micro-organisms: from single cells to global climate. *FEMS microbiology reviews* **24**, 263-290 (2000).

173 Yancey, P. H., Clark, M. E., Hand, S. C., Bowlus, R. D. & Somero, G. N. Living with water stress: evolution of osmolyte systems. *Science* **217**, 1214-1222 (1982).

174 Baskakov, I. & Bolen, D. W. Forcing thermodynamically unfolded proteins to fold. *The Journal of biological chemistry* **273**, 4831-4834 (1998).

175 Qu, Y., Bolen, C. L. & Bolen, D. W. Osmolyte-driven contraction of a random coil protein. *Proceedings of the National Academy of Sciences of the United States of America* **95**, 9268-9273 (1998).

176 Lopez, C. S., Alice, A. F., Heras, H., Rivas, E. A. & Sanchez-Rivas, C. Role of anionic phospholipids in the adaptation of Bacillus subtilis to high salinity. *Microbiology* **152**, 605-616 (2006).

177 Piuri, M., Sanchez-Rivas, C. & Ruzal, S. M. Cell wall modifications during osmotic stress in Lactobacillus casei. *Journal of applied microbiology* **98**, 84-95 (2005).

178 Chateau, A., van Schaik, W., Six, A., Aucher, W. & Fouet, A. CodY regulation is required for full virulence and heme iron acquisition in Bacillus anthracis. *FASEB journal : official publication of the Federation of American Societies for Experimental Biology* **25**, 4445-4456 (2011).

179 Hoffmaster, A. R. & Koehler, T. M. The anthrax toxin activator gene atxA is associated with CO2-enhanced non-toxin gene expression in Bacillus anthracis. *Infection and immunity* **65**, 3091-3099 (1997).

180 Chen, Y., Tenover, F. C. & Koehler, T. M. Beta-lactamase gene expression in a penicillin-resistant Bacillus anthracis strain. *Antimicrobial agents and chemotherapy* **48**, 4873-4877 (2004).

181 Fortinea, N., Trieu-Cuot, P., Gaillot, O., Pellegrini, E., Berche, P. & Gaillard, J. L. Optimization of green fluorescent protein expression vectors for in vitro and in vivo detection of Listeria monocytogenes. *Research in microbiology* **151**, 353-360 (2000).

182 Araki, Y., Oba, S., Araki, S. & Ito, E. Enzymatic deacetylation of N-acetylglucosamine residues in cell wall peptidoglycan. *Journal of biochemistry* **88**, 469-479 (1980).

183 Murphy, E. Nucleotide sequence of a spectinomycin adenyltransferase AAD(9) determinant from Staphylococcus aureus and its relationship to AAD(3") (9). *Molecular & general genetics : MGG* **200**, 33-39 (1985).

184 Rygus, T. & Hillen, W. Inducible high-level expression of heterologous genes in Bacillus megaterium using the regulatory elements of the xylose-utilization operon. *Applied microbiology and biotechnology* **35**, 594-599 (1991).

185 Bui, N. K., Eberhardt, A., Vollmer, D., Kern, T., Bougault, C., Tomasz, A., Simorre, J. P. & Vollmer, W. Isolation and analysis of cell wall components from Streptococcus pneumoniae. *Analytical biochemistry* **421**, 657-666 (2012).

186 Etienne-Toumelin, I., Sirard, J. C., Duflot, E., Mock, M. & Fouet, A. Characterization of the Bacillus anthracis S-layer: cloning and sequencing of the structural gene. *Journal of bacteriology* **177**, 614-620 (1995).

187 Horton, R. M., Cai, Z. L., Ho, S. N. & Pease, L. R. Gene splicing by overlap extension: tailor-made genes using the polymerase chain reaction. *BioTechniques* **8**, 528-535 (1990).

188 Arnaouteli, S., Giastas, P., Andreou, A., Tzanodaskalaki , M., Aldridge, C., Tzartos, S., Vollmer, W., Eliopoulos, E. & Bouriotis, V. Two putative polysaccharide deacetylases are required for osmotic stability and cell shape maintenance in *Bacillus anthracis. Journal of Biological Chemistry* (2015) in press.

189 Notredame, C., Higgins, D.G. & Heringa, J. T-Coffee: A novel method for fast and accurate multiple sequence alignment. *Journal of Molecular Biology* **302**, 205-217 (2000).

190 Robert, X. & Gouet, P. Deciphering key features in protein structures with the new ENDscript server. *Nucleic Acids Res.* **42**, W320-324 (2014).

191 Palomino, M. M., Sanchez-Rivas, C. & Ruzal, S. M. High salt stress in Bacillus subtilis: involvement of PBP4* as a peptidoglycan hydrolase. *Research in microbiology* **160**, 117-124 (2009).

192 Jolliffe, L. K., Doyle, R. J. & Streips, U. N. The energized membrane and cellular autolysis in Bacillus subtilis. *Cell* **25**, 753-763 (1981).

193 Braun, V. & Wu, H.C. Lipoproteins: structure, function, biosynthesis and model for protein export. *New Comparative Biochemistry* **27**, 319–341 (1994).

194 Sutcliffe, I.C. & Russell, R.R. Lipoproteins of gram-positive bacteria. *Journal of Bacteriology* **177**, 1123-1128 (1995).

195 Taylor, E.J., Gloster, T.M., Turkenburg , J.P., Vincent, F. , Brzozowski, M.A., Dupont, C., Shareck, F., Centeno, M.S., Prates, J.A., Puchart, V., Ferreira, L.M., Fontes, C.M., Biely, P. & Davies, G.J. Structure and activity of two metal ion-dependent acetylxylan esterases involved in plant cell wall degradation reveals a close similarity to peptidoglycan deacetylases. *Journal of Biological Chemistry* **281**, 10968–10975 (2006).

196 Pokrovskaya, V., Poloczek, J., Little, D.J., Griffiths, H., Howell, P.L. & Nitz, M. Functional characterization of *Staphylococcus epidermidis* IcaB, a de-N-acetylase important for biofilm formation. *Biochemistry*. **52**, 5463-5471 (2013).

197 Strunk, R.J , Piemonte, K.M. , Petersen, N.M., Koutsioulis, D., Bouriotis, V., Perry, K. & Cole, K.E. Structure determination of BA0150, a putative polysaccharide deacetylase

from *Bacillus anthracis. Acta Crystallographica F Struct Biol Commun*. **70**, 156-159 (2014).

198 Oberbarnscheidt, L., Taylor, E.J., Davies, G.J. & Gloster, T.M. Structure of a Carbohydrate Esterase from *Bacillus anthracis. Proteins*. **66**, 250–252 (2007).

199 Fadouloglou, V. E., Kapanidou, M., Agiomirgianaki, A., Arnaouteli, S., Bouriotis, V., Glykos, N. M. & Kokkinidis, M. Structure determination through homology modelling and torsion-angle simulated annealing: application to a polysaccharide deacetylase from Bacillus cereus. *Acta crystallographica. Section D, Biological crystallography* **69**, 276-283 (2013).

200 Deng, D.M., Urch J.E., ten Cate J.M., Rao, V.A., van Aalten, D.M. & Crielaard, W. *Streptococcus mutans* SMU.623c codes for a functional, metal-dependent polysaccharide deacetylase that modulates interactions with salivary agglutinin. *Journal of Bacteriology* **191**, 394–402 (2009).

201 Antelmann, H., Williams, R. C., Miethke, M., Wipat, A., Albrecht, D., Harwood, C. R. & Hecker, M. The extracellular and cytoplasmic proteomes of the non-virulent Bacillus anthracis strain UM23C1-2. *Proteomics* **5**, 3684-3695 (2005).

202 Chitlaru, T., Gat, O., Grosfeld, H., Inbar, I., Gozlan, Y. & Shafferman, A. Identification of in vivo-expressed immunogenic proteins by serological proteome analysis of the Bacillus anthracis secretome. *Infection and immunity* **75**, 2841-2852 (2007).

203 Bernhardt, T. G. & de Boer, P. A. Screening for synthetic lethal mutants in Escherichia coli and identification of EnvC (YibP) as a periplasmic septal ring factor with murein hydrolase activity. *Molecular microbiology* **52**, 1255-1269 (2004).

204 Uehara, T., Parzych, K. R., Dinh, T. & Bernhardt, T. G. Daughter cell separation is controlled by cytokinetic ring-activated cell wall hydrolysis. *The EMBO journal* **29**, 1412-1422 (2010).

205 Candela, T., Balomenou, S., Aucher, W., Bouriotis, V., Simore, J. P., Fouet, A. & Boneca, I. G. N-acetylglucosamine deacetylases modulate the anchoring of the gamma-glutamyl capsule to the cell wall of Bacillus anthracis. *Microbial drug resistance* **20**, 222-230 (2014).

206 Kataeva, I. A., Seidel, R. D., 3rd, Shah, A., West, L. T., Li, X. L. & Ljungdahl, L. G. The fibronectin type 3-like repeat from the Clostridium thermocellum cellobiohydrolase CbhA promotes hydrolysis of cellulose by modifying its surface. *Applied and environmental microbiology* **68**, 4292-4300 (2002).

207 Nelson, D. E., Ghosh, A. S., Paulson, A. L. & Young, K. D. Contribution of membrane-binding and enzymatic domains of penicillin binding protein 5 to maintenance of uniform cellular morphology of Escherichia coli. *Journal of bacteriology* **184**, 3630-3639 (2002).

208 Chen, Y., Zhang, W., Shi, Q., Hesek, D., Lee, M., Mobashery, S. & Shoichet, B. K. Crystal structures of penicillin-binding protein 6 from Escherichia coli. *Journal of the American Chemical Society* **131**, 14345-14354 (2009).

209 Campbell, I. D. & Spitzfaden, C. Building proteins with fibronectin type III modules. *Structure* **2**, 333-337 (1994).

210 Frirdich, E., Vermeulen, J., Biboy, J., Soares, F., Taveirne, M. E., Johnson, J. G., DiRita, V. J., Girardin, S. E., Vollmer, W. & Gaynor, E. C. Peptidoglycan LD-carboxypeptidase Pgp2 influences Campylobacter jejuni helical cell shape and pathogenic properties and provides the substrate for the DL-carboxypeptidase Pgp1. *The Journal of biological chemistry* **289**, 8007-8018 (2014).

211 Barendt, S. M., Sham, L. T. & Winkler, M. E. Characterization of mutants deficient in the L,D-carboxypeptidase (DacB) and WalRK (VicRK) regulon, involved in peptidoglycan maturation of Streptococcus pneumoniae serotype 2 strain D39. *Journal of bacteriology* **193**, 2290-2300 (2011).

212 Sycuro, L. K., Wyckoff, T. J., Biboy, J., Born, P., Pincus, Z., Vollmer, W. & Salama, N. R. Multiple peptidoglycan modification networks modulate Helicobacter pylori's cell shape, motility, and colonization potential. *PLoS pathogens* **8**, e1002603, doi:10.1371/journal.ppat.1002603 (2012).

213 Hoyland, C. N., Aldridge, C., Cleverley, R. M., Duchene, M. C., Minasov, G., Onopriyenko, O., Sidiq, K., Stogios, P. J., Anderson, W. F., Daniel, R. A., Savchenko, A., Vollmer, W. & Lewis, R. J. Structure of the LdcB LD-carboxypeptidase reveals the molecular basis of peptidoglycan recognition. *Structure* **22**, 949-960 (2014).

214 Dramsi, S. & Cossart, P. Listeriolysin O-mediated calcium influx potentiates entry of Listeria monocytogenes into the human Hep-2 epithelial cell line. *Infection and immunity* **71**, 3614-3618 (2003).

215 El Hidri, D., Guesmi, A., Najjari, A., Cherif, H., Ettoumi, B., Hamdi, C., Boudabous, A. & Cherif, A. Cultivation-dependent assessment, diversity, and ecology of haloalkaliphilic bacteria in arid saline systems of southern Tunisia. *BioMed research international* **2013**, 648141 (2013).

216 Browne, N. & Dowds, B. C. Heat and salt stress in the food pathogen Bacillus cereus. *Journal of applied microbiology* **91**, 1085-1094 (2001).

217 Senior, A. & Moir, A. The Bacillus cereus GerN and GerT protein homologs have distinct roles in spore germination and outgrowth, respectively. *Journal of bacteriology* **190**, 6148-6152 (2008).

218 Reffuveille, F., Leneveu, C., Chevalier, S., Auffray, Y. & Rincé, A. Lipoproteins of Enterococcus faecalis: bioinformatic identification, expression analysis and relation to virulence. *Microbiology* **157**, 3001-3013 (2011).

219 Schmaler, M., Jann, N.J., Götz, F. & Landmann, R. Staphylococcal lipoproteins and their role in bacterial survival in mice. *International Journal of Medical Microbiology* **300**, 155-160 (2010).